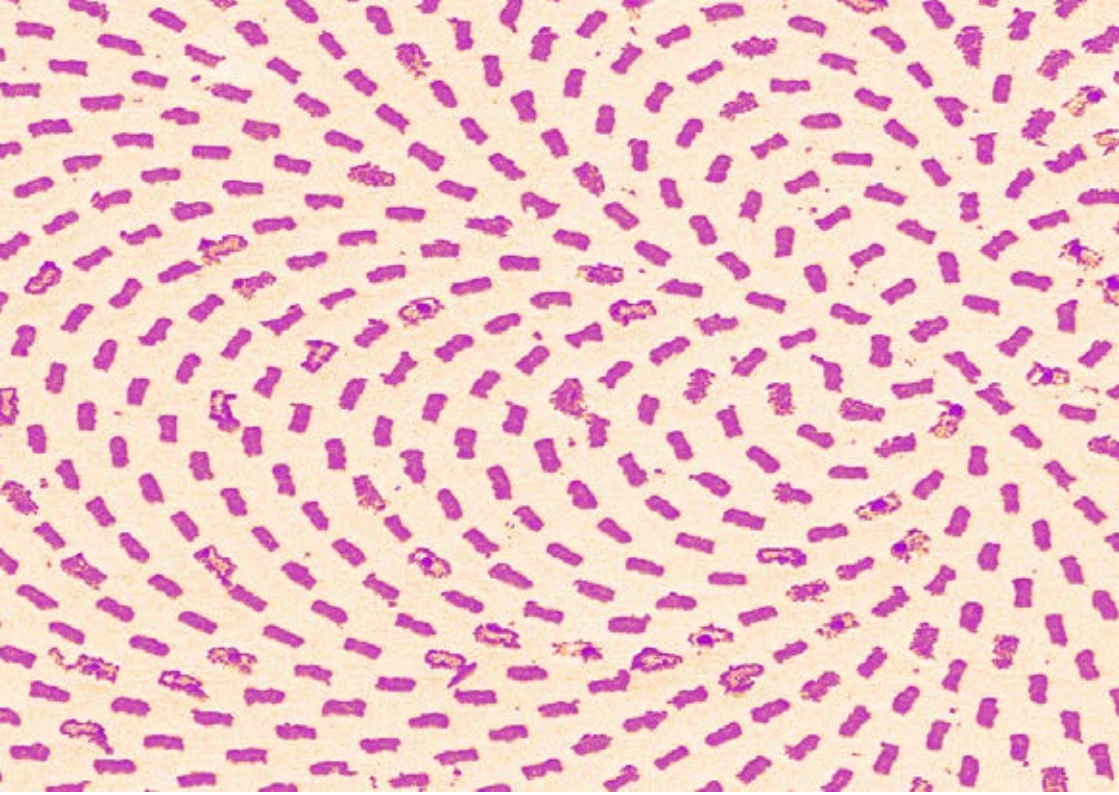

ACTIVITY REPORT 2022

CNR NANO

ISTITUTO NANOSCIENZE CONSIGLIO NAZIONALE DELLE RICERCHE

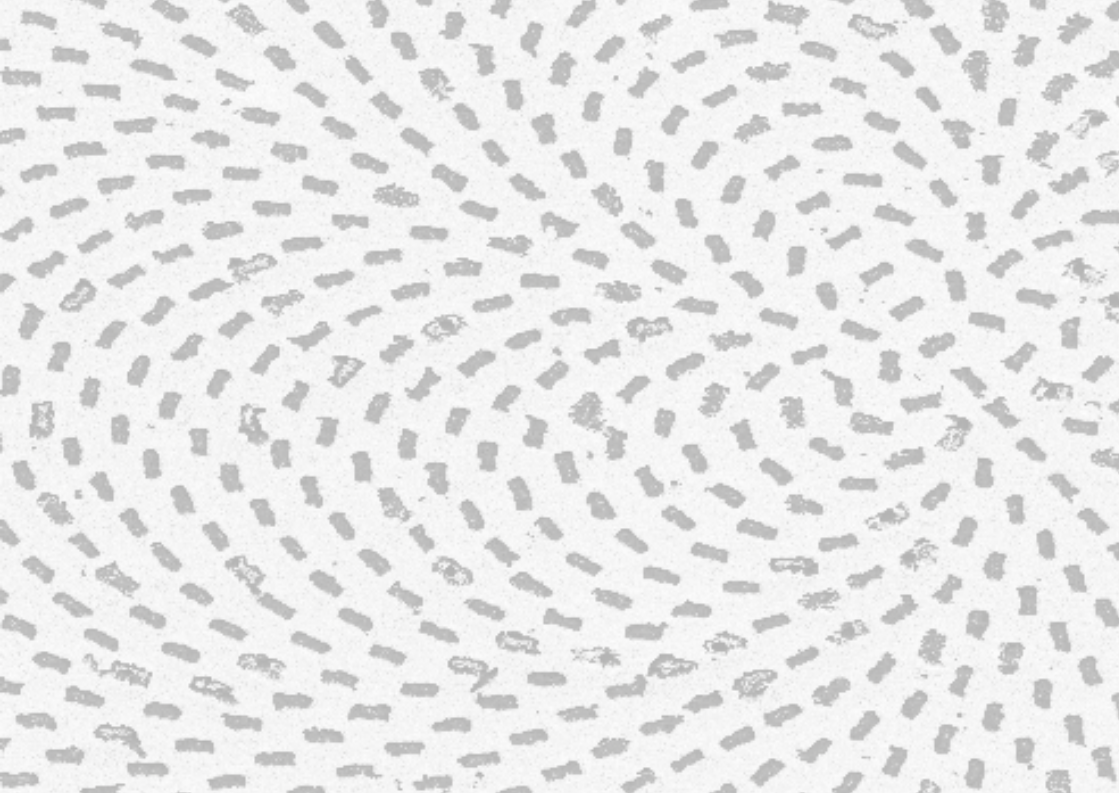

ACTIVITY REPORT 2022

CNR NANO

ISTITUTO NANOSCIENZE CONSIGLIO NAZIONALE DELLE RICERCHE

Table of contents

Institute director
Lucia Sorba

Coordinators of units
Modena: Massimo Rontani
Pisa: Lucia Sorba

Administrative director
Giovanna Diprima

Executive board
Cnr researchers
Giorgia Brancolini, Stefania Benedetti, Marco Cecchini, Stefan Heun, Valentina Tozzini, Filippo Troiani

Cnr technical/administrative staff
Maria Grazia Angelini

Affiliated researchers
Elisa Molinari, Alessandro Tredicucci

CONTACTS
Piazza San Silvestro, 12
I-56127 Pisa, Italy
ph. +39 050 509418
website: www.nano.cnr.it
e-mail: segreteria.nest@nano.cnr.it

Modena unit
via Campi, 213A
I-41125 Modena, Italy
ph. +39 059 2055629
website: www.nano.cnr.it
e-mail: segreteria.s3@nano.cnr.it

Foreword

This is the sixth biennial report of the Institute Nanoscience of the National Research Council (Cnr Nano). We have collected in brief most of the activity of the past two years. At the core of the report are the scientific highlights of years 2020-2021: short articles on the most prominent lines of research of our Institute on solid-state quantum technology; fundamental and translational nanobiophysics; nanoscale theory, modelling, and computational; physics and technology of light at the nanoscale; and surfaces and interfaces: nanofabrication, imaging, and spectroscopy. A complete list of running projects, published papers, and events of 2020-2021 are also included in the report and help give a rich overview of Cnr Nano's outputs.

In the years 2020-2021, due to the pandemic health emergency, research activities were carried out with many difficulties and restrictions. Nonetheless the Cnr Nano people were able to adapt to the new scenario and were up and running both at research and administration level. As a result, 12 new projects started under the framework of Horizon H2020 and Horizon Europe, growing the overall number of European projects to 23. In particular, three FET-open projects, and a FETPROACT, a NMP-to-IND, a Marie Curie individual fellowship, and a LC-BA projects were granted in 2020-2021. In addition, four regional projects and one national FISR started. Moreover, a new Cnr infrastructure for quantum simulation and computation, named "Pasqua", was funded, and a state-of-the-art MBE facility dedicated to the realization of Quantum Cascade Lasers is being established.

By the same token, we enlarged our staff with 12 new researchers and technologists, and almost 40 new post-docs. Almost 5 hundred papers in high impact journals were published in 2020-2021. The Institute also managed to adapt scientific and outreach events to a virtual and hybrid format. By this way, it was possible to hold monthly colloquia, in order to share the ongoing research activities among the Cnr Nano researchers and affiliates. Along with these well-established activities, in the next three years many Cnr Nano researchers will be involved in different initiatives connected to the Italian Plan of Recovery and Resilience (PNRR) that will bring new funds, personnel, and the chance of developing novel and exciting research activities.

I would like to acknowledge Stefania Benedetti, Andrea Camposeo, Claudia Cardoso, Luisa Neri, Maddalena Scandola, Antonella Sgarbossa, and Fabio Taddei for their contribution to drafting this report.

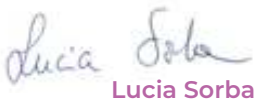

Lucia Sorba

Director of the Institute Nanoscience of Cnr

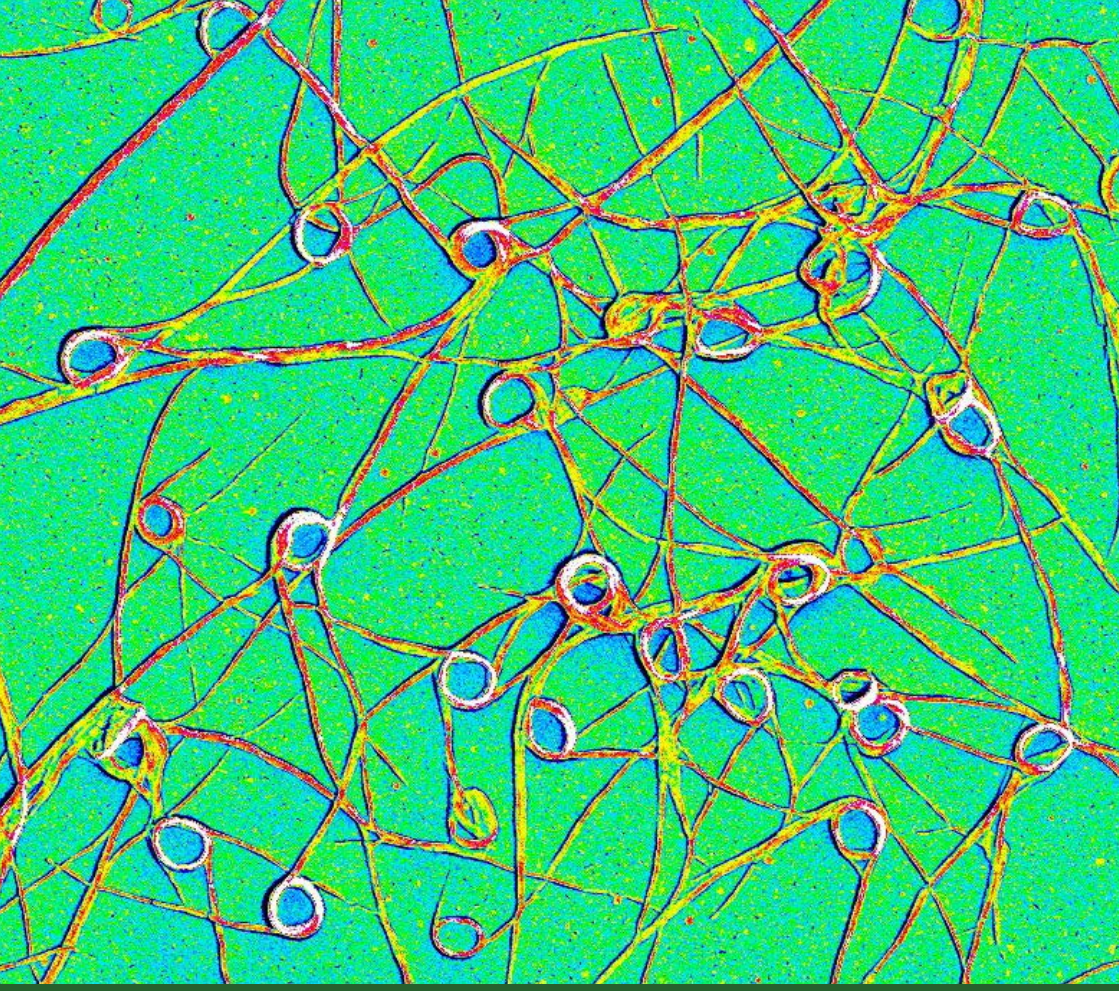

Highlights - Fundamental and translational nanobiophysics

Introduction to Fundamental and translational nanobiophysics

Nanobiophysics research relies on a wide range of multidisciplinary expertise, from biology and biotechnology to physics, chemistry and nanotechnology. The synergy between theoretical-computational methodologies and experimental techniques permits us to face the complexity of biological systems and processes at a nanoscale resolution. The recent pandemic of coronavirus disease 2019 (COVID-19) is increasingly highlighting the need to address and strengthen scientific research in key and critical areas that constitute social emergencies, such as emerging infectious diseases caused by virus and antibiotic resistant bacteria, nano-diagnostic, nano-therapy and precision medicine, and neuroscience and neuropharmacology, to combat serious genetic and neurodegenerative diseases. Nanobiophysics research activities at Cnr Nano focus on these topics, and more, as presented here.

Emerging infectious diseases. Molecular interactions among SARS-CoV-2 and host cells have been investigated at nanoscale by means of a multi-scale microscopy imaging toolbox using both confocal and super-resolution microscopy. Thanks to this combined approach, the entry phase of SARS-CoV-2 variants in model cells has been revealed.

Because of its critical role in the virus replication cycle, SARS-CoV-2 main protease (Mpro) is an appealing target for drug development. In order to design antiviral drugs against SARS-CoV-2, a hybrid quantum classical approach, namely Perturbed Matrix Method, was developed to study the catalytic proton transfer reaction required for the covalent binding of inhibitors to Mpro.

Antimicrobial PhotoDynamic Therapy (aPDT) is particularly effective against microorganisms capable of producing and storing intrinsic photosensitizer pigments as in the case of *Helicobacter pylori* (Hp), a major cause of severe gastric diseases. The main properties of porphyrins produced by Hp in a biofilm were studied using advanced fluorescence microscopy techniques to shed light on potential diagnostic and therapeutic approaches to fight antibiotic resistant infections.

Nano-diagnostic, nano-therapy and precision medicine. Nanotechnologies suitable for point-of-care (PoC) diagnostics are currently under investigation to detect early biomarkers of brain pathologies in circulating blood, avoiding invasive procedures. Effective functionalization strategies for the detection of glial-fibrillary-acidic-protein, a reliable indicator of brain damage, have been explored and the best-performing protocol has been validated with an ultra-high-frequency surface-acoustic-wave (SAW) based lab-on-a-chip.

Molecular simulations can provide atomistic insight into the interactions between a biomolecule and an inorganic/organic surface. The structure and dynamics of functionalized gold surfaces of an Acoustic Wave biosensor were elucidated using fully atomistic MD simulations, with the goal of designing functionalized nanoscale materials for biotechnological applications in nanomedicine. Furthermore, a computational protocol that combines the development of force field parameters, flexible docking with Brownian Dynamics, and s-long MD simulations has been demonstrated to clarify the microscopic working mechanism of sophisticated bio-nanosystems such as nanozymes.

Artificial nanoscaffolds may open up new possibilities for nerve regeneration applications. Chitosan micro-grooved membranes with enhanced asymmetry have been demonstrated to be an efficient performing pattern inducing fast and persistent cell oriented migration in glial Schwann cells.

Neuroscience. Monogenic diseases of the central nervous system are frequently characterized by genetic mosaicism, a phenomenon in which an organ contains cells with different genotypes. The understanding of the mechanisms of these diseases requires the creation of sparse mosaic models, in which the genotype of each neuron is unambiguously recognized by the expression of a fluorescent protein *in vivo*. A dual-color reporter system, Beatrix, has been shown to lead to the development of mosaics with tunable degree when expressed in a floxed mouse strain for a target gene.

Antimicrobial PhotoDynamic Therapy (aPDT): a promising therapeutic strategy to fight antibiotic resistant pathogens

During the last decades bacteria have been developing increasing resistance against conventional antibiotics. This event leads to the demand for new therapeutic strategies to eradicate bacterial infections and in the last years nonpharmacological approaches gained growing importance as alternative treatments. Among these, Antimicrobial PhotoDynamic Therapy (aPDT) is particularly effective against microorganisms able to produce and store up pigments that can be exploited as intrinsic photosensitizers. With this aim, we explored the main characteristics of porphyrins produced by *Helicobacter pylori* in a biofilm in order to shed light on possible diagnostic and therapeutic approaches.

Conventional PhotoDynamic Therapy (PDT) relies on the administration of a photosensitizing drug that upon light irradiation reacts with molecular oxygen in and around cells, producing cytotoxic reactive oxygen species (ROS) able to induce photodamage to host cells. It can be converted in a drugless therapeutic strategy when applied against microorganisms (Antimicrobial PhotoDynamic Therapy, aPDT) that naturally produce and store up photosensitizing pigments. It has long been known that *Helicobacter pylori* (Hp), a major cause of severe gastric diseases, spontaneously produces photosensitising porphyrins, making it a suitable target for aPDT. In order to maximise the photokilling effect, the best illumination parameters have been determined and for the first time endogenous photosensitizing molecules other than porphyrins, such as flavins, were suggested to be involved in the bacterial photoinactivation. Fluorescence lifetime imaging microscopy (FLIM) of intrinsic bacterial por-

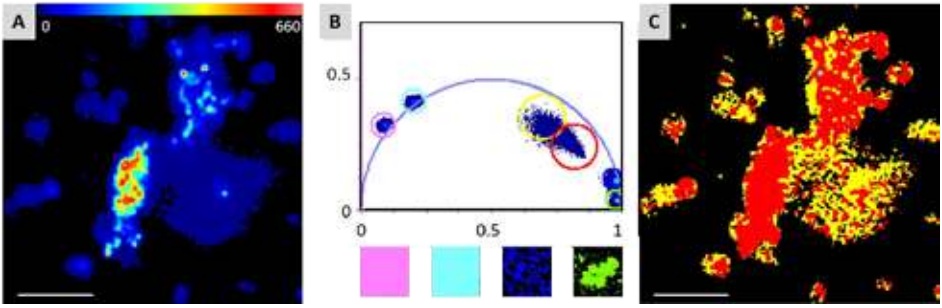

Fig. 1
(A) False-colour intensity-based image of bacterial biofilm. (B top) Overlap of the phasor plots of standard porphyrins PPIX (pink circle: methanol solution, green circle: crystal) and CPI (cyan circle: methanol solution, blue circle: crystal) and biofilm sample (red circle: bacteria, yellow circle: biofilm matrix). (B bottom) Phasor images of the standards, colour code as in the plot. (C) Corresponding phasor image of the biofilm in A. Scale bar in A and C: 25 µm.

phyrins was also performed and data were analysed by the 'fit-free' phasor approach to map the distribution of the different fluorescent species within Hp biofilm. The relevant phasor plot indicates that intracellular porphyrins may be organised in more packed structures than those dispersed in the extracellular matrix. This finding can drive the phototherapeutical approach because, due to the short diffusion path of cytotoxic ROS, a closer bond between the photosensitizer and the cellular target can produce a more effective photokilling activity. As the intracellular pigment concentration varies with the age of bacteria, the detection and the spatial distribution pattern of porphyrin fluorescence in Hp biofilm could provide some hints for the choice of the best time window to perform aPDT. In general, this analysis can be a useful tool to assess the extent of bacterial contamination and the presence of a biofilm inside an infected tissue, suggestive of an advanced stage of infection, in order to develop and optimise novel antimicrobial strategies.

Contact persons
Antonella Sgarbossa (antonella.sgarbossa@nano.cnr.it)
Antonella Battisti (antonella.battisti@nano.cnr.it)

References

[1] Fluorescence lifetime imaging microscopy of porphyrins in *Helicobacter pylori* biofilms. A. Battisti, P. Morici, and A. Sgarbossa. Pharmaceutics 13 (10), 1674 (2021).
[2] The *in vitro* photoinactivation of *Helicobacter pylori* by a novel LED-based device. P. Morici, A. Battisti, G. Tortora, A. Menciassi, G. Checcucci, F. Ghetti, and A. Sgarbossa. Front. Microbiol. 11, 283 (2020).

Design of functionalized nanoscale materials for biotechnological applications

Well-designed molecular simulations can give atomistic insight into the interactions between a biomolecule and an inorganic/organic surface, revealing details that cannot be accessed through experiments alone. In turn, experiments can validate some key aspects of the simulation to build confidence in the theoretical predictions. The activity report shows two examples on how the synergy between experiment and simulation has been harnessed to optimize the design of functionalized nanoscale systems, and indeed provide rational design tools to create new technologies.

The bottom-up design of engineered functional nano-materials largely depends on the accuracy by which each of the inherent nanometric components can be functionally designed with predictive methods.
In a first work, fully atomistic MD simulations have been applied to reveal the structure and dynamics of functionalized gold surfaces of an Acoustic Wave biosensor, which could not be easily captured by experiments [1]. The paper clarified the role of the grafted linker density of biotinylated polyethylene glycol chains on a gold surface and disclosed the influence of the pegylation ratio on the sensitivity of the biosensor.
In a second contribution, we have shown how a computational protocol combining the development of force field parameters, flexible docking with Brownian Dynamics and μs-long MD simulations can gain the microscopic picture at the basis of experimental results for complicated bio-nanosystems such as nanozymes [2]. Our results show the importance of a rational design of the peptide to enhance the catalytic activity of peptide-nanoparticle conjugates and present a viable computational approach which can be generalized, not only to tune catalytically active peptide-nano conjugate but also to design proper nano-receptor with target affinity in domain of nano-medicine and industrial applications in future.

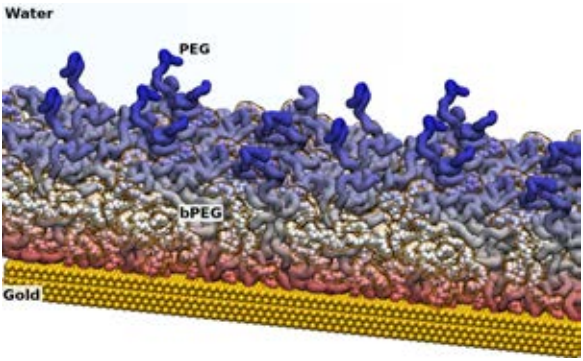

Fig. 1
Fully atomistic MD simulations of large pegylated gold surfaces, functionalized with a different number and types of linkers, are applied to reveal the structure and dynamics of functionalized gold surfaces of an Acoustic Wave biosensor, which cannot be easily captured by experiments.

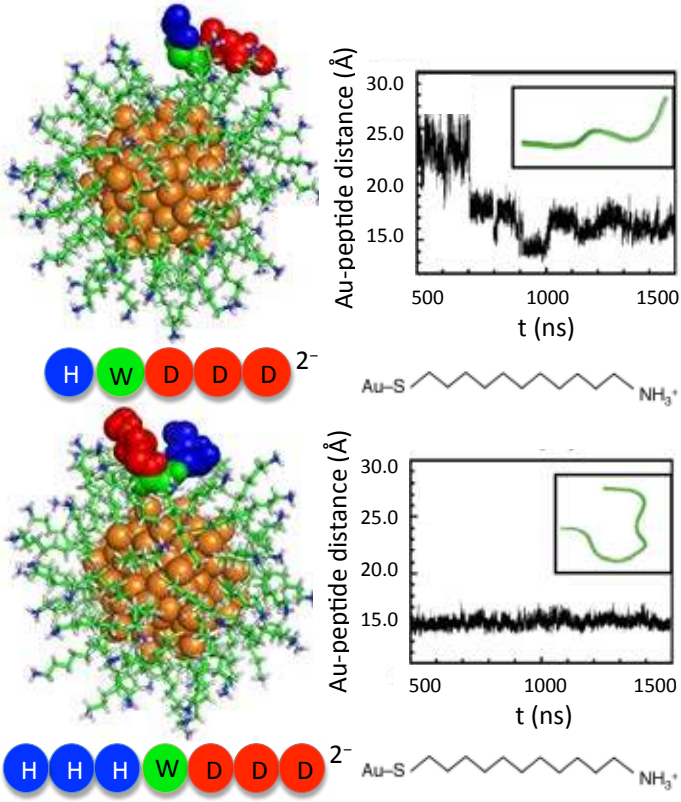

Fig. 2
A multiscale iterative approach is applied to nanozymes, resulting from the assembling between a small peptide and the surface of cationic self-assembled monolayers on gold nanoparticles. Starting from published experimental data [J Am Chem Soc 134, 8396 (2012)] we have shown how a computational protocol able to tackle multiple time scales can be used to clarify the microscopic working mechanism of such nano-biosystems. In particular, we were able to identify the mechanisms that make the bound peptide catalytically active, as opposed to the inactive free peptide.

Contact person
Giorgia Brancolini (giorgia.brancolini@nano.cnr.it)

References
[1] Atomistic simulations of gold surface functionalization for nanoscale biosensors applications. S. Dutta, L. Bellucci, M. Agostini, M. Gagliardi, S. Corni, M. Cecchini, and G. Brancolini. Nanotechnology 32, 095702 (2021).
[2] Molecular Dynamics Simulations of a Catalytic Multivalent Peptide–Nanoparticle Complex. S. Dutta, S. Corni, and G. Brancolini. Int. J. Mol. Sci. 22, 3624 (2021).

Glial-fibrillary-acidic-protein (GFAP) biomarker detection in serum-matrix: Functionalization strategies and detection by an ultra-high-frequency surface-acoustic-wave (UHF-SAW) lab-on-chip

Glial-fibrillary-acidic-protein (GFAP) has recently drawn significant attention as a promising biomarker for brain damage. Here, we develop three detection strategies for GFAP, among the most popular in the biosensing field and never examined side by side. We compare their capability of detecting GFAP in a clean-buffer and serum-matrix by a quartz-crystal-microbalance (QCM). Then, we select the best-performing protocol and validate its detection performance with an ultra-high-frequency surface-acoustic-wave (SAW) based lab-on-a-chip (LoC). GFAP detection is demonstrated in a clean-buffer and serum-matrix at a concentration of 35 pM. This GFAP level is compatible with clinical diagnostics.

The presence of GFAP in circulating blood has been linked to severe brain damage, such as glioblastoma multiforme and traumatic brain injuries. The interest in GFAP as a biomarker is related to two main aspects. First, the importance of the pathologies that could be addressed. Second, the possibility to detect this biomarker in circulating blood, avoiding invasive procedures. In this direction, the common aim is to propose technologies suitable for point-of-care (PoC) diagnostics. In the context of label-free methods with electrical readout and on-chip sample manipulation, the surface acoustic wave (SAW) technology can be used as a sensor for detecting adhesion of molecules onto surfaces, and for manipulating fluids at the micrometer scale

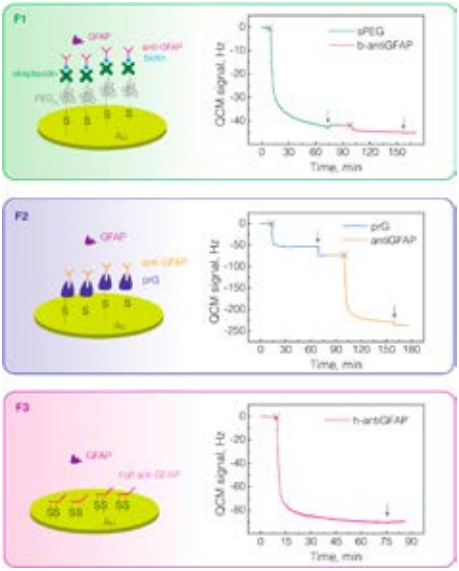

Fig. 1
The three functionalization strategies explored for GFAP detection with gold QCM sensors. F1 comprises an sPEG functionalization followed by the immobilization of the b-anti-GFAP through the biotin-streptavidin binding. F2 comprises a functionalization with prG followed by the immobilization of the antiGFAP by the prG binding immunoglobulins. F3 makes use of the thiol-bridges of the reduced anti-GFAP. On the right-hand side, the binding kinetics during the different steps are shown. The cross symbol corresponds to solution injection, while the arrow to the rinsing with buffer.

as well [1,2]. We explored three different functionalization strategies for GFAP detection, all of them based on antibodies. The first strategy (F1) exploited a PEG layer for antifouling, the second (F2) the protein-G for antibody-orientation, and the third (F3) an antibody-splitting protocol for an enhanced surface-coverage (Fig. 1). Their performance in terms of limit-of-detection and selectivity was evaluated by a QCM. All three functionalizations were effective in clean buffers, but only F1 and F3 could also significantly detect at least one concentration of GFAP in presence of serum. F1 was the best performing both in terms of lowest significant concentration and specificity. We then chose F1 and demonstrated its use with a UHF-SAW LoC. This device exploited ~1 GHz SAW resonators as mass-sensors, and a microfluidic network for fluid routing. GFAP was significantly detected at clinically-relevant concentrations both in clean-buffers (>23 pM) and in serum-matrix (35 pM) (Fig. 2) [3]. This device can be further developed with the aim of realizing a PoC platform for the detection of multiple brain-pathology biomarkers in serum or whole blood. Yet, it has also the potential to be tailored for other, non-CNS, relevant pathologies, where a PoC diagnosis could be a breakthrough, such as a virus and bacteria detection.

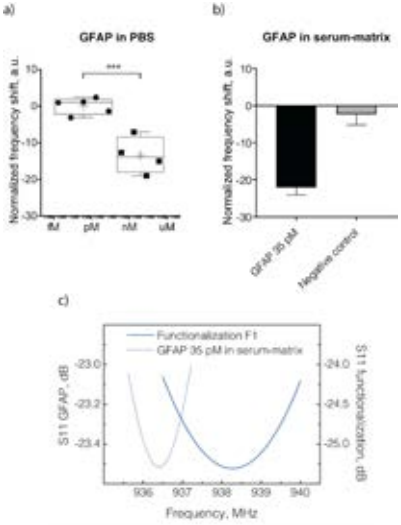

Fig. 2
GFAP detection with the UHF-SAW LoC. a) Experiments with GFAP in PBS at several concentrations. t-test with 23 pM as grouping threshold P < 0.001. b) Experiments with GFAP in serum-matrix error bars are the SD of the signal resulting from repeated sensor washings. c) Reflected power spectrum (S11) of the resonator showing the resonance shift in the F1 and GFAP in the serum-matrix case.

Contact person
Marco Cecchini (marco.cecchini@nano.cnr.it)

References
[1] Ultra-high-frequency Love surface acoustic wave device for real-time sensing applications. G. Greco, M. Agostini, and M. Cecchini. IEEE Access 8, 112507 (2020).
[2] Ultra-high-frequency (UHF) surface-acoustic-wave (SAW) microfluidics and biosensors. M. Agostini and M. Cecchini. Nanotechnology 32, 312001 (2021).
[3] Glial-fibrillary-acidic-protein (GFAP) biomarker detection in serum-matrix: Functionalization strategies and detection by an ultra-high-frequency surface-acoustic-wave (UHF-SAW) lab-on-chip. M. Agostini, F. Amato, M. L. Vieri, G. Greco, I. Tonazzini, L. Baroncelli, M. Caleo, E. Vannini, M. Santi, G. Signore, and M. Cecchini. Biosens. Bioelectron. 172, 112774 (2021).

DNA-based regenerative amplifier for the creation of novel models of genetic diseases

Genetic mosaicism, a condition in which an organ includes cells with different genotypes, is frequently present in monogenic diseases of the central nervous system due to mutations affecting a subset of neurons. The comprehension of the mechanisms of these diseases and of the cell-autonomous effects of specific mutations requires the generation of sparse mosaic models in which the genotype of each neuron is univocally identified by the expression of a fluorescent protein *in vivo*. Here we have developed a sensor/effector that causes the silencing of a gene along with the binarized expression of a fluorescent tag that identifies univocally the cell genotype by two-photon microscopy *in vivo*.

Genetic mosaicism refers to the presence of genetically distinct cellular populations within the same individual. This condition originates from DNA mutations occurring through different biological mechanisms, associated with several brain disorders and cancer. Therefore it is not surprising that mosaic modelling has attracted wide interest with the long-term goal of studying the physiology of cells carrying the mutation intermingled with normal cells. For this aim it is necessary to design a tool that a) generates an expression mosaic for a gene of choice with a controllable degree ratio of mutated vs normal cells and b) allows the cell genotype to be identified on the basis of the expression of two different fluorescent proteins and the presence of the mutation. The most commonly used tool for the cell specific control of gene expression is the creation of a mouse line where the gene is "floxed". This indicates the insertion of a brief DNA sequence in the genome (loxP sequence) that surrounds the gene. In these mice the gene is expressed normally but if a plasmid encoding for the protein Cre-recombinase is inserted in a cell, the gene is edited and the floxed gene is removed. In this study, we have created a fragment of DNA that amplifies in a non linear way the activity of Cre leading to the creation of a genetic mosaic for the gene under study where cells are tagged with proteins of different colours: red for cells with normal genotype, green for mutant cells. We demonstrated that Beatrix, a bicolor sensor/effector for CRE-recombinase activity, is a reliable reporter of Cre-mediated recombination allowing the creation of genetic mosaics of arbitrary degree, amenable to be imaged *in vivo* by two photon microscopy. As a proof of principle, we created a mosaic of expression of the autism-related gene PTEN, a constitutive inhibitor of the mTOR pathway, and we demonstrated that the cortical mosaic is characterised by impaired network activity and by transient episodes of hyperexcitability strongly reminiscent of the electrophysiological signature of the human disease.

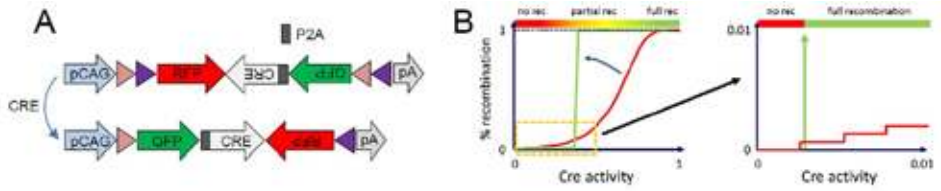

Fig. 1
Structure and operation of Beatrix: a bicolor sensor/effector for Cre-recombinase activity.

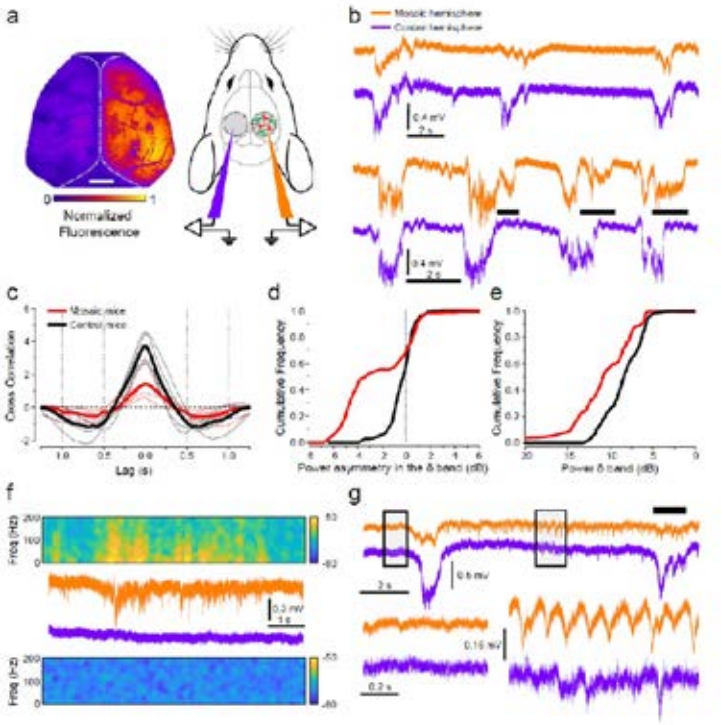

Fig. 2
Electrophysiological impairment of the resting state EEG in the PTEN-KO mosaic.

Contact person
Gian Michele Ratto (gianmichele.ratto@nano.cnr.it)

Reference

[1] Modelling genetic mosaicism of neurodevelopmental disorders in vivo by a Cre-amplifying fluorescent reporter. F. Trovato, R. Parra, E. Pracucci, S. Landi, O. Cozzolino, G. Nardi, F. Cruciani, V. Pillai, L. Mosti, A. W. Cwetsch, L. Cancedda, L. Gritti, C. Sala, C. Verpelli, A. Maset, C. Lodovichi, and G. M. Ratto. Nat Commun 11, 6194 (2020).

A spatial multi-scale fluorescence microscopy toolbox discloses functional features of SARS-CoV-2 cell cycle

To address molecular interactions among SARS-CoV-2 and host cells, a multi-scale microscopy imaging toolbox was explored using both conventional and super-resolution fluorescence microscopy. By this toolbox we revealed the entry phase of SARS-CoV-2 variants in model cells. Of note, alpha variant (B.1.1.7) is associated with much faster kinetics uptake compared to its ancestor B.1.177. Given the cell-entry scenario dominated by the endosomal "late pathway", the faster internalization of B.1.1.7 seems directly related to the N501Y mutation in the S protein, which strengthens its binding with ACE2. Our approach represents a general strategy to investigate the interplay of SARS-CoV-2 with cells.

In the last years, SARS-CoV-2 has rapidly spread worldwide generating a pandemic with devastating social consequences. In this context, elucidation of structure-property relationships that modulate virus-cell host checkpoints, such as entry and egress, is crucial to assess the role of virus infectivity. The virus-cell interactions were imaged by conventional fluorescence microscopy (confocal or TIRF). However,

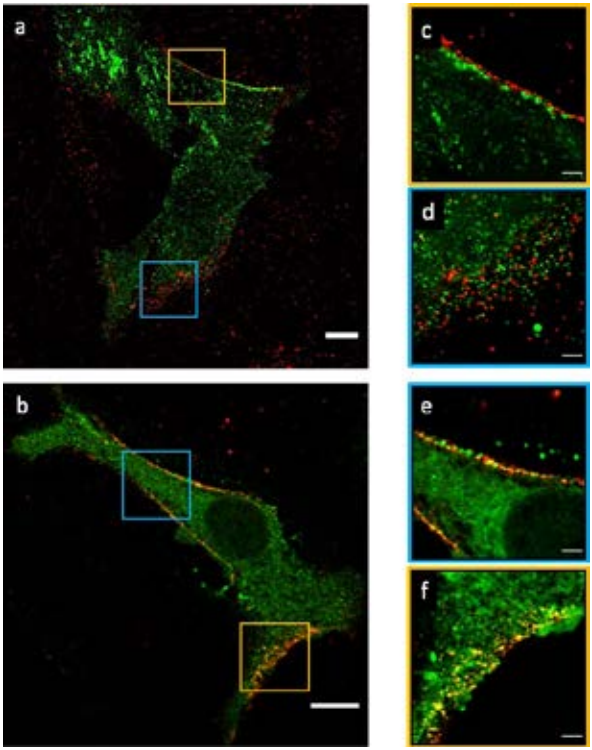

Fig. 1
During the early entry phase virions on the membrane colocalize with clathrin but not with Caveolin-1. (a) Confocal images of B.1.177 at 3 hpi (in red) with Caveolin-1 (in green); Green: Caveolin-1, red: S protein, scale bar: 10 µm. (b) Same as in (a) but Caveolin-1 is replaced by clathrin. (c-f) ISM images of regions in (a) or (b) enclosed in cyan and orange squares. Scale bar: 10 µm (a,b), 2 µm (c-f).

viruses have a size around 100 nm, i.e., well below the optical resolution of these microscopes (200-300 nm). Optical super-resolution methods that break the light-diffraction barrier may reach the 20-150 nm spatial scale. STimulated Emission Depletion (STED) and Single Molecule Localization Microscopy (SMLM) have been recently applied to image single viruses at <100 nm in the cellular context. In this context, we deployed for the first time a multi-scale fluorescence microscopy toolbox to investigate entry and replication checkpoints of SARS-CoV-2 [1] with two general goals: 1) demonstrate that imaging SARS-CoV-2 at single virus level does help answering biological questions, and 2) highlight the ability of super-resolution techniques to afford morphology details of virus structure and molecular interactions with the cell. Our multi-scale toolbox was organized according to the resolution capability of each technique: confocal and TIRF microscopy were applied to visualize interactions at cell level; super-resolution microscopy techniques were applied to reveal single-virus morphology and interactions with cell substructures. By our approach we shed light on the different endocytic uptake kinetics of alpha variant (B.1.1.7) compared to B.1.177, an older D614G lineage with large diffusion in Europe in late 2020, as well as on the role of clathrin and caveolin in mediating the endocytic uptake of the virus in the late pathway occurring in Vero E6 cells. Beside their own relevance, we believe that our results are representative of a new and fertile approach for the study of SARS-CoV-2 (and other viruses) interactions with cells.

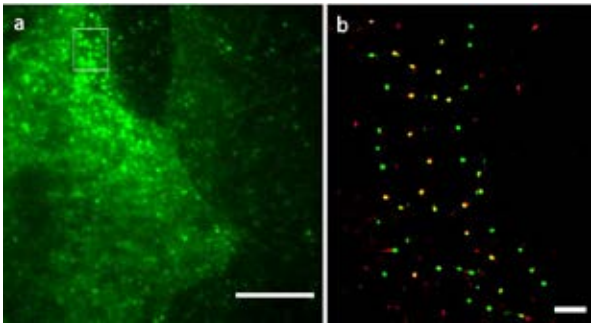

Fig. 2
Virions are embedded into clathrin-coated pits. (a) TIRF image of Vero E6 cell after 3 h post-incubation at 4C (B.1.177 infection). (b) Two-color map of dSTORM-TIRF localization density of clathrin (green) and S (red): colocalized particles appear yellow; pixel size: 10 nm, average localization precision (±SD): 32 ± 10 nm (both channels). Green: clathrin, red: S protein. Scale bar: 10 μm (a), 1 μm (b).

Contact person
Barbara Storti (barbara.storti@nano.cnr.it)

Reference
[1] A spatial multi-scale fluorescence microscopy toolbox discloses entry checkpoints of SARS-CoV-2 variants in Vero E6 cells. B. Storti, P. Quaranta, C. Di Primio, N. Clementi, N. Mancini, E. Criscuolo, P. G. Spezia, V. Carnicelli, G. Lottini, E. Paolini, G. Freer, M. Lai, M. Costa, F. Beltram, A. Diaspro, M. Pistello, R. Zucchi, P. Bianchini, G. Signore, and R. Bizzarri. Comput. Struct. Biotechnol. J. 19, 6140 (2021).

Chitosan Micro-Grooved Membranes with Increased Asymmetry for the Improvement of the Schwann Cell Response in Nerve Regeneration

There are still no efficient therapeutic treatments for peripheral nerve injuries. Here, artificial scaffolds can offer new opportunities for nerve regeneration applications, and chitosan is emerging as a promising biomaterial. We set up an effective method for the production of micro-structured chitosan films by solvent casting, with high fidelity in the micro-pattern reproducibility. We developed chitosan directional micro-grooved patterns with different levels of symmetricity, and tested them *in vitro* with Schwann cells, the glial cells driving the regeneration. The better performing pattern was the most asymmetrical one, which induced a faster and more persistent cell-oriented migration.

In this work we developed and tested in vitro chitosan-based micro-structured substrates, aiming to introduce new strategies to improve scaffolds for peripheral nerve regeneration. Chitosan membranes were fabricated and micro-patterned with directional topographies having different levels of axial symmetry, by solvent casting (Fig. 1a): gratings pattern (GR), with two symmetry axes; zigzag pattern with isosceles triangles (ISO) and one symmetry axis; zigzag pattern with scalene triangles (SCA) and no symmetry axis (Fig. 1b). The films presented precise and stable directional and asymmetric patterns, with dimensionality of 4 µm ridges, 6 µm grooves, and depth of 1.6 µm. This soft lithography technique with a two-molds-step allows developing conveniently micro-grooved chitosan films at room temperature and avoids silicon mold deterioration over time, thanks to the intermediate PDMS mold. The chitosan films were then tested in vitro with the RT4-D6P2T-GFP glial Schwann cells (SCs) to investigate cell proliferation, single-cell and collective migration, and actin cytoskeleton organisation. SCs grew optimally on our chitosan membranes, they were guided by the underlying directional signal but also behaved according to the patterns' asymmetry (Fig. 2). All the films were effective in inducing cell alignment to the

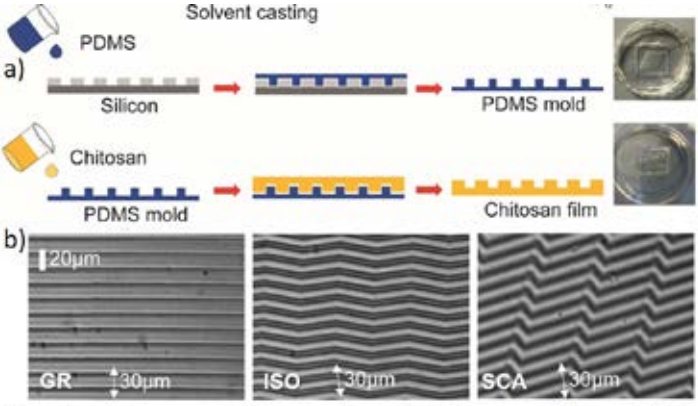

Fig. 1
a) Micro-patterned chitosan membrane fabrication process with two molds by solvent casting, with images of a PDMS mold and a chitosan micropatterned membrane. b) Optical microscope images of the chitosan patterns GR, ISO and SCA, after 24h in liquid.

pattern (Fig. 2a), and directing cell migration along the pattern. The most asymmetric pattern, SCA, polarised and aligned less strictly SCs, leaving a higher degree of freedom to cell orientation. Importantly, SCA promoted a farther displacement of SCs (Fig. 2b), a faster collective migration (Fig. 2c), and an increased persistence on one direction of migration, by inducing the establishment of asymmetric cell fronts with different actin fibers organisation (Fig. 2d). Overall, SCA chitosan membranes result in a promising topography for improving SCs migration performance. These results show how specific topographical features can be exploited for tissue engineering applications, and for new scaffolds with better performances in peripheral nerve regeneration.

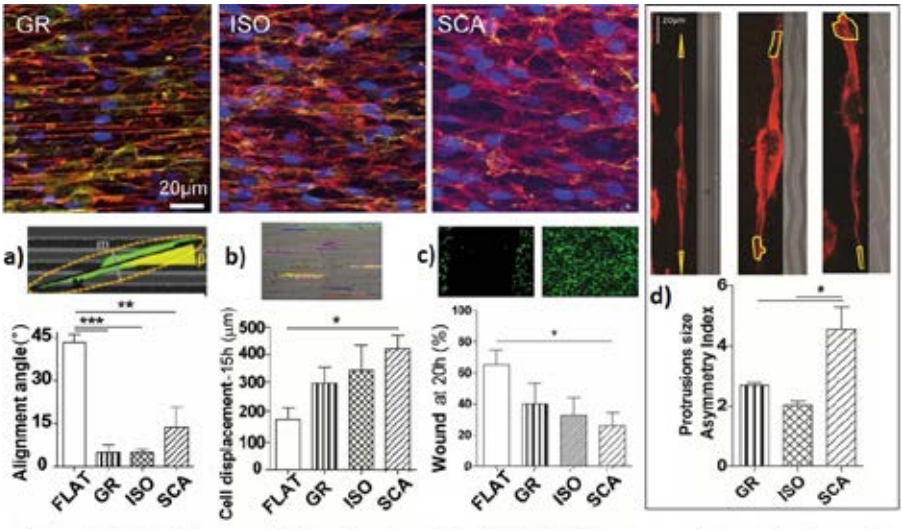

Fig. 2
Virions are embedded into clathrin-coated pits. (a) TIRF image of Vero E6 cell after 3 h post-incuConfocal images of SCs cultured on GR, ISO, SCA chitosan membranes showing actin fibers (red), N-Cadherin (yellow), nucleus (blue). a) Single-cell alignment: it is the angle between the cell major axis and the main axes of the pattern. b) Single-cell migration: cell final displacement from the t=0 position, on different substrates. c) Collective migration: the % of wound area at t=20h was reported in respect to the initial wound area. d) Cell asymmetry on SCA pattern: confocal images of SCs cultured on GR, ISO, SCA stained for actin fibers. Cell protrusion (drawn in yellow) size asymmetry index: the ratio of protrusions' area (the ratio between the area of the bigger cell's protrusion over the minor one), as parameter of cell-ends asymmetry. */*** P<0.05/0.001 One-way Anova; data= mean ± SEM, n ≥ 3.

Contact persons
Ilaria Tonazzini (ilaria.tonazzini@nano.cnr.it), Marco Cecchini (marco.cecchini@nano.cnr.it)

Reference
[1] Chitosan Micro-Grooved Membranes with Increased Asymmetry for the Improvement of the Schwann Cell Response in Nerve Regeneration. L. Scaccini, R. Mezzena, A. De Masi, M. Gagliardi, G. Gambarotta, M. Cecchini, and I. Tonazzini. Int. J. Mol. Sci. 22, 7901 (2021).

Computational insights into SARS-CoV-2 main protease for the development of novel inhibitors

In order to fight COVID-19, a tremendous effort is being put into developing both vaccines and antiviral drugs against SARS-CoV-2. A good target for antiviral therapeutics is SARS-CoV-2 main protease (Mpro). We investigated the structural stability of Mpro as a function of protonation assignments, and also showed that the most stable protonation states vary in a ligand-dependent manner. With a quantum/classical approach we studied the catalytic proton transfer reaction that also relevantly contributes to the rate-determining step for the formation of covalent complexes with inhibitors. The present results provide indications to be used in high-throughput screening procedures for the design of novel inhibitors.

The main protease of SARS-CoV-2 (Mpro) is an attractive target for drug design given i) its critical role in the virus replication cycle, ii) its similarity to main proteases from other coronaviruses, suggesting that broad-spectrum antiviral drugs might be obtained by targeting this enzyme, iii) its unique substrate specificity, with a recognition sequence unknown to host cell proteases. For computational drug design strategies to be effective, the details of the structure and dynamics of the active site and its neighborhood are required. It is also crucial to achieve a deep understanding of the catalytic reaction that is activated by a proton transfer (PT) at the active site (Fig. 1A). We performed molecular dynamics simulations of Mpro in its apo state and complexed to two inhibitors: the peptidomimetic N3 and an α-ketoamide [1]. We investigated how the structure and dynamics of Mpro are affected by the protonation states of a number of crucial residues in the substrate binding site. We found that the conformational stability of the binding site, bound inhibitors, and the hydrogen

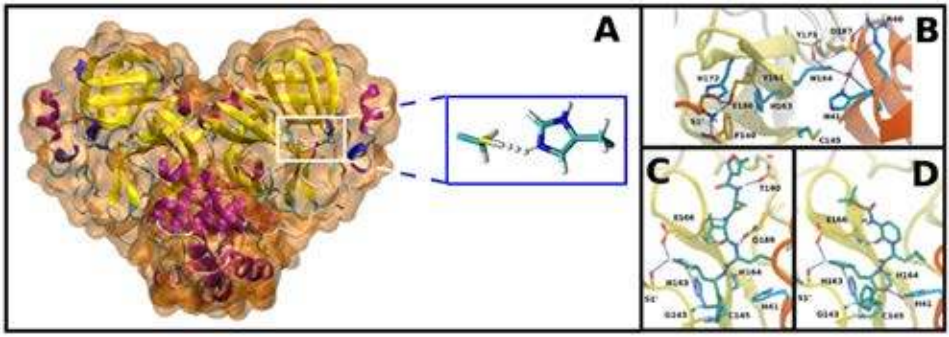

Fig. 1
(A) Crystal structure of SARS-CoV-2 Mpro. The inset highlights the PT reaction in the Cys-His catalytic dyad. Hydrogen bonding interactions in the catalytic site for the apo (B), N3-bound (C), and ketoamide-bound (D) structures. In B and D, the catalytic His41 hydrogens are rendered in magenta, highlighting the alternate protonation for the N3 and ketoamide-bound non-covalent complex.

bond networks are highly sensitive to protonation assignments (Fig. 1B) and that the two inhibitors studied display distinct protonation-state-dependent stabilities (Fig. 1C-D).
Then we used a multiscale approach [Zanetti-Polzi 2018] to investigate the thermodynamics of the PT reaction that activates the catalytic reaction and that is also required for the covalent binding of inhibitors. We studied the PT in the apo enzyme and in complex with the same two inhibitors, focusing on the identification of the enzyme regions that can be targeted to inhibit its catalytic activity [2]. We showed that the free energy cost to reach the charge-separated state of the active-site dyad is lower with the inhibitors, with N3 inducing the most significant reduction. We also showed that a few key sites (including specific water molecules) significantly enhance or reduce the thermodynamic feasibility of the PT reaction, with selective desolvation of the active site playing a crucial role (Fig. 2).

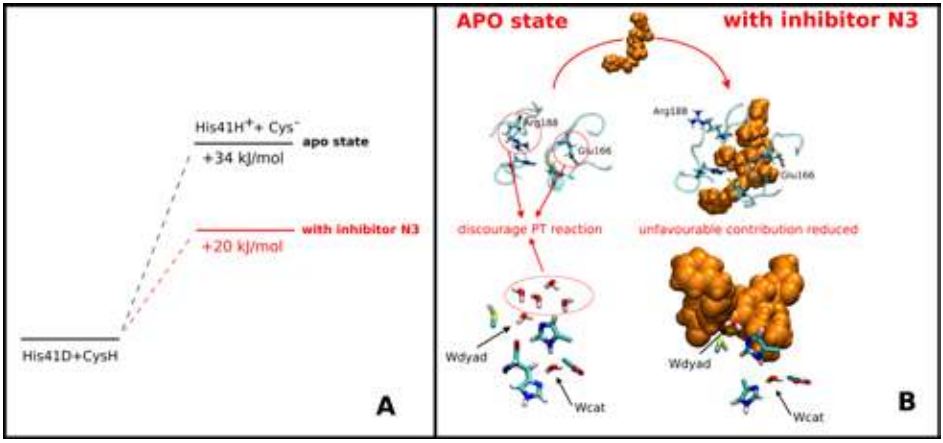

Fig. 2
(A) Representation of the free energy change upon PT in the apo state and in the presence of inhibitors N3 and 13b. (B) Representation of the mechanism that determines a lower PT free energy in the presence of the N3 inhibitor. In the upper panels, the positions of the side chains of two crucial residues are highlighted in the apo and N3-bound systems. In the bottom panels, the positions of the water molecules closer to the catalytic dyad are highlighted in the apo and N3-bound systems.

Contact person
Laura Zanetti-Polzi (laura.zanettipolzi@nano.cnr.it)

References
[1] Inhibitor binding influences the protonation states of histidines in SARS-CoV-2 main protease. A. Pavlova, D. L. Lynch, I. Daidone, L. Zanetti-Polzi, M. D. Smith, C. Chipot, D. W. Kneller, A. Kovalevsky, L. Coates, A. A. Golosov, C. J. Dickson, C. Velez-Vega, J. S. Duca, J. V. Vermaas, Y. T. Pang, A. Acharya, J. M. Parks, J. C. Smith, and J. C. Gumbart. Chem. Sci. 12, 1513 (2021).
[2] Tuning Proton Transfer Thermodynamics in SARS-CoV-2 Main Protease: Implications for Catalysis and Inhibitor Design. L. Zanetti-Polzi, M. D. Smith, C. Chipot, J. C. Gumbart, D. L. Lynch, A. Pavlova, J. C. Smith, and I. Daidone. J. Phys. Chem. Lett. 12, 4195 (2021).

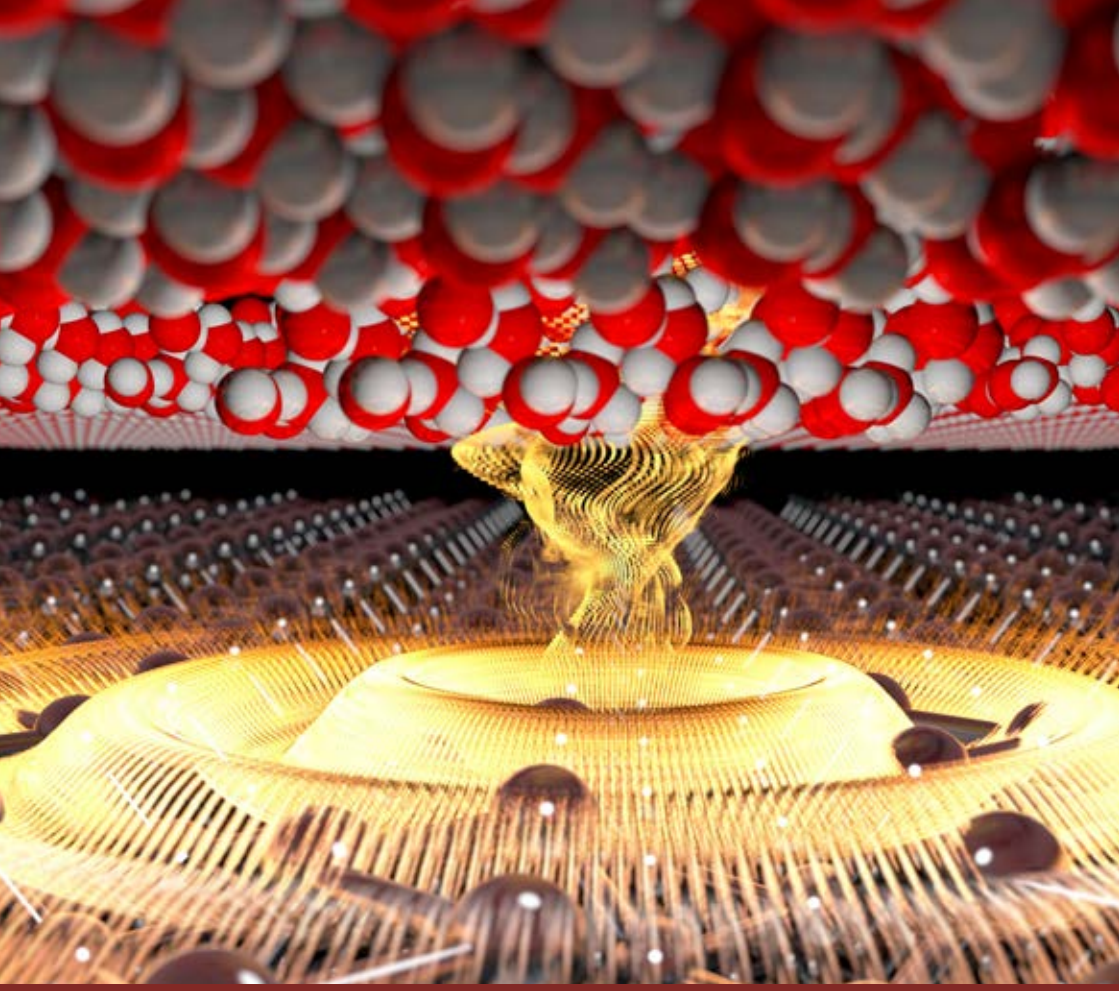

Highlights
-
Physics and technology of light at the nanoscale

Introduction to Physics and technology of light at the nanoscale

The thematic field ***physics and technology of light at the nanoscale*** is devoted to the investigation of nanoscale photonic systems and to the understanding of the phenomena occurring when light is emitted, scattered, transported, and confined by nanostructured materials. These research activities are leading to innovative experimental approaches for the study of the optical properties of nanomaterials and for nanoscale imaging, as well as to various advanced nanophotonic devices for the generation, modulation and detection of light in spectral ranges spanning from ultraviolet to millimeter waves.

Understanding the **properties of light interacting with patterned surfaces** is crucial for many applications such as the switching of light by light, the control of light polarization and of the intensity spatial profiles. In this context, an experimental study performed on thin metal patches on a dielectric slab highlights the dependence of the spectra of the light transmitted through complementary metal patterns on the thickness of the substrate. In particular, the Babinet complementarity principle, that relates the fields scattered by geometrically complementary patterns, is demonstrated to be applicable for ultrathin dielectric slabs.

Disordered **networks of nanofibers** have also intriguing light diffusion properties especially if made of materials with properties tailorable by light. The optically-programmable light scattering properties of textured non-wovens are exploited for the realization of non-colorimetric time-temperature indicators which display a warning sign following the exposure to pre-defined time-temperature profile. Lasers based on disordered fiber networks and materials are also realized with emission in the UV and visible range and interesting spatial coherence properties, which make them ideal light sources for speckle-free imaging.

The design of **novel optical resonators** is also critically important for controlling the emission properties of laser devices. In the field of **optomechanics**, the coupling of a mechanical resonator with a photonic crystal structure is investigated, demonstrating a full opto-electro-mechanical platform for microwave to near-infrared unidirectional wavelength conversion. Moreover, a resonator based on a surface grating with the Octonacci design is exploited for realizing surface-emitting terahertz (THz) quantum cascade lasers, which feature high slope efficiency and low divergence. For THz radiation also the detection, switching and modulation of light is highly relevant. **THz photodetectors** with sub-nanosecond response time are realized by using single layer graphene, whereas THz receivers are demonstrated with both homogeneous and heterostructured nanowires. Single layer graphene turns out to be exploitable also for **THz modulators**, with high modulation depth and electrical bandwidth, while the realization of a polaritonic saturable absorber coupled to a quantum cascade laser paves the way for passively mode-locked sources.

Another vibrant field concerns the **imaging with nanoscale spatial resolution** of the optical properties of nanostructured materials. An elegant novel approach for mapping the absorption properties of materials with sub-wavelength spatial resolution has been recently proposed based on the cathodoluminescence and scanning electron beam microscopy. By exploiting the cathodoluminescence generated by a substrate as a broadband light source, a quantitative analysis of the absorption properties of various monolayer materials is reported. Advanced nanoimaging methodologies, based on a combination of THz quantum cascade lasers and scattering near-field optical microscopy (s-SNOM), allows the photo-response properties of individual InAs nanowires to be investigated with high spatial resolution (35 nm), whereas the physical properties of layered topological insulators are investigated by hyperspectral time domain THz spectroscopy nano-imaging and s-SNOM.

Nanofibers networks for light amplification and intelligent time-temperature indicators

In this work we realized ZnO nanowires-in-nanofiber hybrids, which exhibit a combination of polarized stimulated emission, transport of light with low propagation losses, and structural flexibility. Moreover, the potentiality of electrospun nanofibers for non-colorimetric time-temperature indicators is also demonstrated by realizing nano-textured non-wovens with optically-programmed properties. The cross-linking degree of the non-wovens is exploited to achieve a desired time-temperature response by visual contrast.

Nanofibers networks are emerging as a novel platform for managing light properties at subwavelength scales. Such networks can be designed with variable topological complexity and degree of structural flexibility, making them conformable to non-planar surfaces.
We have fabricated hybrid networks of poly(methyl methacrylate) (PMMA) nanofibers incorporating UV-emitting ZnO nanowires (NWs) with internal NWs alignment (Fig. 1a) [1]. Time-resolved pump-probe spectroscopy shows stimulated emission at 380-400 nm (Fig. 1b), resulting in line narrowing (down to 4 nm) of the emission spectrum at an excitation threshold of 650 $\mu J\ cm^{-2}$, as typical of amplified spontaneous emission (ASE). ASE is linearly polarized along the longitudinal axis of the fibers and has very low divergence (5 mrad). The fiber networks can be wrapped around curved surfaces, such as a capillary glass tube (Fig. 1c). The UV light emitted by the hybrid fibers networks can be in turn used to excite the fluorescence of a solution of chromophores in the tube, whereas the light emitted by the chromophores is guided along the same tube at distances of centimeters and it is visible as a bright spot in the container of the solution.
Non-colorimetric labels made of nanofiber networks are also realized [2]. To this aim, non-wovens made of SU-8 photosensitive resin are realized as disordered fiber networks with optically-programmable light scattering properties. In particular, the SU-8 nanofibers are exposed first to a dose of UV light, which allows the degree of cross-linking of the resin to be controlled (1st photo-programming step), whereas a second exposure to a UV light pattern (2nd photo-programming step) activates a warning sign (Fig. 1d). Depending on the achieved degree of cross-linking at the first step, the light scattering properties of the networks are made responsive to pre-defined time-temperature profiles. Such property allows the pattern activated during the second step to be visually disclosed only upon exposure of the fiber networks to the pre-defined time-temperature profile (Fig. 1e-h). The realized photo-programmable networks are exploited for the realization of smart time-temperature indicators for the supply chain of perishable food and drugs (Fig. 1i).

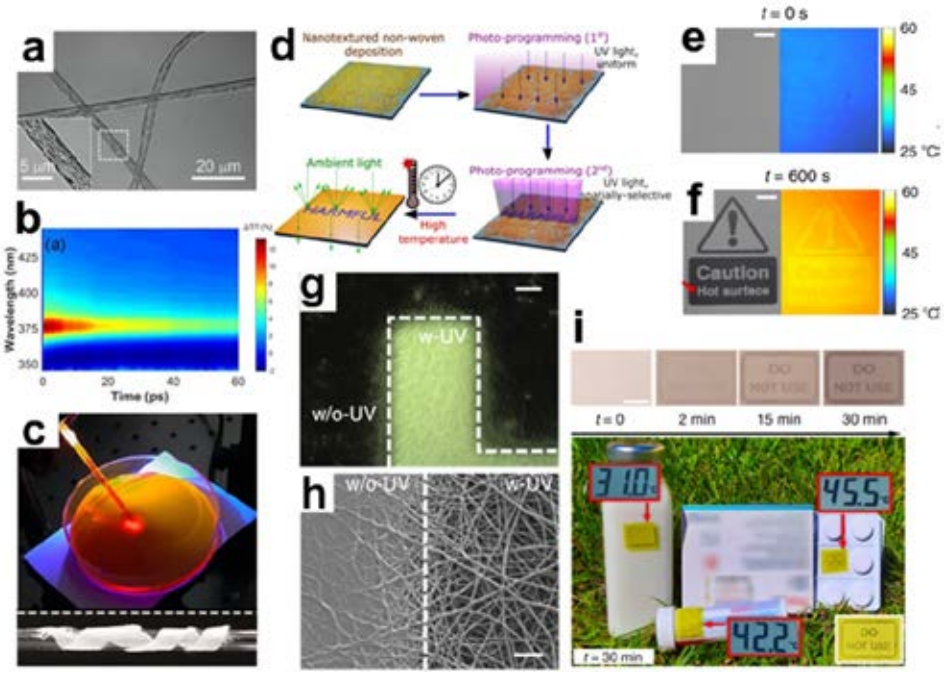

Fig. 1
a) Scanning electron microscope micrographs of ZnO PMMA fibers. b) Spectral and temporal (pump–probe time delay) dependence of ΔT/T. c) Fiber mat coupled with a curved surface (bottom image). The emitted UV light from NW-in-fibers excites a red dye solution in the tube. Reproduced from ref. [1] under the terms of CC-BY-NC-ND license. © 2020 American Chemical Society. d) Schematic working principle of the non-colorimetric indicator. SU-8 non-woven network deposition is followed by photo-programming (blue vertical rays) at calibrated optical dose (first step) and pattern activation (second step). A warning sign will appear when the faced time–temperature profile overcomes the targeted programmed values by diffuse reflectance contrast (green rays). e-f) Optical and thermal images of the SU-8 fiber networks at different times during heating at 55 °C. g-h) Close-up of the letter "H" in the sign "Hot" (red arrow in f) and corresponding SEM images showing the interface between the UV exposed and unexposed areas during the second step of photo-programming. i) Sunlight-induced warming on typical supplies (milk, drugs) after 30 min exposure. Inset: photographs of the indicator while working at 35 °C with 30 min response timescale. Reproduced from ref. [2] under CC-BY 4.0 license, © The Author(s) 2020, published by Springer Nature.

Contact person
Andrea Camposeo (andrea.camposeo@nano.cnr.it)

References
[1] Conformable nanowire-in-nanofiber hybrids for low-threshold optical gain in the ultraviolet. A. Portone, R. Borrego-Varillas, L. Ganzer, R. Di Corato, A. Qualtieri, L. Persano, A. Camposeo, G. Cerullo, and D. Pisignano. ACS Nano 14, 8093 (2020).
[2] Intelligent non-colorimetric indicators for the perishable supply chain by non-wovens with photo-programmed thermal response. L. Romano, A. Portone, M.-B. Coltelli, F. Patti, R. Saija, M. A. Iatì, G. Gallone, A. Lazzeri, S. Danti, O. M. Maragò, A. Camposeo, D. Pisignano, and L. Persano. Nat. Commun. 11, 5991 (2020).

Development of cathodoluminescence-based hyper-spectral optical absorption technique with nanoscale resolution

Scanning confocal spectroscopic techniques have provided important insights on the optical properties of layered materials. However, this class of techniques is limited to a spatial resolution of a few hundred nanometers at least. In order to overcome the diffraction limit, the near-field regime is required. This is particularly true for light absorption spectroscopic mapping. The novel approach employed for overcoming the diffraction limit is based on the electron beam excited light emissions of substrate, where layered materials are grown or transferred on. With this novel approach it is possible to obtain both the local absorption spectrum and the map of the fraction of absorbed light.

The quantitative nanoscale absorption mapping (QNAM) technique is based on the following approach (Fig. 1): the electron beam excites light emission of the substrate (cathodoluminescence, CL), then the substrate cathodoluminescence is absorbed by the top layered material. Therefore, it is possible to evaluate quantitatively the absorption of such material at the nanoscale.

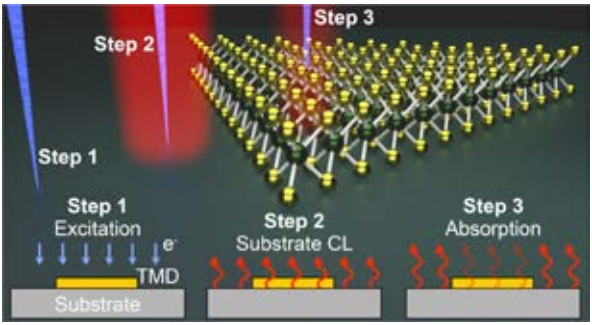

Fig. 1
Sketch of the working principle of the technique. Step 1: a focused electron beam rasters the sample surface. Step 2: the electron beam excites the CL of both the substrates and the flake; due to the limited interaction volume, the emission from the flake is too weak, and it is not detected. Step 3: the flake absorbs part of the substrate CL emission, which results in the QNAM contrast between bare and ML covered regions of the substrate.

Considering different substrates, such as silicon dioxide or sapphire, it is possible to probe different optical ranges, from deep ultraviolet up to infrared. The computational simulation of the electron-beam interaction with the sample allows evaluating the spatial resolution of this technique (from 80 nm up to 150 nm depending on the electron beam parameters, as accelerating voltage and beam current). The experimental activity has been carried out on monolayer (ML) molybdenum disulphide (MoS_2) and molybdenum diselenide ($MoSe_2$), strategic materials belonging to the class of the semiconducting transition metal dichalcogenides (TMD), and related van der Waals (vdW) hetero-structures (Fig. 2). The main result was that the heterostructure has a 19.2% absorption at 323 nm, that is three times the absorption of the single monolayer (7.3%) due to interlayer interactions among the materials composing the heterostructure [1].

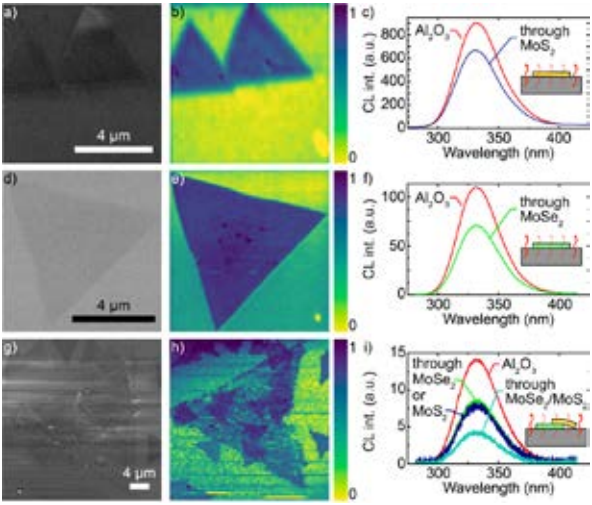

Fig. 2
a) Secondary electron image at 5 kV of MoS_2 ML on sapphire substrate. b) QNAM map of MoS_2 ML. c) CL spectra from the bare substrate and from the MoS_2 ML area. d) Secondary electron image at 5 kV of $MoSe_2$ flake on Al_2O_3. e) QNAM map of the $MoSe_2$. f) CL spectra from the bare substrate and from the $MoSe_2$ ML area ML. g) Secondary electron image at 5 kV of a van der Waals heterostructure composed of $MoSe_2$ ML (larger) and several MoS_2 MLs (smaller) on sapphire. h) QNAM map of the vdW heterostructures. i) CL spectra of bare substrate, MoS_2 ML, $MoSe_2$ ML, and MoS_2–$MoSe_2$ vdW heterostructures.

In addition, recent investigation [Nanoscale 14, 1179 (2022)] has demonstrated the possible application of the QNAM technique to three dimensional MoS_2 pyramidal microstructures in the visible range (Fig. 3), revealing the peculiar absorption properties of the pyramid edges and vertexes. In this last work, two novel aspects of this technique have been shown: the analysis at cryogenic temperature, allowing to evaluate the temperature shift of the MoS_2 excitonic absorption and the comparison between the absorption and the emission spectra, which allows the evaluation of the Stokes shift of excitons in MoS_2.

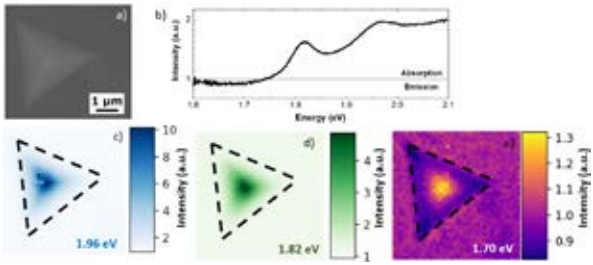

Fig. 3
a) Scanning electron micrograph of the MoS_2 pyramid.
b) Absorption-emission spectrumobtained by renormalizations of CL spectra, integrated over the whole pyramid. c) Absorption map of the B exciton (1.96 eV). d) Absorption map of the A exciton. e) CL absorption-emission map of the defect related state (1.70 eV).

Contact person
Filippo Fabbri (filippo.fabbri@nano.cnr.it)

Reference
[1] Quantitative Nanoscale Absorption Mapping: a novel technique to probe optical absorption of two-dimensional materials. M. Negri, L. Francaviglia, D. Dumcenco, M. Bosi, D. Kaplan, V. Swaminathan, G. Salviati, A. Kis, F. Fabbri, and A. Fontcuberta i Morral. Nano Letters 20, 567-576 (2020).

Organic complex lasers with electrically controlled emission intensity and transient function

Complex lasers are gaining interest for applications in speckle-free imaging, white lasing and high-resolution spectroscopy. We have realized various complex lasers, including a white-emitting laser based on a polymer matrix with dispersed droplets of liquid crystals, doped with multiple organic chromophores. The phase separation of the hydrophilic matrix and the hydrophobic liquid crystals leads to the formation of a complex optically active layer, featuring lasing emission tunable from blue to red with intensity controllable by electric fields. Moreover, by combining dry–wet transient materials, a light-emitting heterostructure is realized, which is exploited as a transient illumination source for speckle-free, full-field imaging, and as transient optical labels that incorporate QR-codes with stably encoded information.

Complex lasers are gaining interest for their spatial and temporal coherence properties and broadband emission. Here, we demonstrate organic devices providing emission tunability and low spatial coherence, which can be exploited in spectroscopy, imaging, lighting, and optical sensing.

The first system is composed of phase-separated hydrophobic droplets of liquid crystals (LCs) dispersed into a hydrophilic polyvinyl alcohol (PVA) matrix [1]. Optical gain is provided by a blue-emitting dye incorporated in the polymer matrix and green- or red-emitting dyes dispersed in LC droplets (Fig. 1a-e). The wavelength of emission can be varied by adjusting the relative content of the dyes (Fig. 1f), while lasing emission is achieved by a balanced mixture of the three emitting components (Fig. 1g). Emission features reveal a random lasing mechanism due to diffusive scattering and amplification of the emitted photons in the multiphase active material, with optical excitation thresholds of 7–12 mJ cm^{-2}. Reversible control over the emission intensity of the white lasers is demonstrated by applying a DC electric field, which induces a re-arrangement of the LC droplets, and a consequent change of the excitation and scattering processes.

A different approach for realizing complex lasers is based on an organic heterostructure [2], composed by a polymer bilayer with red light-emission properties that is deposited onto a nonpolar cyclic hydrocarbon sublimating substrate (Fig. 1h). Such heterostructures can be engineered by properly selecting the thickness ratio of the optically active layers, to keep them mechanically stable upon substrate sublimation. These systems have physically transient properties, namely the capability to evolve into a univocally designed function, which may include a self-elimination phase. Amplified spontaneous emission (ASE) is observed upon optical pumping, with an excitation threshold of 0.2 mJ cm^{-2}, along with an operational lifetime of 1.5×10^3 excitation pulses under continuous operation in ambient condition (Fig. 1i-j). Application of the device for speckle-free full-field imaging is demonstrated (Fig. 1k).

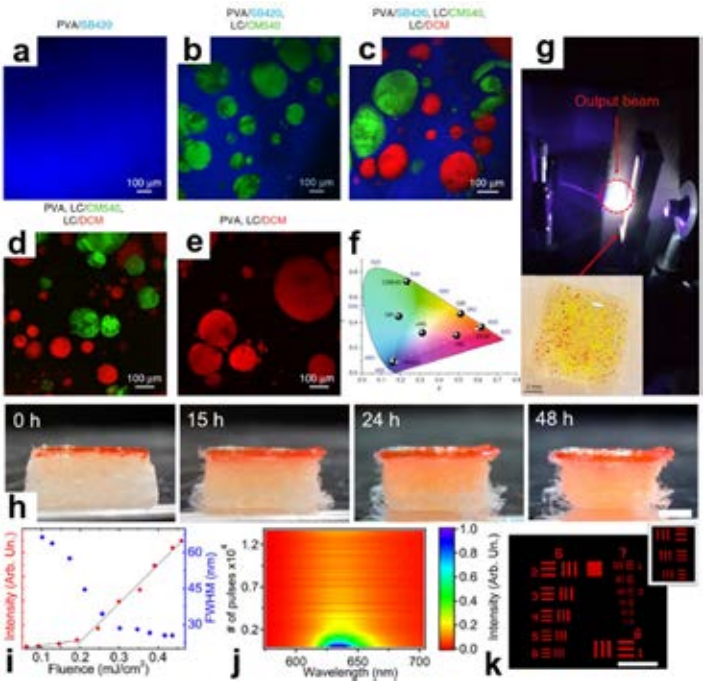

Fig. 1
a-e) Confocal fluorescence images of samples containing different dyes combinations [blue-emitting 2,2'-([1,1'-biphenyl]-4.4'-diyldi-2,1-ethenediyl)bis-benzenesulfonic acid disodium salt (SB420); green-emitting (3-(2- benzothiazolyl)-7-(diethylamino)-2H-1-benzopyran-2-one) (CM540) and red emitting 4-(dicyanomethylene)-2-methyl-6-(4-dimethylaminostyryl)-4H-pyran (DCM)]. f) CIE chromaticity coordinates for devices with various dyes combinations. g) Photograph of the white light lasing emission of the multiphase device under optical excitation. Inset: image of the PVA matrix embedding blue dye and LC/green/red droplets. Reproduced from ref. [1] under the CC BY 4.0 License © The Author(s) 2020, published by Springer Nature. h) Images of the ASE transient device while the substrate sublimates at 55 °C. Scale bar: 2 mm. i) Light-in light-out intensity (red circles) plot and dependence of the full width at half maximum (FWHM, blue circles) on the excitation fluence. j) Dependence of the emission spectrum on the pulses number at 0.3 mJ cm^{-2}. k) Images of a US Air Force resolution test chart illuminated by the ASE from the transient device. Scale bar: 115 µm. Top right inset: close-up view of the test patterns in column 7. Reproduced from ref. [2] under the CC BY 4.0 License, © The Author(s) 2020. Published by Wiley-VCH GmbH.

Contact person
Francesca Matino (francesca.matino@nano.cnr.it)

References
[1] Electrically controlled white laser emission through liquid crystal/polymer multiphases. A. Adamow, A. Szukalski, L. Sznitko, L. Persano, D. Pisignano, A. Camposeo, and J. Mysliwiec. Light Sci. Appl. 9, 19 (2020).
[2] Naturally degradable photonic devices with transient function by heterostructured waxy-sublimating and water-soluble materials. A. Camposeo, F. D'Elia, A. Portone, F. Matino, M. Archimi, S. Conti, G. Fiori, D. Pisignano, and L. Persano. Adv. Sci. 7, 2001594 (2020).

SAW-based, GHz mechanical excitation of Si micromechanical resonators and photonic crystals

We investigate the coupling of mechanical waves into micromechanical resonators and photonic crystals operating in the near-infrared range for optomechanical applications. The hybrid SOI/AlN platform allows for launching Surface Acoustic Wave (SAW) into the silicon layer. By analysing the displacement field via Laser Doppler Vibrometry, we evaluate the coupling efficiency of SAWs with focusing interdigitated transducers. By decorating the mechanical resonator with a photonic crystal pattern, we achieve a full opto-electro-mechanical platform for microwave to near-infrared unidirectional wavelength conversion, with potential impact on quantum communications and technologies.

Hybrid systems are one of the most versatile and interesting platforms for the manipulation of classical and quantum information on chips. Along with electrons, photons and spins, recently phonons have emerged in this research line: their pervasive nature and long lifetimes make them the quintessential tool for creating interconnects on chip. They can be used for addressing photonic and electronic networks, which can be coupled with no need for spatial overlap, with great advantages for fabrication and device performances.

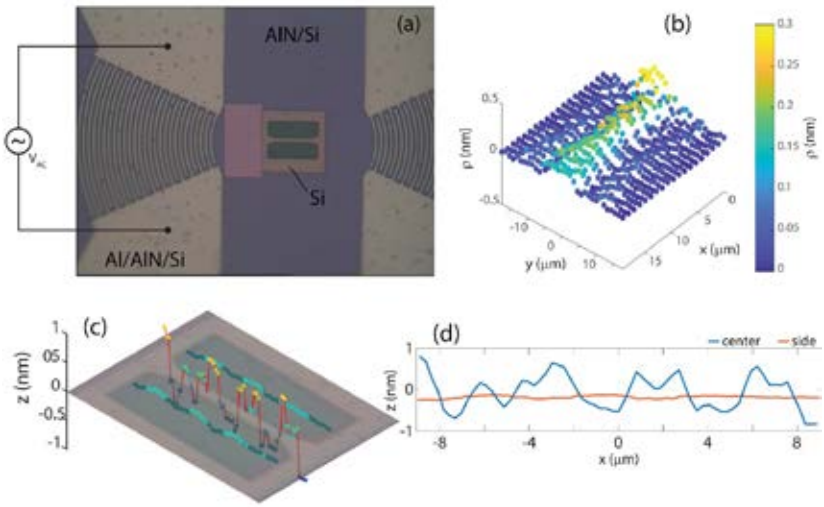

Fig. 1
a) Microscope image of the device. b) SAW focusing effect. c-d) Out of plane displacement on the nanostring and on the bottom of the etched well.

In this research line we have developed a platform for coherent control of high frequency phonons (1 – 2 GHz) through deposition of piezoelectric materials such as AlN on a Si device layer. This approach combines the electrical generation of Surface Acoustic Waves (SAWs) with the ultimate characteristics of Si as a photonic and electronic material. The basic device for testing our technology is shown in Fig. 1a. The device characteristics were inspected by using light interferometry to assess the out-of-plane mechanical displacement at room-temperature. Semi-circular, focusing Interdigitated Transducers (IDTs) were fabricated of Al on top of an AlN layer deposited on a Si wafer; full details can be found elsewhere [1]. The IDT periodicity was such to excite 1 GHz SAWs which were focused at the edge on a suspended Si nanostring (see the measured z-displacement amplitude ρ in Fig. 1b, mapped on the read area in 1a). The focused SAW excited mechanical modes on the string resonators with an external efficiency of 500 pm/V, as can be seen in Fig. 1c and 1d, where the interferometric measured z-displacement on top of the string and on the bottom of the etched well are compared. The high efficiency allowed us to operate a full opto-electro-mechanical device where the Si nanostring was decorated with a photonic crystal pattern [ACS Photonics 9, 413 (2022)]. The full device, along with a sketch of the experimental bench, is shown in Fig. 2a. The slightly higher frequency (2 GHz) SAWs generated by the IDTs excite mechanical modes in an optomechanical nanobeam (see SEM inset). Using a twisted fiber loop, the optical modes of the nanobeam can be probed with an infrared laser. Mechanical actuation shifts the mechanical modes, modulating reflected light at a fixed wavelength. Coherent detection of the modulated light versus the RF drive of the IDT allows one to get the number of coherent phonons excited within the nanobeam via SAWs (Fig. 2b). With a minimum of 2.6 injected coherent phonons, our device enables single phonon level operation in a room-temperature environment.

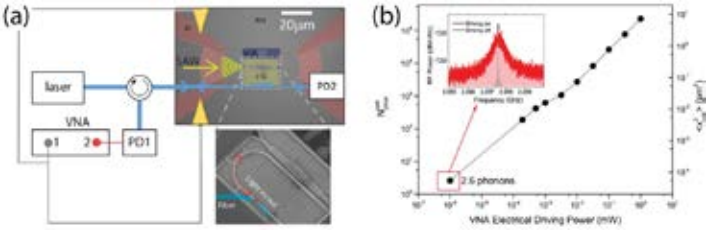

Fig. 2
a) Sketch of the experimental setup including a microscope image of the whole device and a SEM of the photonic crystal. b) Characterization of the number of coherently excited phonons.

Contact persons
Alessandro Pitanti (alessandro.pitanti@nano.cnr.it)
Simone Zanotto (simone.zanotto@nano.cnr.it)

Reference
[1] High-frequency mechanical excitation of a silicon nanostring with piezoelectric aluminum nitride layers. A. Pitanti, T. Makkonen, M. F. Colombano, S. Zanotto, L. Vicarelli, M. Cecchini, A. Griol, D. Navarro-Urrios, C. Sotomayor-Torres, A. Martinez, and J. Ahopelto. Phys. Rev. Appl. 14, 014054 (2020).

Near-field nanoscopy at terahertz frequencies

Near-field optical microscopy techniques have shown an amazing potential in the last few years for investigating optoelectronic properties of nanoscale materials and devices thanks to the unique capability of inspecting charge carrier density, plasmon-polariton, and phonon-polariton modes with unprecedented spatial resolution. Furthermore, near-field microscopy can allow mapping the spatial variation and the bias dependence of local currents induced by light illumination, therefore tracking the photo-carrier transport and the electronic band bending in electronic and photonic nanodevices. Here we combine hyperspectral, photocurrent, and detectorless near field nanoscopy techniques at terahertz frequencies, to investigate quantum materials and nanostructures.

We exploit a combination of hyperspectral time domain THz spectroscopy nano-imaging and detectorless scattering near-field optical microscopy (s-SNOM), at multiple terahertz frequencies, either with single mode lasers or with random lasers, to explore the rich physics of layered topological insulators as Bi_2Se_3 and $Bi_2Te_{2.2}Se_{0.8}$, hyperbolic materials with topologically protected surface states. By mapping the near-field scattering signal from a set of thin flakes of Bi_2Se_3 and $Bi_2Te_{2.2}Se_{0.8}$ of various thicknesses, we shed light on the nature of the collective modes dominating their optical response in the 2-3 THz range. We capture snapshots of the activation of transverse and longitudinal optical phonons and reveal the propagation of sub-diffractional hyperbolic phonon-polariton modes influenced by the Dirac plasmons arising from the topological surface states and of bulk plasmons. The interaction of the probed phonon-polaritons modes with the electrons from the TSS suggests possible ultrafast optical control by above interband photoexcitation to ideally switch on and off the hybridized modes, opening intriguing technological perspectives in plasmonics, ultrafast photonics, spintronics, nanophotonics, and quantum optics.
We also innovatively capture snapshots of the photo-response of individual InAs nanowires via high spatial resolution (35 nm) THz photocurrent nanoscopy. By coupling a THz quantum cascade laser to the s-SNOM and monitoring both electrical and optical readouts, we simultaneously measure transport and scattering properties. The spatially resolved electric response provides unambiguous signatures of photo-thermoelectric and bolometric currents whose interplay is discussed as a function of photon density and material doping, therefore providing a route to engineer the nanowires photo-response as room-temperature THz detectors.

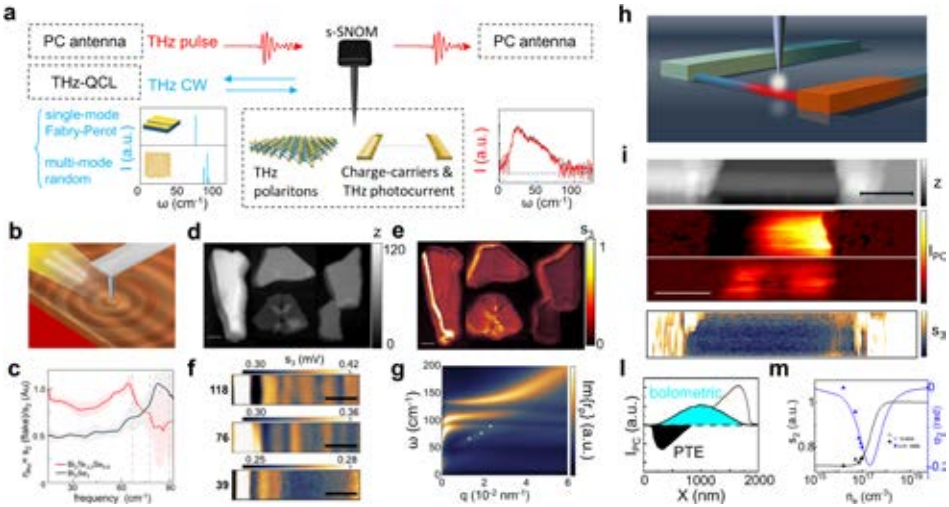

Fig. 1

a) Sketch of the THz multimodal near-field microscope coupled to broadband TDS systems based on two photoconductive antennae or THz-QCL with single mode or multimode emission. b) Illustration of the s-SNOM tip launching THz polaritons in a topological insulator. c) Near-field contrast spectrum measured on Bi_2Se_3 and $Bi_2Te_{2.2}Se_{0.8}$ thin films showing peaks attributed to long-wavelength phonons. d) AFM-topography z in nanometer of thin flakes of Bi_2Se_3. e) Near-field contrast at the third harmonic s_3 in arbitrary units measured at 66cm^{-1} (ca 2THz). f) Interference intensity pattern generated by propagating THz polaritons in Bi_2Se_3. g) Energy dispersion of collective excitations of $Bi_2Te_{2.2}Se_{0.8}$ (colored map) compared with the experimental data (white crosses). h) Schematics of THz photocurrent experiment based on detection of local currents in a InAs nanowire. i) (top to bottom) Topography (z), photocurrent profile in high and low doping conditions (I_{PC}), near-field scattering contrast at the third harmonics s_3. l) Fingerprints of bolometric and PTE photocurrents profiles. m) Scattering contrast and phase as a function of carrier density.

Contact persons

Miriam Serena Vitiello (miriam.vitiello@nano.cnr.it)
Eva A. A. Pogna (eva.pogna@nano.cnr.it)

References

[1] Mapping propagation of collective modes in Bi2Se3 and Bi2Te2.2Se0.8 topological insulators by near-field terahertz nanoscopy. E. A. A. Pogna, L. Viti, A. Politano, M. Brambilla, G. Scamarcio, and M. S. Vitiello. Nat. Commun. 12, 1-11 (2021).

[2] Unveiling the detection dynamics of semiconductor nanowire photodetectors by terahertz near-field nanoscopy. E. A. A. Pogna, M. Asgari, V. Zannier, L. Sorba, L. Viti, and M. S. Vitiello. Light Sci. Appl. 9, 1-12 (2020).

[3] Self-mixing interferometry and near-field nanoscopy in quantum cascade random lasers at terahertz frequencies. K. S. Reichel, E. A. A. Pogna, S. Biasco, L. Viti, A. Di Gaspare, H. E. Beere, D. A. Ritchie, and M. S. Vitiello. Nanophotonics 10, 1495-1503 (2021).

[4] Terahertz near-field nanoscopy based on detectorless laser feedback interferometry under different feedback regimes. E. A. A. Pogna, C. Silvestri, L. L. Columbo, M. Brambilla, G. Scamarcio, and M. S. Vitiello. APL Photonics 6, 061302 (2021).

Highly-efficient semiconductor lasers

Photonic engineering of semiconductor laser cavities has been extensively investigated over the last years as a versatile approach to control the spectral, spatial, and temporal emission of lasers operating in different regions of the electromagnetic spectrum. Here, we conceive and demonstrate quasi-crystal THz quantum cascade laser resonators exploiting a surface grating following the Octonacci design, which are capable of significantly boosting the state-of-the-art performance of surface emitting THz lasers. We also demonstrate intracavity mmWave generation within THz QCLs over the unprecedented range of 25 GHz to 500 GHz.

Quantum cascade lasers (QCLs) represent the most fascinating achievement of quantum engineering, showing how artificial materials can be generated through quantum design, with tailor-made properties. Their inherent quantum nature deeply affects their core physical parameters. QCLs indeed display intrinsic linewidths approaching the quantum limit, show spontaneous phase-locking of their emitted modes via intracavity four-wave-mixing, ultrafast gain relaxation and high nonlinearities meaning and can naturally operate as random quantum emitters or photonic crystal lasers, also in frontier frequency domains, as the far-infrared, yet unexplored in quantum science. We have recently engineered the first one-dimensional quasi-crystal distributed feedback laser by lithographically patterning a series of air slits of different widths, following the Octonacci sequence, on the top metal layer of a THz QCL. We tuned the emission from single-mode to multi-mode over a 530 GHz bandwidth, achieving a maximum peak optical power of 240 mW (190 mW) in multimode (single-mode) lasers with record slope efficiencies up to ≈570 mW/A at 78 K and ≈700 mW/A at 20 K, wall-plug efficiencies of $\eta \approx 1\%$ and low divergent emission. Those performances represent the state of art in the field of surface emitting THz frequency lasers.
We also demonstrate intracavity mmWave generation within THz QCLs over the unprecedented range of 25 GHz to 500 GHz. We highlight the importance of modal phases and that the process is a result of a giant second-order nonlinearity combined with a phase matched process between the THz and mmWave emission. Importantly, this work opens up the possibility of compact, low noise mmWave generation using modelocked QCLs. We then discuss their optical properties and potential in all areas of quantum science. The ability to generate mm waves from highly-stable lasers promises to be a key method to achieve the spectrally-pure, low-phase noise, and microwave signals that are targeted for local oscillators in high frequency communications.

Fig. 1

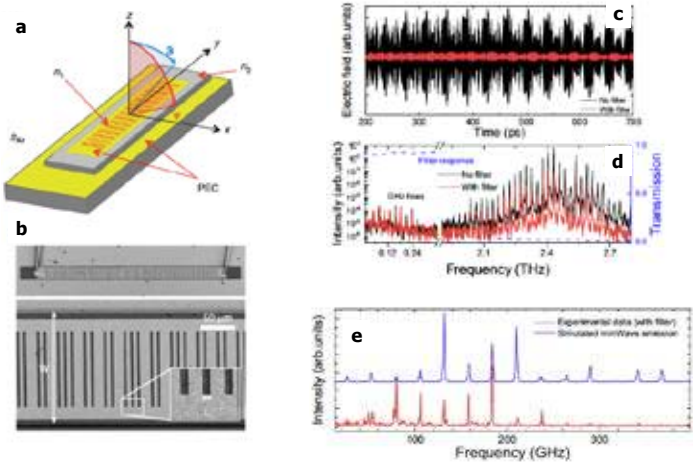

a) Device schematics. A fully three-dimensional device simulation is performed through a finite element method (FEM) to extract the resonating modes via Maxwell's equations. The laser active material is modelled with a refractive index n_1 = 3.6, while the external border of the ridge covered by a 7-nm-thick Cr layer is described by the effective complex value n_2 = 4.43+ i0.31, accounting for the optical losses induced by chromium. The laser is surrounded by a volume of air with n_{Air} = 1. b) SEM image of a prototypical device with a ridge width of W = 160 μm and length of 2.9 mm, featuring the Octonacci grating on the laser top surface with a slit length of L = 3.5 μm. c) Time-resolved electric field from injection seeded QCL with (red) and without (black) the low-pass filter. Electric field oscillations of the laser emission are not visible owing to the long temporal scan. d) Intensity spectrum of emission from QCL1 with (red) and without (black) the low pass filter. The QCL is driven in pulsed mode (10% duty cycle) and at a fixed heat sink temperature of 10 K. The THz emission is centred around 2.4 THz. The filter (blue curve) removes an order of magnitude of the intensity of the THz emission but does not change the mmWave emission. This unambiguously illustrates the mmWave emission is from the QCL and not an artefact of the detection technique. e) Enhanced view of mmWave spectral emission from QCL1 (red) showing comparison with simulated results (blue) from the QCL THz spectrum. mmWave emission is observed up to 367 GHz.

Contact persons
Miriam Serena Vitiello (miriam.vitiello@nano.cnr.it)
Alessandra Di Gaspare (alessandra.digaspare@nano.cnr.it)

References

[1] Highly efficient surface-emitting semiconductor lasers exploiting quasi-crystalline distributed feedback photonic patterns. S. Biasco, A. Ciavatti, L. Li, A. G. Davies, E. H. Linfield, H. Beere, D. Ritchie, and M. S. Vitiello. Light Sci. Appl. 9, 1-11 (2020).
[2] Millimeter wave photonics with terahertz semiconductor lasers. V. Pistore, H. Nong, P.-B. Vigneron, K. Garrasi, S. Houver, L. Li, A. G. Davies, E. H. Linfield, J. Tignon, J. Mangeney, R. Colombelli, M. S. Vitiello, and S. S. Dhillon. Nat. Commun. 12, 1-7 (2021).
[3] Polarization analysis of random THz lasers. A. Di Gaspare and M. S. Vitiello. APL Photonics 6, 070805 (2021).
[4] Terahertz quantum cascade lasers as enabling quantum technology. M. S. Vitiello and P. De Natale. Adv. Quantum Technol. 5, 2100082 (2021).
[5] Physics and technology of Terahertz quantum cascade lasers. M. S. Vitiello and A. Tredicucci. Adv. Phys.: X 6, 1893809 (2021).
[6] One-dimensional, surface emitting, disordered Terahertz lasers. L. Salemi, K. Garrasi, S. Biasco, T. Crisci, H. E. Beere, D. A. Ritchie, and M. S. Vitiello. APL Photonics 5, 036102 (2020).

Nanoscale terahertz photonic devices for light detection and manipulation

Key photonic applications in the far-infrared, i.e., 1–10 THz frequencies, require detection, modulation, and switching of optical signals with high signal-to-noise ratios and high speeds. Low-dimensional systems and designer architectures represent a promising platform for manipulating, controlling, and capturing photons in this frequency range, thanks to their inherent versatility and tunable-by-design optoelectronic properties. Here we review our latest results on the development of THz nano-detectors based on low-dimensional systems (graphene-based field effect transistors and quantum dots embedded in axially heterostructured semiconductor nanowires) and on the realisation of on-chip photonic components for the active or passive modulation of the emission of THz quantum cascade laser (QCL) frequency combs (FCs).

Terahertz Detectors. The conversion of light into an electrical signal, with large quantum efficiencies and controllable physical dynamics, is a major need in THz photonics and optoelectronics. The rich physics of semiconductor nanostructures such as two-dimensional materials, one-dimensional semiconductor nanowires (NWs) and zero-dimensional nanostructures, offers a unique platform to investigate light-matter interaction in the far-infrared, and to achieve state-of-the-art detection performances by taking advantage of different physical mechanisms.

We develop graphene-based room temperature photo-thermoelectric (PTE) detectors realised by exploiting both high-quality, hBN encapsulated, single layer graphene (SLG), and large-area CVD-grown SLG. By combining the ultrafast carrier thermodynamics of electrons in SLG with on-chip radio-frequency architectures, we achieve noise equivalent power (NEP) <120 $pWHz^{-½}$ and sub-ns response times.

Furthermore, we devise NW-based THz receivers, featuring homogeneous InAs NWs or axially heterostructured InAs/$InAs_{0.3}P_{0.7}$ quantum-dot receivers, where the detection is driven by thermally activated dynamics. These nanostructured devices reached NEP <8 $pWHz^{-½}$ at low temperature, opening intriguing perspectives for quantum key distributions, quantum communications, and quantum cryptography at terahertz frequencies.

Terahertz Modulators and saturable absorbers. Future high-speed communications and quantum applications in the THz domain will rely on the development of fast, reconfigurable components for amplitude, frequency, and phase stabilisation. In this context, the realisation and on-chip integration of active modulators or passive non-linear elements with compact and high power THz QCLs can open important perspectives in emerging fields such as tunable transformation-optics, adaptive and quantum optics, and metrological tools for spectroscopy.

We design and engineer a SLG-based modulator with a tunable-by-design optical bandwidth, achieving large modulation depths (90%) and ≥20 kHz electrical bandwidth, operating in the 1.9–2.7 THz range. We then integrate our device on-chip, with miniaturised THz QCL sources to alter the oscillating phase of the reflected intracavity field.

Furthermore, by ultrastrong coupling intersubband transitions of semiconductor

quantum wells to the photonic mode of a metallic cavity in order to custom-tailor the population and polarisation dynamics of intersubband cavity polaritons in the saturation regime, we obtained absorption bleaching at a peak intensity one order of magnitude lower than previous all-integrated approaches and well achievable by QCLs. Our results highlight a path towards passively mode-locked sources based on polaritonic saturable absorbers in a monolithic single-chip design.

Fig. 1

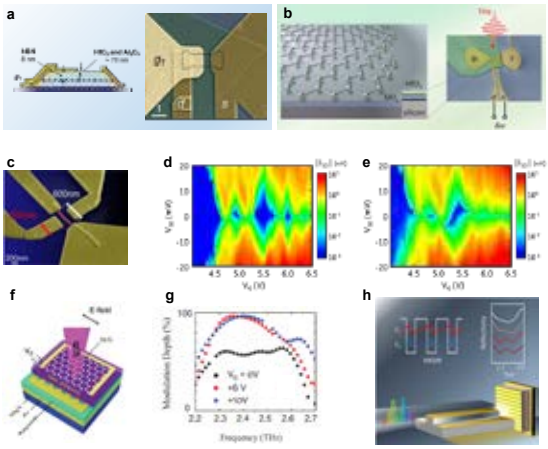

a) Schematics of a hBN-encapsulated graphene-based THz detector and false colour SEM image of an antenna-coupled device. b) Schematics of a THz detector based on large-area CVD graphene. c) False colour SEM of an antenna coupled THz detector based on a quantum dot (QD) axially grown along a nanowire. d) Coulomb blockade pattern measured in the dark and e) when a 0.3 THz radiation (power 1 mW) is focused on the QD-based detector. The distortion of the charge-stability diagram is a direct consequence of the THz-induced Seebeck effect in the QD device. f) Sketch of a graphene-on-polymide THz intensity modulator and g) its spectral response. h) Principle of operation of a polaritonic saturable absorber coupled to a QCL.

Contact persons
Miriam Serena Vitiello (miriam.vitiello@nano.cnr.it)
Leonardo Viti (leonardo.viti@nano.cnr.it)

References

[1] Tailored nano-electronics and photonics with two-dimensional materials at terahertz frequencies. L. Viti and M. S. Vitiello. J. Appl. Phys. 130, 170903 (2021).
[2] Chip-scalable, room-temperature, zero-bias, graphene-based Terahertz detectors with nanosecond response time. M. Asgari, E. Riccardi, O. Balci, D. De Fazio, S. M. Shinde, J. Zhang, S. Mignuzzi, F. H. L. Koppens, A. C. Ferrari, L. Viti, and M. S. Vitiello. ACS Nano 15, 17966 (2021).
[3] Thermoelectric graphene photodetectors with sub-nanosecond response times at terahertz frequencies. L. Viti, A. R. Cadore, X. Yang, A. Vorobiev, J. E. Muench, K. Watanabe, T. Taniguchi, J. Stake, A. C. Ferrari, and M. S. Vitiello. Nanophotonics 10, 89-98 (2020).
[4] HBN-encapsulated, graphene-based, room-temperature Terahertz receivers, with high speed and low noise. L. Viti, D. G. Purdie, A. Lombardo, A. C. Ferrari, and M. S. Vitiello. Nano Lett. 20, 3169 (2020).
[5] Semiconductor nanowire field-effect transistors as sensitive detectors in the far-infrared. M. Asgari, L. Viti, V. Zannier, L. Sorba, and M. S. Vitiello. Nanomaterials 11, 3378 (2021).
[6] Quantum-dot single-electron transistors as thermoelectric quantum detectors at terahertz frequencies. M. Asgari, D. Coquillat, G. Menichetti, V. Zannier, N. Dyakonova, W. Knap, L. Sorba, L. Viti, and M. S. Vitiello. Nano Lett. 21, 8587 (2021).
[7] Ultrafast terahertz saturable absorbers using tailored intersubband polaritons. J. Raab, F. P. Mezzapesa, L. Viti, N. Dessmann, L. K. Diebel, L. Li, A. Giles Davies, E. H. Linfield, C. Lange, R. Huber, and M. S Vitiello. Nat. Commun. 11, 1-8 (2020).
[8] Tunable, grating-gated, graphene-on-polyimide Terahertz modulators. A. Di Gaspare, E. A. A. Pogna, L. Salemi, O. Balci, A. R. Cadore, S. M. Shinde, L. Li, C. di Franco, A. Giles Davies, E. H. Linfield, A. C. Ferrari, G. Scamarcio, and M. S. Vitiello. Adv. Funct. Mater. 31, 2008039 (2021).

Dealing with asymmetries in photonics: Babinet screens and light-light switches

The operational capabilities of photonic devices are strongly affected by underlying symmetries, either of geometrical kind or of more abstract, invariant-related ones. Such (a)symmetries, ultimately dictated by the physics laws that underlie the photonic component, can be either detrimental or useful for the component operation. Here we show that Babinet complementarity is violated in substrate-supported geometrically complementary screens, and that Hermitian symmetry violation (i.e., in photonics, gain-loss symmetry) is essential for the performance of fully optical switches.

The Babinet complementarity principle relates the fields scattered by geometrically complementary screens, as for instance a hole in a continuous metal and an isolated metal disk of the same radius. Such symmetry is useful as it essentially doubles the yield of a photonic design process. For arrays of subwavelength objects, the relation is simply that $T = 1 - T_C$, where T (T_C) is the transmittance of the original (complementary) screen. We name this relation spectral complementarity. A rigorous treatment shows that Babinet principle is indeed a theorem, but only under stringent hypotheses: the screen must be infinitesimally thin and perfectly conducting. More practical settings require that the screen (usually a metal) is lying on a dielectric slab, as shown in Fig. 1a. We have shown that a dielectric slab of subwavelength thickness ($< \lambda/5$) has a strong impact on the Babinet-predicted spectral complementarity. Our results are summarised in Fig. 1b-d, where spectra corresponding to structures with geometrical complementarity are reported. We have also shown [1] that the spectral complementarity, i.e., the original Babinet principle/theorem, is recovered if the thickness of the supporting dielectric slab tends to zero – or better, if its thickness is less than a tiny fraction (~ 1/100) of the radiation wavelength.
On the other hand, we show in Fig. 2 a situation where symmetry breaking is useful for a specific application in photonic data processing. Here, a strong beam is switched on and off by means of a phase-controlled, weak beam. In order to render this process efficient, i.e., if no intensity loss of the signal beam is required, the photonic structure must show a special kind of internal asymmetry: it must embed a space- and time-asymmetric profile of the permittivity (where time-asymmetry in the frequency domain refers to the complex conjugation of the permittivity). In [Opt. Express 26, 3618 (2018)] we have determined the exact conditions that the permittivity profile must fulfil in order to implement the perfect asymmetric switch of Fig. 2a, that, in brief, is a gain-loss bilayer with specific thicknesses and complex refractive indices ($n + ik$) (Fig. 2b). Noticeably, the energy flux displays a peculiar sign-inversion inside the structure (Fig. 2c).

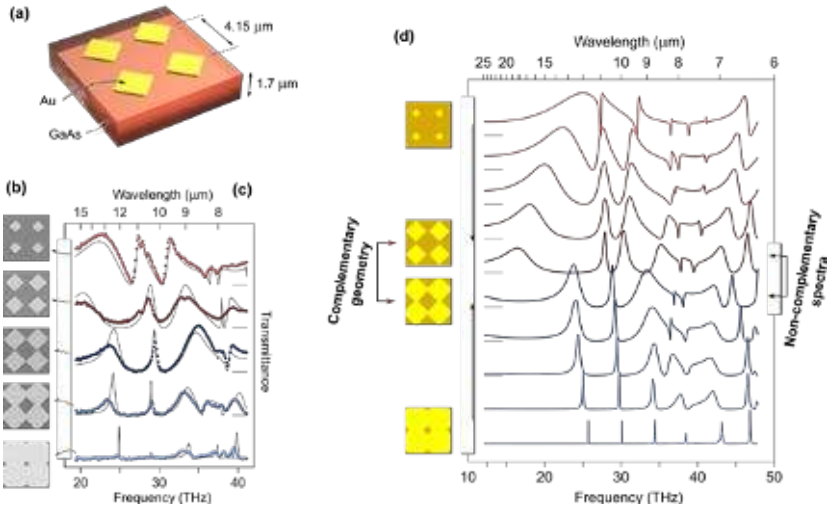

Fig. 1
a) Schematic of a dielectric-slab-supported metal screen. The gold patches can be either disconnected or connected, as illustrated in the SEM images reproduced in b) where the dashed arrow indicates a pair of quasi-complementary screens. The colored traces reported in c) are measured infrared transmittance spectra; the black traces are calculated spectra. By accurate numerical calculations it is possible to compare the spectra of structures with exact geometrical complementarity, like the pair indicated in d). Noticeably, the corresponding spectra are not complementary.

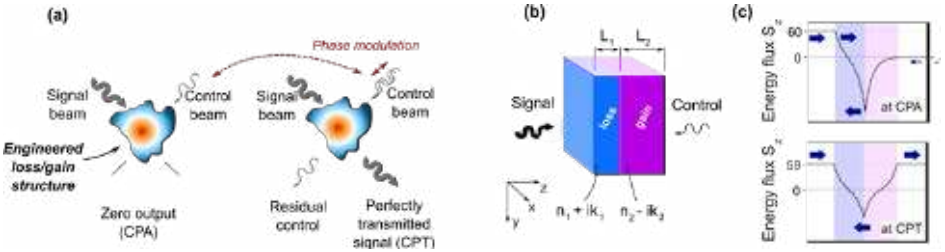

Fig. 2
a) Schematic of a photonic device with two inputs (signal and control) of different intensity. By exploiting the coherent perfect absorption and transparency (CPA and CPT) concepts, it is possible to fully switch the strong signal by acting on the weak control beam's phase. In order to implement this operation, a specially engineered scatterer with loss and gain must be employed, like that in b). Under these circumstances, the energy flux inside the structure is that indicated in c).

Contact person
Simone Zanotto (simone.zanotto@nano.cnr.it)

Reference
[1] Departure from the Babinet principle in metasurfaces supported by subwavelength dielectric slabs. G. Biasiol and S. Zanotto. Opt. Lett. 45, 3402 (2020).

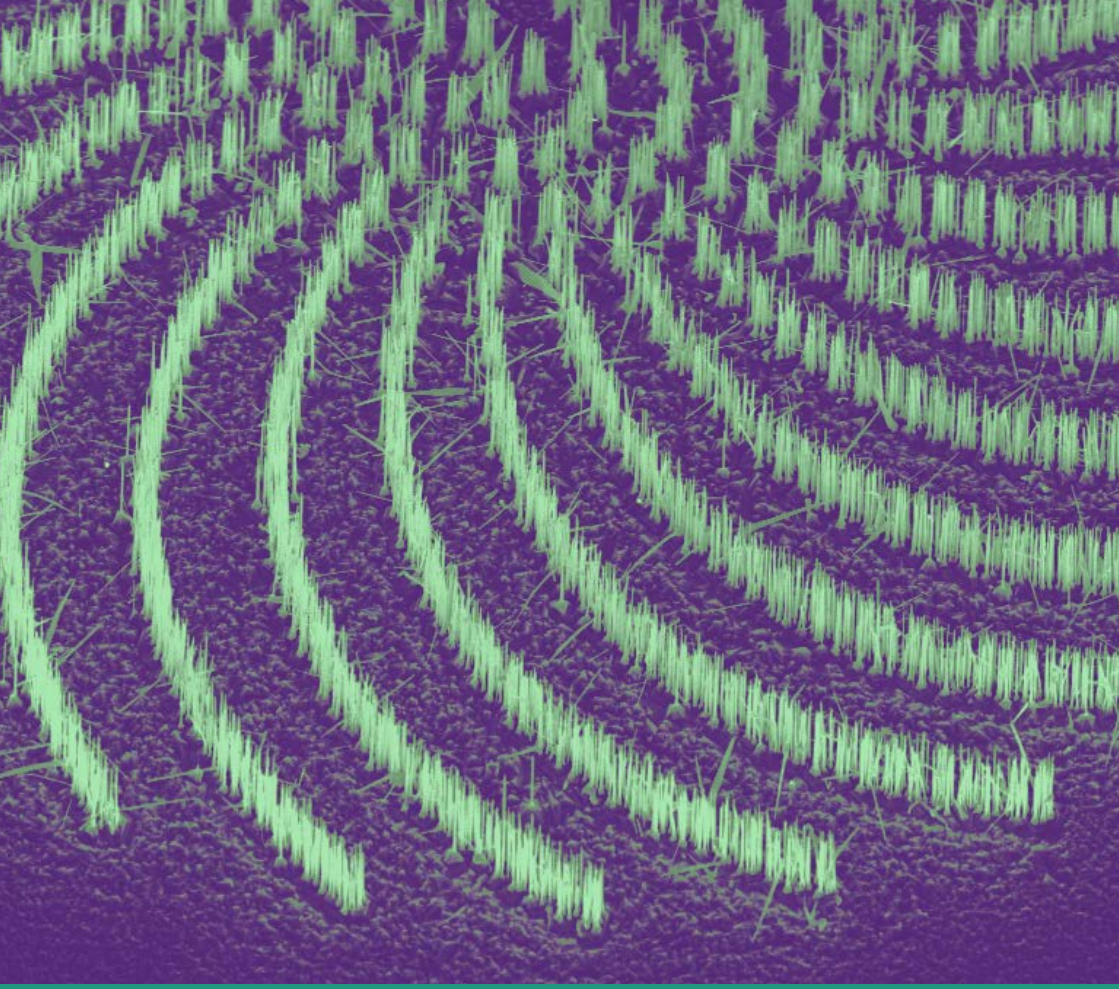

Highlights
-
Solid-state quantum technology

Introduction to Solid-state quantum technology

Research in solid-state quantum technology focuses on the **fabrication, investigation, and implementation of novel nanodevices** both for fundamental science and for new applications. Joint experimental and theoretical activity is devoted to the study of quantum systems and phenomena, and aims at developing novel concepts and ideas, with potential impact on future applications. Advanced fabrication techniques and low-temperature magneto-transport measurements are developed along **four main research lines**, as described below.

Charge and thermal transport at the nanoscale. Precise control of charge and heat transport at the nanoscale is at the heart of new technological advances, including quantum technologies. Manipulation and harvesting of heat fluxes can be achieved in coherent superconducting nanodevices, where photonic heat transport and rectification in circuits and qubits are currently investigated. Thermal transport in Josephson junctions (conventional and topological) and electrical transport in twisted bilayer graphene are also among our interests. More pieces of evidence on systems based on Josephson junctions are collected on the unexpected gating effects occurring in fully metallic superconducting systems, while the first theoretical scenarios are proposed. Finally, high-quality nanostructures, such as defect-free InSb quantum dots embedded into InAs nanowires, are demonstrated.

Superconducting spintronics. One of the promising perspectives of spintronics is the possibility to control spin and charge at the nanometer scale, both at classical and quantum (qubit) level. Recent advances allowed combining ferromagnetic insulators with superconductors, enabling the possible implementation of a superconducting logic memory based on spin valves and the control of the superconducting phase to implement a quantum phase battery.

Moreover, molecular spin ensembles can be engineered and coherently manipulated with suitable protocols through planar superconducting microwave resonators, even considering advanced two-tone transmission spectroscopy.

Topologically protected quantum technology. The study of topological states of matter, systems that are intrinsically robust to external perturbations, is of great interest for new quantum computing architectures. Hybrid superconductor/semiconductor devices with strong-spin-orbit coupling represent an ideal platform to inspect this new physics. Systems based on Josephson junctions, topological insulators and InSb nanoflags are modelled and investigated by means of low-temperature quantum transport experiments.

Quantum information and quantum thermodynamics. With the advent of the quantum technology revolution, mastering of quantum states has become a reality. Our efforts span from devising new methods to master information processing and energy transfers in quantum systems, devices and transmission lines, to modelling low temperature solid-state quantum devices. The latter comprise superconducting circuits, NV centres in diamond, Silicon-channel p-MOSFET (hole-spin qubit), quantum thermal machines based on thermoelectric effects and miniaturized THz frequency comb synthesizers. Finally, quantum computers are used to advance quantum thermodynamic theory.

Quantum thermoelectricity and caloritronics in superconducting nanodevices

Superconducting circuits are the core platform for quantum technologies. The continuous increase of the qubits surface density sets stringent requirements in controlling heat losses. So, we mainly investigated the possibility to manipulate, harvest and use heat phenomena in coherent superconducting nanodevices. We considered photonics heat transport and rectification in circuits and qubits. We demonstrated an unexpected bipolar thermoelectricity as induced by spontaneous breaking of the particle-hole symmetry and discussed applications of phase-coherent thermodynamics and thermal transport in conventional and topological Josephson junctions.

Superconducting quantum technology requires extremely low temperatures to operate. This represents a major bottleneck, especially for quantum computing platforms, where the increasing qubit density poses serious difficulties to the cooling and the proper management of heat losses. For quantum processors this is crucial, since heating leads to a fast loss of coherence degrading the qubit fidelity. In this research we have investigated the fundamental problem of heating and non-equilibrium physics of coherent superconducting circuits proposing novel technological solutions for the quantum technology community to manage the heat bottleneck.

In this perspective, we have proposed and investigated photonic heat transport rectifiers in superconducting circuits [1] or qubits [2] which may play an important role in manipulating and monitoring quantum resources. At extremely low temperatures, the photonic heat channels become comparable with other more conventional heat transport processes, such as phononic and electronic channels, so this represents a novel, and mainly unexplored, route toward the heat management and control in coherent circuits.

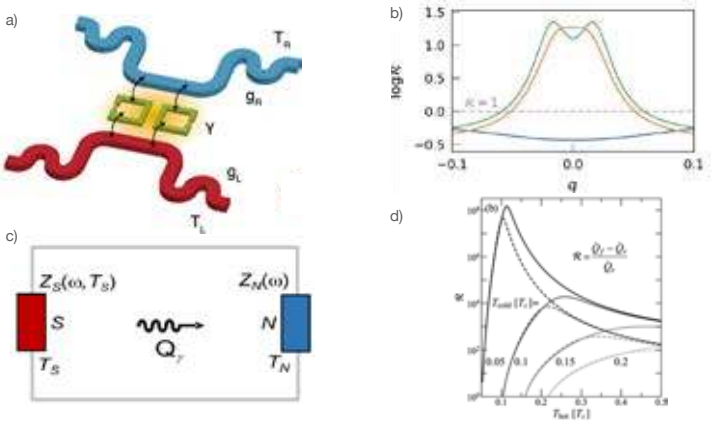

Fig. 1
Photonic heat transport diodes. a) Two-qubit heat diode [1]. b) Photonic heat transfer rectification ratio R of the qubit heat diode as a function of normalized flux. c) Photonic superconducting-normal metal heat diode [2]. d) Photonic heat transfer rectification ratio R as a function of hot temperature.

Another important strategy is heat harvesting, where the unavoidable heat produced in a circuit is used to add novel functionalities to the same circuit. In this perspective, we have discovered that the superconducting tunnel junctions, done with different materials, can host a novel and astounding strong bipolar thermoelectric effect induced by spontaneous breaking of the particle-hole symmetry [3]. So we have proposed a simple phase controlled thermoelectric engine [4] showing that it can be fruitfully patented as a novel current-controlled thermoelectric superconducting memory [5].
Finally, we have investigated the rich coherent thermodynamics [Sci. Rep. 9, 3228 (2019)] and the thermal transport of Josephson junctions, proposing new methods to identify it [6] and test the not-trivial topological phases [7] or even to realize novel cooling cycles with a concrete applicative potential [8].

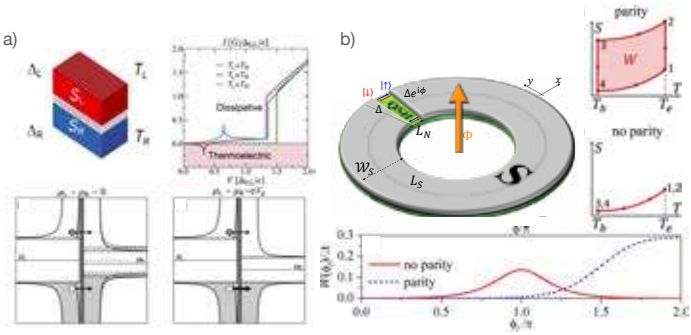

Fig. 2
Thermoelectricity and coherent thermodynamics in superconducting junctions. a) Nonlinear bipolar thermoelectric effect of a SIS' tunnel junction [3,4]. b) Coherent thermodynamics of a topological Josephson junction: work is done only when the nontrivial junction has parity conserved after 2pi evolution [6].

Contact persons
Alessandro Braggio (alessandro.braggio@nano.cnr.it)
Francesco Giazotto (francesco.giazotto@nano.cnr.it)

References

[1] Highly efficient phase-tunable photonic thermal diode. G. Marchegiani, A. Braggio, and F. Giazotto. App. Phys Lett. 118, 022602 (2021).
[2] Photonic Heat Rectification in a System of Coupled Qubits. A. Iorio, E. Strambini, G. Haack, M. Campisi, and F. Giazotto. Phys. Rev. Applied 15, 054050 (2021).
[3] Nonlinear Thermoelectricity with Electron-Hole Symmetric Systems. G. Marchegiani, A. Braggio, and F. Giazotto. Phys. Rev. Lett. 124, 106801 (2020).
[4] Superconducting nonlinear thermoelectric heat engine. G. Marchegiani, A. Braggio, and F. Giazotto. Phys. Rev. B 101, 214509 (2020).
[5] Superconducting bipolar thermo-electric memory and method for writing a superconducting bipolar thermoelectric memory. G. Germanese, G. Marchegiani, F. Paolucci, A. Braggio, and F. Giazotto. Patent application No. 102021000032042 (2021).
[6] Topological Josephson heat engine. B. Scharf, A. Braggio, E. Strambini, F. Giazotto, and E. M. Hankiewicz. Communications Physics 3, 1 (2020).
[7] Signatures of Jackiw-Rebbi resonance in the thermal conductance of topological Josephson junctions with magnetic islands. D. Gresta, G. Blasi, F. Taddei, M. Carrega, A. Braggio, and L. Arrachea. Phys. Rev. B 103, 075439 (2021).
[8] Systems and Methods for Superconducting Quantum Refrigeration. A. N. Jordan, F. Giazotto, and S. K. Manikandan. US Patent App. 16/593, 781 (2021).

Quantum Thermodynamics and Quantum Information

With the advent of the quantum technology revolution, mastering of quantum states has become a reality. Our pioneering results span from devising new methods to master information processing and energy transfers in quantum systems, devices and transmission lines, at the quantum level, to modelling low-temperature solid-state quantum devices such as superconducting circuits and NV centres in diamond. We use quantum computers to advance quantum thermodynamic theory and, in turn, use quantum thermodynamic theory to improve the performance of quantum computers. We study quantum thermal machines and the management of heat fluxes in nanoscale systems using the thermoelectric effect.

Quantum fluctuation theorems are an invaluable tool of investigation of energy exchanges at the quantum level [Rev. Mod. Phys. 83, 771 (2011)]. In [1] we employed them to estimate the degree of entropy produced during the information processing occurring in a real quantum annealing computation. In [2] instead, we used a quantum computer to experimentally verify a number of quantum fluctuation relations that were predicted theoretically [Phys. Rev. E 83, 041114 (2011); J. Phys. A 47, 245001 (2014)], but lacked a verification so far. Furthermore, quantum fluctuation relations relating to open quantum systems were experimentally verified using NV centres in diamond [3].

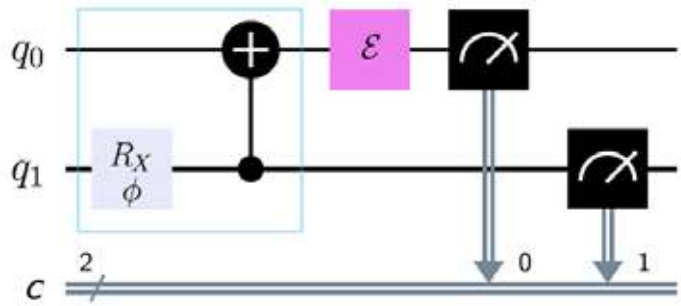

Fig. 1
A quantum algorithm (i.e., a series of instructions for a quantum computer) can be graphically represented as a "quantum score". Like in a music score, "notes" and "chords" (the quantum gates) are sequentially applied to single and multiple keys (the qubits), respectively. The picture shows the basic quantum algorithm used to experimentally validate various quantum fluctuation theorems [2].

A goal in thermodynamics of quantum nanoscale systems is to conceive of and realize thermal machines in the quantum realm. In [4] we have presented a general unified approach for the study of quantum thermal machines operating under periodic adiabatic driving, showing that many physical quantities characterizing the engine performance (e.g., its efficiency) are of geometric nature. In [5] we have investigated the nonlocal thermoelectric effects in systems based on a topological insulator embedded in a Josephson junction, finding a unique signature of the helical nature of the edge states. The performance of a nonlocal heat engine based on the same systems has been thoroughly investigated [6].
Quantum technologies have a chance of being essential also in the management of energy sources. We have studied the transferring of useful energy (work) along a transmission line that allows for partial preservation of quantum coherence [7]. Related to quantum metrology, we have introduced a measure of genuine quantum incompatibility in the estimation task of multiple parameters, that has a geometric character and is backed by a clear operational interpretation [8]. We have also presented upper bounds on the quantum and private capacity of single-mode, phase-insensitive bosonic Gaussian channels based on degradable extensions [9].

Contact persons
Michele Campisi (michele.campisi@nano.cnr.it)
Fabio Taddei (fabio.taddei@nano.cnr.it)

References

[1] Improved bound on entropy production in a quantum annealer. M. Campisi and L. Buffoni. Phys. Rev. E 104, L022102 (2021).
[2] Experimental verification of fluctuation theorems with a quantum computer. A. Solfanelli, A. Santini, and M. Campisi. PRX quantum 2, 030353 (2021).
[3] Experimental test of fluctuation relations for driven open quantum systems with an NV center. S. Hernández-Gómez, N. Staudenmaier, M. Campisi, and N. Fabbri. New J. Phys. 23, 06500 (2021).
[4] Geometric properties of adiabatic quantum thermal machines. B. Bhandari, P. T. Alonso, F. Taddei, F. von Oppen, R. Fazio, and L. Arrachea. Phys. Rev. B 102, 155407 (2020).
[5] Nonlocal thermoelectricity in a superconductor–topological-insulator–superconductor junction in contact with a normal-metal probe: evidence for helical edge states. G. Blasi, F. Taddei, L. Arrachea, M. Carrega, and A. Braggio. Phys. Rev. Lett. 124, 227701 (2020).
[6] Nonlocal thermoelectric engines in hybrid topological Josephson junctions. G. Blasi, F. Taddei, L. Arrachea, M. Carrega, and A. Braggio. Phys. Rev. B 103, 235434 (2021).
[7] Quantum Energy Lines and the optimal output ergotropy problem. S. Tirone, R. Salvia, and V. Giovannetti. Phys. Rev. Lett. 127, 210601 (2021).
[8] Incompatibility in quantum parameter estimation. F. Belliardo and V. Giovannetti. New J. Phys. 23, 063055 (2021).
[9] Estimating quantum and private capacities of gaussian channels via degradable extensions. M. Fanizza, F. Kianvash, and V. Giovannetti. Phys. Rev. Lett. 127, 210501 (2021).

Gate-control of critical supercurrent in mesoscopic metallic transistors

Since 2018, the Superconducting Quantum Electronics group has pioneered the usage of electrostatic gates to modulate down to full suppression the supercurrent flow through a weak link consisting of a constriction in a contiguous superconducting metal or a normal chunk sandwiched between two superconducting contacts [Nat. Nanotech. 13, 802 (2018)]. A comprehensive understanding of the phenomenon is still missing, though theoretical scenarios started to be proposed [1-3]. The experimental fingerprint of ambipolar suppression of critical current has been shown in metallic superconducting films, single Josephson junctions, and superconducting quantum interference devices [4].

The possibility of a local, electrostatic tuning of a dissipationless current in metallic superconductor systems implies applications as magnetometers, heat management systems, radiation detectors, and architectures for quantum and classical computation. Several experiments have tried to unveil the microscopic origin of such gate-induced effect and to characterize it, for instance, in terms of spatial extent and speed of the superconducting/normal switch mechanism.
In 2020-2021, the SQEL group performed two experiments aimed at excluding a possible role of the gate-superconductor *leakage* current in determining the critical current suppression.
The first consists in controlling the supercurrent in a fully suspended superconducting titanium nanobridge [5] shown in Fig. 1a and b. The suspended device architecture min-

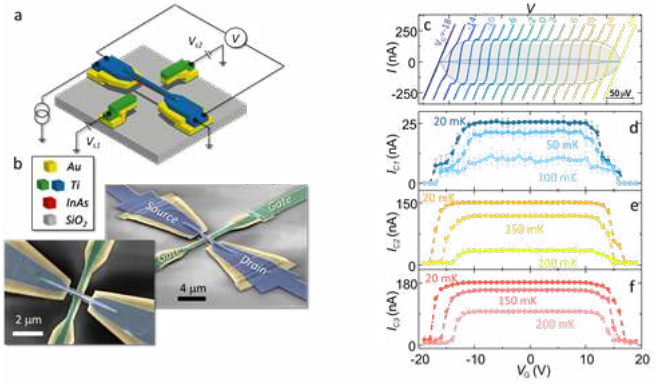

Fig. 1
a) 3D sketch showing a suspended gated Ti nanowire. The wire (blue) is measured in a conventional four-wire configuration. The amplitude of the device supercurrent was controlled by applying a voltage VG to the two side-gate electrodes (green). b) False-colour scanning electron micrographs (top view and 35° tilted, left and right respectively) of a typical device, laid on an intrinsic SiO_2 substrate (grey). The gold pads (yellow) are used to hold the suspended structures while the Ti nanowire is mechanically supported by an InAs nanowire located underneath the Ti wire. The InAs nanowire does not contribute to the conduction. c) Current vs voltage characteristics (back and forth) for different applied gate voltage (V_G) values measured at T = 20 mK. The curves are horizontally offset for clarity. Blue and grey areas, and the dotted grey lines are guides to the eye highlighting the gate-driven evolution of the critical current I_{C1}, I_{C2}, and I_{C3} of three different regions of the nanowire. d) Switching current I_{C1} vs V_G measured at selected bath temperatures T. Similarly to d), e), and f) show the V_G dependence of I_{C2} and I_{C3}, respectively. The error bars represent the standard deviation of $I_{C1;2;3}$ calculated over 25 repetitions.

imizes the electron–phonon interaction between the superconducting nanobridge and the substrate where the gate lies, and hampers the injection of quasiparticles through the substrate. In Fig. 1c we observe the gate influence on the current-voltage characteristics at different gate voltages, resulting in the suppression of wire critical current (see Fig 1d, e, and f).

In a second experiment [6], the gate electrode is not in the vicinity of the niobium constriction, but about 100 μm distant. The electric field is carried to the surface of the metallic weak link by a drop of ionic electrolyte, see Fig. 2a and b. It gets polarized by a gate contact at high temperature (~200K) and then frozen to base temperature (~4K) to retain the polarization of its ions, some randomly placed on the Nb wire surface and thus affecting the behaviour of the bridge. A bipolar suppression of the superconducting critical current of up to 45% is observed in Fig. 1c. The described results point toward an interaction between electrostatic fields and superconductivity which does not rely on heat injection caused by the leakage current.

We acknowledge three European research projects: H2020 FET Open *SuperGate*, H2020 FET Open *Genesis*, and H2021 TRANSITION OPEN *Spectrum*.

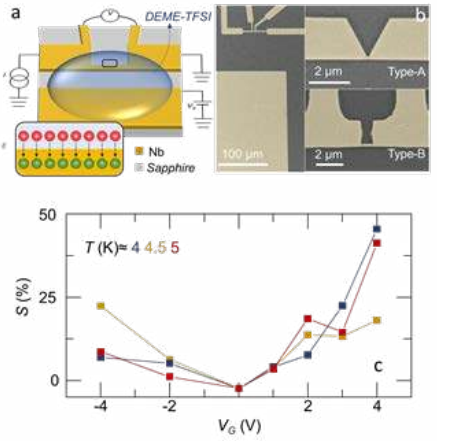

Fig. 2
a) Schematic of a typical ISFET, where the superconducting active region is current-biased and the counter electrode polarizes the electrolyte (DEME-TFSI) droplet through the voltage V_C. The accumulation of ions at the sample surface creates the EDL and generates the electric field (E). b) False-colour SEM picture of typical ISFETs: (top) type-A device realized in the form of a Dayem-bridge-like Josephson junction (the constriction length is ~300 nm, while its width is ~100 nm); (bottom) type-B device consisting of a quasi one-dimensional superconducting nanowire (the wire length is ~1 μm, and its width is ~100 nm). c) Supercurrent suppression parameter S versus V_C for selected values of the temperature T.

Contact persons
Giorgio De Simoni (giorgio.desimoni@nano.cnr.it)
Francesco Giazotto (francesco.giazotto@nano.cnr.it)

References
[1] Sauter-Schwinger Effect in a Bardeen-Cooper-Schrieffer Superconductor. P. Solinas, A. Amoretti, and F. Giazotto. Phys. Rev. Lett. 126, 117001 (2021).
[2] Spectroscopic signatures of gate-controlled superconducting phases. M. T. Mercaldo, F. Giazotto, and M. Cuoco. Phys. Rev. Res. 3, 043042 (2021).
[3] Electrically Tunable Superconductivity Through Surface Orbital Polarization. M. T. Mercaldo, P. Solinas, F. Giazotto, and M. Cuoco. Phys. Rev. App. 14, 034041 (2020).
[4] Gate Control of Superconductivity in Mesoscopic All-Metallic Devices. C. Puglia, G. De Simoni, and F. Giazotto. Materials 14, 1243 (2021).
[5] Gate-Controlled Suspended Titanium Nanobridge Supercurrent Transistor. M. Rocci, G. De Simoni, C. Puglia, D. Degli Esposti, E. Strambini, V. Zannier, L. Sorba, and F. Giazotto. ACS Nano 14, 12621 (2020).
[6] Electrostatic Field-Driven Supercurrent Suppression in Ionic-Gated Metallic Superconducting Nanotransistors. F. Paolucci, F. Crisà, G. De Simoni, L. Bours, C. Puglia, E. Strambini, S. Roddaro, and F. Giazotto. Nano Lett. 21, 10309 (2021).

Coherent Manipulation and Readout of Molecular Spins through Planar Superconducting Microwave Resonators

Molecular spins hold potential for quantum information and quantum technologies when integrated into planar superconducting microwave resonators [Adv. Phys. X 3, 1435305 (2018)]. Along this line, a crucial step is the design and implementation of suitable protocols (i.e., microwave sequences) for initializing, manipulating, and reading out the spins. In this report, we show our recent progress and experimental results on the manipulation of molecular spin ensembles through planar microwave resonators [1] and on advanced two-tone transmission spectroscopy performed in the dispersive regime of the magnetic coupling [2].

We first considered the transmission spectroscopy of diluted Oxovanadyl (VO(TPP)) molecular spin ensembles in the pulsed-wave regime, in both crystalline and solid dispersion form [1]. We showed that it is possible to coherently manipulate the ensembles through the resonator and to measure their phase memory time. We additionally tested two Dynamical Decoupling protocols: Carr-Purcell-Meiboom-Gill and Uhrig Dynamical Decoupling. An enhancement of the memory time up to a factor of 3 after the application of a relatively low number (3-4) of π pulses is found for the crystalline samples for both sequences. We finally applied a storage/retrieval protocol on the ensemble, showing that it is possible to use it as a temporary memory for trains of up to 5 small input excitations (Fig. 1). We also showed that individual control on the output excitations can be achieved by changing the corresponding input. This result demonstrates the potential of molecular spins as (quantum) memories for information [1].

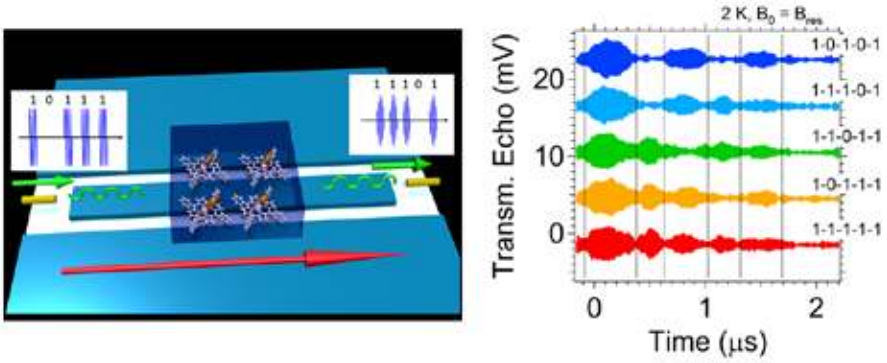

Fig. 1
Left) Sketch of a coplanar resonator with a spin ensemble on it. Red arrow represents the externally applied static magnetic field, while green arrows represent the microwave signal. A sketch of an input pulse sequence and of its corresponding output echo train retrieved from the ensemble are shown. Right) Echo trains measured at 2 K for a 2% VO(TPP) molecular spin ensemble after the application of the readout pulse. The input sequence sent on the ensemble is reported on the right of each trace (0=pulse off and 1=pulse on). Individual control of each echo in the output train is achieved acting on the corresponding input pulse [1].

Afterwards, we considered an advanced two-tone transmission spectroscopy performed on a crystal of diluted Diphenyl-Nitroxide (DPNO) organic radical in the dispersive limit of the coupling to the resonator, where no resonant exchange of photons occurs [2]. Here, one tone is used to drive the spins, while the other is used to monitor the resonator. A shift in both frequency and phase of the resonator is observed when the drive energy matches the one of the spins (Fig. 2). We showed that it is possible to use such a shift for measuring the ensemble indirectly, through the detuned resonator, with sufficient spectral resolution for electronic and nuclear spin transitions. The spin sensitivity can be comparable to the one achieved in the standard, single-tone, resonant spectroscopy. Moreover, the independent tunability of the two input powers allowed us to tune the signal-to-noise ratio of the measurement [2]. Finally, a similar two-tone dispersive spectroscopy repeated in the pulsed-wave regime opens the possibility to estimate the spin-lattice relaxation time of the sample [2].

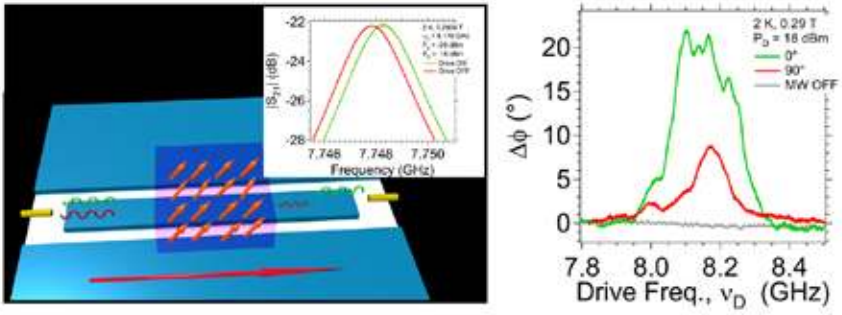

Fig. 2
Left) Sketch of a coplanar resonator coupled to a spin ensemble. Red arrow represents the static magnetic field, while the two sinusoids represent the microwave tones (red = drive frequency, green = readout frequency) used for the transmission spectroscopy in the dispersive regime. The inset shows the transmission of the resonator measured at 2 K when the drive tone is ON or OFF. A shift of the resonant peak is visible when the drive tone excites the spins at large detuning from the resonator. Right) Phase shift of the resonator measured as a function of the frequency of the drive tone for two different orientations of a 1.5% DPNO organic radical crystal with respect to the static magnetic field. All the electronic and nuclear transitions are clearly resolved in the dispersive transmission spectroscopy [2].

Contact person
Alberto Ghirri (alberto.ghirri@nano.cnr.it)

References
[1] Storage and retrieval of microwave pulses with molecular spin ensembles. C. Bonizzoni, A. Ghirri, F. Sanatanni, M. Atzori, L. Sorace, R. Sessoli, and M. Affronte. npj Quantum Inf. 6, 68 (2020).
[2] Transmission Spectroscopy of Molecular Spin Ensembles in the Dispersive Regime. C. Bonizzoni, A. Ghirri, S. Nakazawa, S. Nishida, K. Sato, T. Takui, and M. Affronte. Adv. Quantum Tech. 2, 100039 (2021).

Free-standing InSb nanoflags for quantum device applications

InSb offers a narrow band gap, a high carrier mobility, and a small effective mass, and thus has recently attracted tremendous attention for the implementation of topological superconducting states. Here, we show optimized growth of free-standing 2D InSb nanoflags (NFs) via Au-assisted chemical beam epitaxy (CBE). An electron mobility of 29,500 cm^2/Vs and a mean free path of 500 nm at 4.2 K are measured on Hall-bar devices. InSb NF-based Josephson junctions show gate-tunable proximity-induced supercurrent, with phase-coherent transport and high transparency of the interfaces. Our study places InSb NFs in the spotlight as a versatile and convenient 2D platform for advanced quantum technologies.

High-quality heteroepitaxial two-dimensional (2D) InSb layers are difficult to realize because of the large lattice mismatch with other widespread semiconductor substrates. A way around this problem is to grow freestanding 2D InSb nanostructures on nanowire (NW) stems, thanks to the capability of NWs to relax elastic strain along the sidewalls when lattice-mismatched systems are integrated. Nevertheless, controlling the aspect ratio of freestanding InSb nanostructures is challenging, due to the low vapor pressure of Sb and the surfactant effect. We first investigated the morphology evolution of freestanding InSb nanostructures like NWs (1D), NFs (2D), and nanocubes (NC) (3D) on InAs NW stems by means of Au-assisted CBE as a function of the growth conditions (Fig. 1) [1]. In particular, we found that 2D InSb NFs are single crystalline, defect-free with zinc blende structure, and provide a high degree of freedom in device fabrication. Next, by employing more robust and tapered InP NW stems and precisely orienting the substrate with the aid of reflection high-energy electron diffraction patterns, we could maximize length and width, and minimize the thickness of these NFs (Fig. 2a) [2]. The optimized InSb NFs have been used to fabricate Hall-bar devices, from which we measured electron mobility of 29,500 cm^2/Vs (Fig. 2b) and a mean free path of 500 nm at 4.2 K, which is the highest value reported for free-standing 2D InSb NFs in literature. We also successfully fabricated InSb NF-based Josephson junction devices with Ti/Nb contacts that show gate-tunable proximity-induced supercurrent up to 50 nA at 250 mK (Fig. 2c) and a sizable excess current. The devices show clear signatures of subharmonic gap structures, indicating phase-coherent transport in the junction and a high transparency of the interfaces [3]. We envision the use of 2D InSb NFs for fabrication of advanced quantum devices.

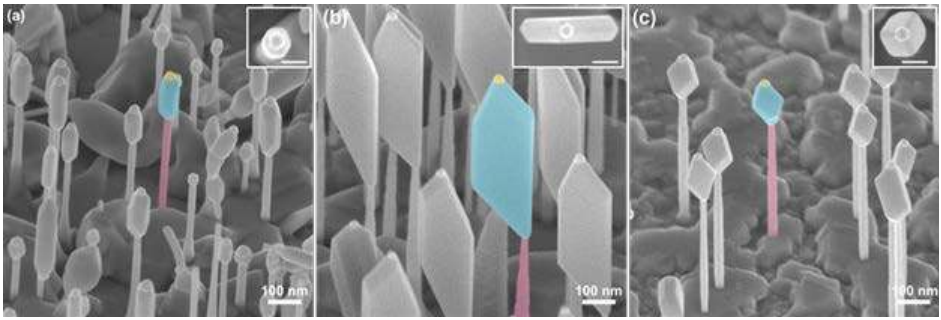

Fig. 1
InAs-InSb hetero-nanostructures with different morphology. 45°-tilted and top view (inset) SEM images of (a) 1D InSb NWs, (b) 2D NFs, and (c) 3D NCs grown on InAs NW stems. All scale bars are 100 nm. The false color is used to highlight the InAs stems (pink) and InSb nanostructures (blue).

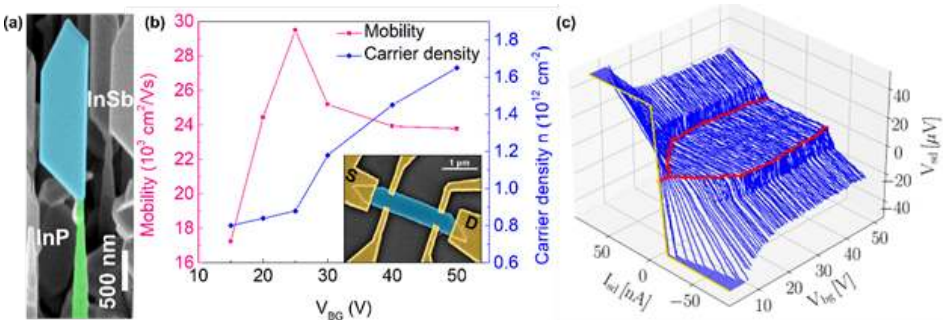

Fig. 2
(a) 45°-tilted SEM image of freestanding InSb NFs on InP NW stems. The false colour is used to highlight the InP stem (green) and InSb NF (blue). (b) Hall mobility and carrier density obtained from Hall measurements. Inset shows the SEM image of an InSb NF Hall-bar device. (c) Voltage drop V_{sd} across an InSb-based Josephson junction versus current bias I_{sd} and back gate voltage V_{bg}. The red line indicates the critical current.

Contact persons
Valentina Zannier (valentina.zannier@nano.cnr.it)
Stefan Heun (stefan.heun@nano.cnr.it)

References
[1] Morphology control of single-crystal InSb nanostructures by tuning the growth parameters. I. Verma, V. Zannier, F. Rossi, D. Ercolani, F. Beltram, and L. Sorba. Nanotechnology 31, 384002 (2020).
[2] High-Mobility Free-Standing InSb Nanoflags Grown on InP Nanowire Stems for Quantum Devices. I. Verma, S. Salimian, V. Zannier, S. Heun, F. Rossi, D. Ercolani, F. Beltram, and L. Sorba. ACS Appl. Nano Mater. 4, 5825 (2021).
[3] Gate-controlled supercurrent in ballistic InSb nanoflag Josephson junctions. S. Salimian, M. Carrega, I. Verma, V. Zannier, M. P. Nowak, F. Beltram, L. Sorba, and S. Heun. Appl. Phys. Lett. 119, 214004 (2021).

Parallel transport and layer-resolved thermodynamic measurements in twisted bilayer graphene

When stacking two-dimensional atomic crystals, their relative crystallographic alignment – so-called twisting – offers a powerful tuning knob for the electronic properties. We focus on the electrical transport of twisted bilayer graphene, with a growth-controlled 30° twist angle that minimizes the interlayer coupling. Employing dual-gated encapsulated devices with ultra-low disorder, we verify that the transport characteristics reproduce those of two parallel-conducting graphene sheets. Moreover, we find that gate-dependent features from one layer can directly probe the chemical potential in the other one, thus enabling a novel approach for high-resolution thermodynamic measurements.

Two-dimensional materials can be engineered in artificial stacks with highly tunable electronic properties. Even the simplest one – bilayer graphene – hosts an extraordinarily rich phase diagram that can be explored by applying gate voltages to field-effect devices, as well as by setting different twist angles at the assembly or synthesis stage. Ultimately, the understanding and control of this kind of systems holds the exciting perspective of realizing programmable condensed matter quantum simulators. In 30°-twisted bilayer graphene – 30TBG, a metastable configuration stabilized by chemical vapor deposition (CVD) on Cu – the superimposed layers effectively decouple (within the energy range probed in transport experiments). Still, a giant interlayer capacitance – matching the capacitance-per-unit-area of two parallel plates separated by a 1.2 Å vacuum layer – determines the response to gate voltages (Fig. 1a). In [1], we experimentally reveal novel implications of these widely-accepted aspects.
By analyzing the resistivity of CVD-grown 30TBG (Fig. 1b), we demonstrate quantitative agreement with simple parallel conduction between two pristine graphene layers. At room temperature, a conductivity as high as 40 mS – unattainable in a single graphene sheet – can be realized. At 4.2 K, we measure a mean free path limited by device width (2.2 μm, Fig. 1b inset), leading to a carrier mobility up to 6×10^5 $cm^2V^{-1}s^{-1}$. Via fine-tuning of the gate potentials, we observe a splitting of the charge neutrality point (CNP) for the two layers (Fig. 1c). Along the CNP of one layer, the chemical potential and carrier density in the other one can be measured using simple electrostatic considerations. This approach is reciprocal (meaning that the upper layer can probe the lower one, and vice versa), relies only on the twist-induced capacitive coupling, and allows a direct measurement of the Fermi velocity. In magnetic fields (Fig. 1d), the crossing between Landau levels from the two layers can be employed to measure jumps in the chemical potential with a few-meV resolution.

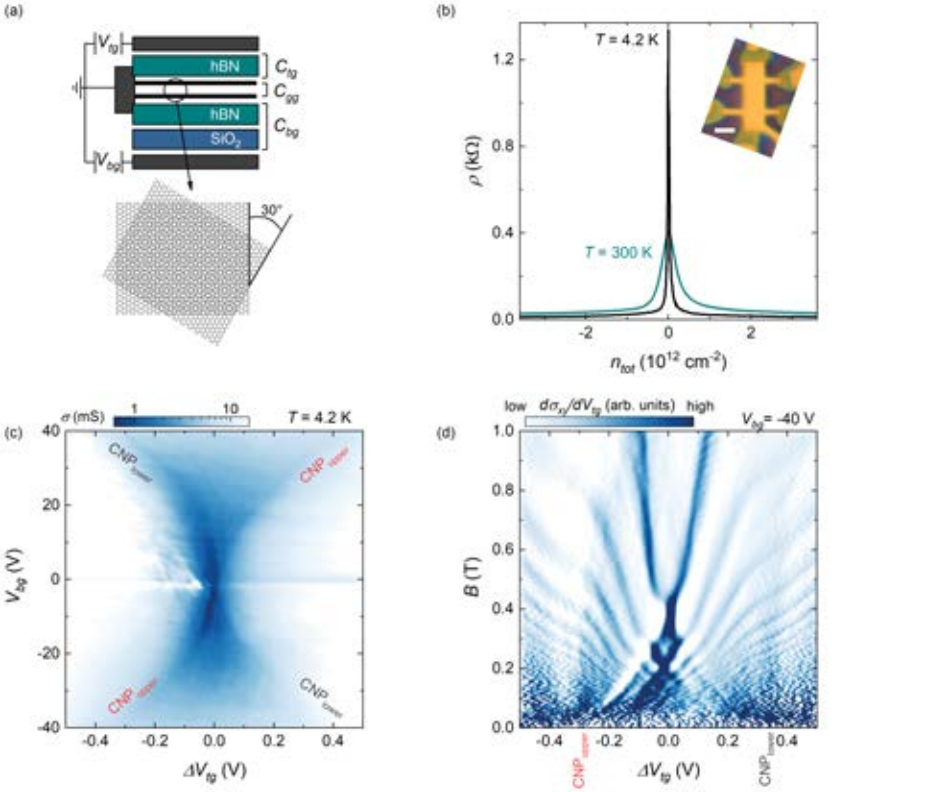

Fig. 1
(a) Sketch of the device (side view): 30TBG is encapsulated in hexagonal boron nitride and contacted by edge-type electrodes. Top and bottom gates can independently control the carrier density and its distribution, determined by the interlayer capacitance C_{gg}. (b) Resistivity as a function of the total carrier density, at room temperature (dark cyan) and at 4.2 K (black). Inset: optical microscopy image of the device; the scale bar is 2 μm. (c) Splitting of the CNP for the two layers controlled by the gate voltages. The color map shows the longitudinal conductivity at 4.2 K. (d) Crossing of Landau fans from coexisting electrons and holes, in the upper and lower graphene layer, respectively. The colour map shows the derivative of the Hall conductivity with respect to the top gate voltage.

Contact person
Sergio Pezzini (sergio.pezzini@nano.cnr.it)

Reference
[1] Parallel transport and layer-resolved thermodynamic measurements in twisted bilayer graphene. G. Piccinini, V. Mišeikis, K. Watanabe, T. Taniguchi, C. Coletti, and S. Pezzini. Phys. Rev. B 104, L241410 (2021).

Superconducting spintronics and phase-coherent quantum technologies

Superconducting quantum electronics is at the base of novel quantum technologies promising enhanced computational power in both classical and quantum approaches. Notably, superconductivity and ferromagnetism, two competing orders in bulk materials, can coexist at the nanoscale and are exploited in novel superconducting spintronic devices. We propose a superconducting logic memory based on a spin valve obtained with thin films of a ferromagnetic insulator and a superconductor. Moreover, we use the ferromagnetic order to control the superconducting phase and implement a quantum phase battery and the bi-stability of the superconducting phase in metallic nanowires for robust superconducting memories.

The macroscopic phase of a superconducting circuit is a robust quantum variable at the base of many fundamental studies and applications based on quantum coherence. Recent experimental findings of the SQEL group at Cnr Nano have pushed this field further towards innovative quantum technologies. The first-ever battery for the quantum phase [1] – a device that maintains a phase difference between two points in a superconducting circuit – has been constructed. The battery, which consists of an indium arsenide (InAs) nanowire in contact with aluminum (Al) superconducting leads, could be used in quantum computing circuits and for novel superconducting interferometers [2]. Demonstration of the battery operation is shown in Fig. 1.
Based on a fully metallic Al nanowire is the phase-slip memory [3], another phase coherent device able to store information, a logic bit, in the winding number of the superconducting phase along the nanowire. The strength of the phase-slip barrier generated in the device makes the memory robust against noise and persistence up to few days. The logic state can be read with a small probing current injected by a

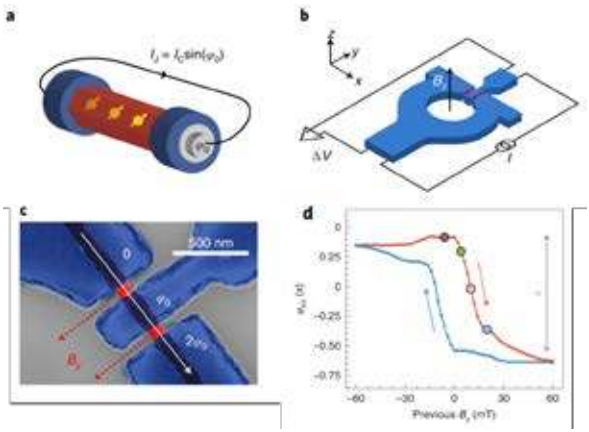

Fig. 1
Josephson phase-battery. a, Conceptual scheme of a Josephson phase battery composed of an InAs nanowire (red) embedded between two superconducting poles (blue) converting the spin polarization of surface unpaired spins (yellow) into a phase bias ϕ_0. b, Schematic illustration of the hybrid InAs-nanowire–aluminum SQUID interferometer used to quantify the phase bias ϕ_0 provided by the two JJs (in red). c, False-coloured scanning electron microscopy image of the active region of the phase battery. d, phase bias ϕ_0 accumulated thanks to the ferromagnetic polarization of the unpaired spins controlled by the in-plane magnetic field B_y.

tunnel probe integrated in the device as shown in Fig. 2a. Write and erase operations are performed through magnetic pulses as shown in Fig. 2b-c.
Finally, the coexistence of superconductivity and magnetic order have been further investigated in Europium Sulfide/Aluminum thin films [4]. Europium Sulfide is a ferromagnetic insulator which can induce a strong exchange field in an adjacent superconductor (Aluminum) via the magnetic proximity effect. This manifests as spin splitting of the BCS density of states of the superconductor, an important ingredient for numerous superconducting spintronics applications and the realization of Majorana fermions. Our results demonstrate the important role of the S layer thickness, which is particularly relevant for the fabrication of high-quality samples towards the realization of low dissipation logic memory based on a superconducting spintronic tunnel junction [5].

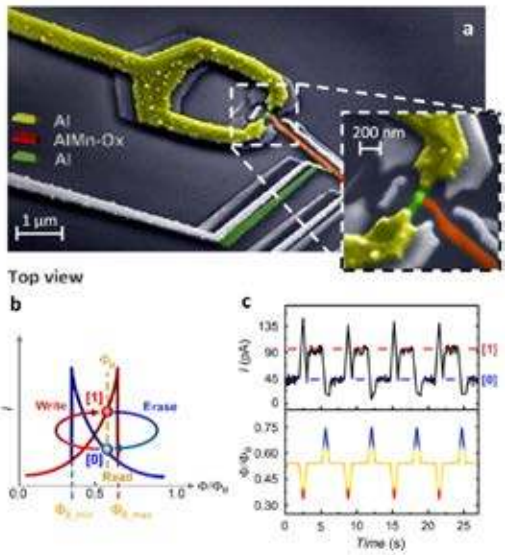

Fig. 2
Phase-slip memory. a, Pseudo-color scanning electron micrograph of a typical phase-slip memory. An Al nanowire (green) is inserted in a micron-size Al ring (yellow), whereas an AlMn probing electrode (red) is tunnel-coupled to the middle of the nanowire and to a second Al electrode (green) via an insulating oxide layer (grey) to allow the memory operation.
b, Sketch of the memory operation principle at a constant voltage bias (V). Low (blue, $I_{[0]}$) and high (red, $I_{[1]}$) current branches at the bias flux φB encode the [0] and [1] logic states, respectively. The erase (write) operation is performed by applying a flux pulse with amplitude $\varphi_E > \varphi_{B\_max}$ ($\varphi_W > \varphi_{Bmin}$). c, Write and erase operations observed in the readout tunnelling current (top panel) measured at V =300 µV for the evolution of the magnetic flux shown in the bottom panel.

Contact persons
Elia Strambini (elia.strambini@nano.cnr.it)
Francesco Giazotto (francesco.giazotto@nano.cnr.it)

References

[1] A Josephson Phase Battery. E. Strambini, A. Iorio, O. Durante, R. Citro, C. Sanz-Fernández, C. Guarcello, I. V. Tokatly, A. Braggio, M. Rocci, N. Ligato, V. Zannier, L. Sorba, F. S. Bergeret, and F. Giazotto. Nature Nanotechnology 15, 656 (2020).
[2] Rf-SQUID Measurements of Anomalous Josephson Effect. C. Guarcello, R. Citro, O. Durante, F. S. Bergeret, A. Iorio, C. Sanz-Fernández, E. Strambini, F. Giazotto, and A. Braggio. Phys. Rev. Res. 2, 023165 (2020).
[3] Preliminary Demonstration of a Persistent Josephson Phase-Slip Memory Cell with Topological Protection. N. Ligato, E. Strambini, F. Paolucci, and F. Giazotto. Nat. Commun. 12, 5200 (2021).
[4] Coexistence of Superconductivity and Spin-Splitting Fields in Superconductor/Ferromagnetic Insulator Bilayers of Arbitrary Thickness. A. Hijano, S. Ilić, M. Rouco, C. González-Orellana, M. Ilyn, C. Rogero, P. Virtanen, T. T. Heikkilä, S. Khorshidian, M. Spies, N. Ligato, F. Giazotto, E. Strambini, and F. S. Bergeret. Phys. Rev. Research 3, 023131 (2021).
[5] Superconducting logic element. F. Giazotto, E. Strambini, G. De Simoni, and F. S. Bergeret. US Patent, US2020227617 (A1), US11005023B2 (2020).

Toward Hole-Spin Qubits in Si p-MOSFETs within a Planar CMOS Foundry Technology

Hole spins in semiconductor quantum dots represent a viable route for the implementation of electrically controlled qubits. In particular, the qubit implementation based on Si p-MOSFETs offers great potentialities in terms of integration with the control electronics and long-term scalability. Within the present activity, a multi-scale approach is used to simulate a hole-spin qubit in a down-scaled Si-channel p-MOSFET, the structure of which is based on a commercial 22-nm fully depleted silicon-on-insulator device. Our calculations show the formation of well-defined hole quantum dots within the Si channel and the possibility of a general and fast electrical control.

Spin qubits in semiconductors have gained a renewed interest, thanks to the high degree of control achieved in the last years on the single- and few-particle states in Si and Ge quantum dots. Within this platform, high- fidelity single- and two-qubit gates have been recently demonstrated, as well as qubit read out and coherent spin transfer. Crucially, carrier spins in Si and Ge benefit from long coherence times, thanks to the limited impact of hyperfine interactions. Besides, Si and Ge represent key materials in modern electronics, and thus provide a common platform for integrating qubits and control circuits, possibly based on the same building blocks, such as scaled MOSFETs. In particular, hole spins are amenable to all-electric qubit manipulation, thus avoiding the introduction in the circuit design of elements that are incompatible with the industrial fabrication processes.

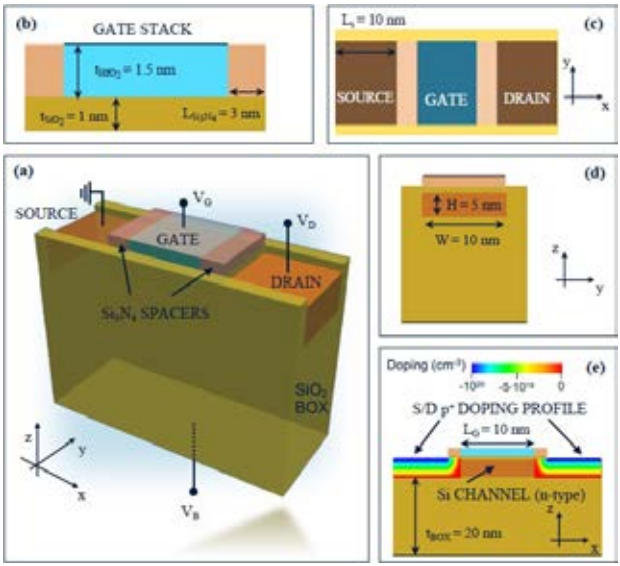

Fig. 1
(a) Schematics of the simulated pMOSFET fully depleted silicon on insulator (FDSOI) transistor. (b) Composition and geometry of the high-k metal gate stack. Top (c), side (d), and front (e) views of the device; in the latter we highlight the non-uniform Gaussian doping profile in the source and drain. The holes are confined in the dot, which is electrostatically defined in the silicon channel by suitably selecting the top-gate voltage.

Here, we have theoretically investigated the possibility of generating hole-spin qubits in a downscaled Si pMOSFET, derived from 22nm fully-depleted silicon-on-insulator (FDSOI) CMOS foundry technology (Fig. 1). We find that these devices indeed allow the formation of well-defined quantum dots, for a realistic set of values of the applied (sub-threshold) gate voltages. Besides, the application of time-dependent voltages to the top gate would allow one to perform qubit rotations around both a longitudinal (Z) and transverse (X, Y) directions, with Rabi frequencies of the order of 102 MHz (in the presence of static magnetic field of 1 T). Despite the fact that the two rotations display complementary dependencies on the magnetic field orientation (Fig. 2), a good trade-off has been identified, demonstrating the possibility of efficiently implementing the two qubit rotations within the same geometry. Besides, both the absolute values and the correlation between the Rabi frequencies are shown to be highly tunable by means of the channel geometry. These results support the viability of the approach based on the hole-spin qubits in FDSOI silicon MOSFETs.

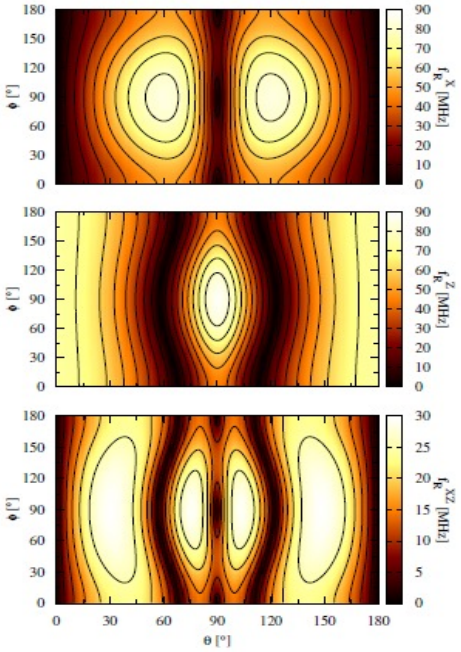

Fig. 2
Dependence of the Rabi frequencies f^{x}_{R} (upper panel, corresponding to rotations around the X axis of the Bloch sphere), f^{z}_{R} (middle, rotations around Z), and of f^{xz}_{R} (lower panel, sequential rotations around X and Z) on the orientation of the static magnetic field. This is defined by the polar angle σ and the azimuthal angle ϕ.

Contact persons
Filippo Troiani (filippo.troiani@nano.cnr.it)
Andrea Bertoni (andrea.bertoni@nano.cnr.it)

References

[1] Toward Hole-Spin Qubits in Si p-MOSFETs within a Planar CMOS Foundry Technology. L. Bellentani, M. Bina, S. Bonen, A. Secchi, A. Bertoni, S. P. Voinigescu, A. Padovani, L. Larcher, and F. Troiani. Phys. Rev. Applied 16, 054034 (2021).
[2] High-Throughput Investigation of the Electron Transport Properties in $Si_{1-X}Ge_{X}$ Alloys. B. I. Adetunji, A. Supka, M. Fornari, and A. Calzolari. IEEE Access 9, 141121 (2021).
[3] Inter- and intraband Coulomb interactions between holes in silicon nanostructures. A. Secchi, L. Bellentani, A. Bertoni, and F. Troiani. Phys. Rev. B 104, 205409 (2021).
[4] Interacting holes in Si and Ge double quantum dots: From a multiband approach to an effective-spin picture. A. Secchi, L. Bellentani, A. Bertoni, and F. Troiani. Phys. Rev. B 104, 035302 (2021).

Fully phase-stabilized quantum cascade laser frequency combs

Metrological-grade frequency comb (FC) synthesizers are the ideal sources for quantum sensing, metrology, communications and simulations. At terahertz (THz) frequencies, electrically pumped quantum cascade lasers (QCLs) have shown quantum-limited frequency noise operation, phase/frequency absolute referencing and self-starting FC operation, albeit over a rather restricted dynamic range, governed by the nature of the quantum gain media that entangles group velocity dispersion at the different bias points. Here, we conceive a set of technological approaches to achieve FC operation over the entire available gain bandwidth and across almost the whole lasing regime at THz frequencies.

The ability to engineer quantum-cascade-lasers (QCLs) with ultrabroad gain spectra, and with a full compensation of the group velocity dispersion, at terahertz (THz) frequencies, is key for devising monolithic and miniaturized optical frequency comb-synthesizers (FCSs) in the far-infrared. In THz QCLs four-wave mixing, driven by intrinsic third-order susceptibility of the intersubband gain medium, selflocks the optical modes in phase, allowing stable comb operation, albeit over a restricted dynamic range (~20% of the laser operational range). Here, we engineer miniaturized THz FCSs, comprising a heterogeneous THz QCL, integrated with a tightly coupled, on-chip, solution-processed, graphene saturable-absorber reflector that preserves phase coherence between lasing modes, even when four-wave mixing no longer provides dispersion compensation. This enables a high power (8 mW) FCS with over 90 optical modes, through 55% of the laser operational range. We also achieve stable injection locking, paving the way to a number of key applications, including high-precision tunable broadband spectroscopy, and quantum metrology.
We also conceive an alternative integrated architecture for the generation of high power (>10 mW) THz FCs comprising an ultrafast THz polaritonic reflector, exploiting intersubband cavity polaritons, and a broad bandwidth (2.3–3.8 THz) heterogeneous THz QCL. By tuning the group-delay dispersion through the exploitation of light-induced bleaching of the intersubband-based THz polaritons, we demonstrate spectral reshaping of the QCL emission and stable FC operation over an operational range up to 38%, characterized by a single and narrow (down to 700 Hz) intermode beatnote.
Our QCL FCs are then exploited in a sophisticated arrangement to assess its phase coherence, reconstructing its intensity emission profile, instantaneous frequency and electric field, thus proving its metrological nature. We then highlight future perspectives of this frontier research field in disruptive areas of quantum technologies, such as quantum sensing, quantum metrology, quantum imaging, and photonic-based quantum computation.

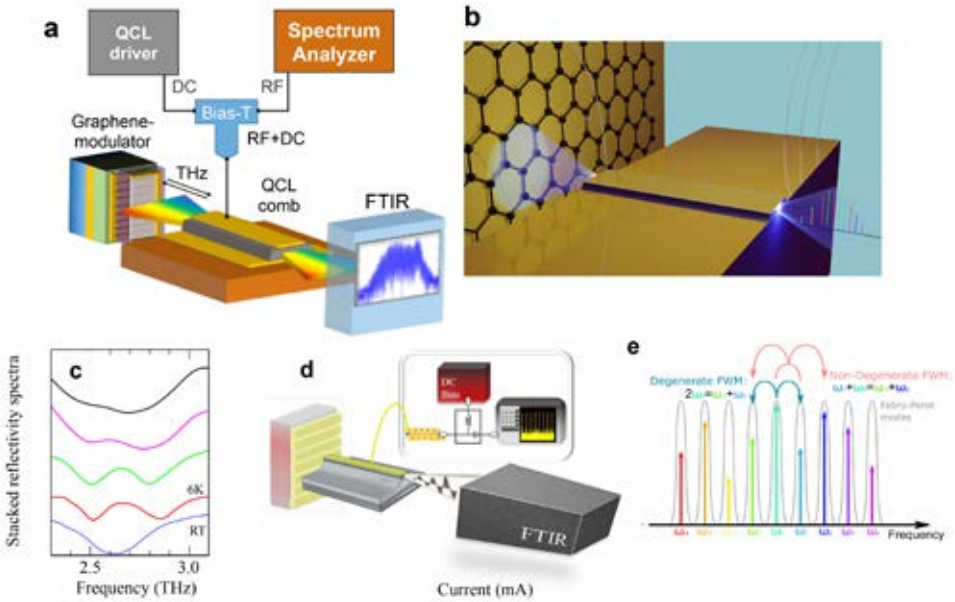

Fig. 1
(a) Schematic experimental setup: the SLG modulator is mounted on a piezoelectric stage 50μm away from the back facet of a multimode heterogeneous THz QCL. The coupled system is then mounted on the cold head of a He-flow cryostat. The radiation back-reflected by the modulator is injected into the QCL waveguide, while the emission from the front facet is sent into a Fourier-Transform InfraRed (FTIR) spectrometer. (b) Terahertz frequency combs exploiting an on-chip, solution-processed, graphene-quantum cascade laser coupled cavity. (c) Reflectivity spectra of the polaritonic structure measured at T = 300 K (blue curve), and at T= 6 K while pumping on it a continuous-wave QCL (laser A) driven at I = 0 mA (red curve), I = 520 mA (green curve), I = 580 mA (pink curve), I = 632 mA (black curve). (d) Schematic diagram showing the experimental arrangement. (e) Schematic representation of frequency comb formation mechanisms through degenerate and non-degenerate four wave mixing (FWM).

Contact person
Miriam Serena Vitiello (miriam.vitiello@nano.cnr.it)

References

[1] Chip-Scale Terahertz Frequency Combs through Integrated Intersubband Polariton Bleaching. F. P. Mezzapesa, L. Viti, L. Li, V. Pistore, S. Dhillon, A. G. Davies, E. H. Linfield, and M. S. Vitiello. Lasers and Photonics Reviews 2000575 (2021).
[2] Terahertz Frequency Combs Exploiting an On-Chip, Solution-Processed, Graphene-Quantum Cascade Laser Coupled-Cavity. F. P. Mezzapesa, K. Garrasi, J. Schmidt, L. Salemi, V. Pistore, L. Li, A. G. Davies, E. H. Linfield, M. Riesch, C. Jirauschek, T. Carey, F. Torrisi, A. C. Ferrari, and M. S. Vitiello. ACS Photonics 7, 3489-3498 (2020).
[3] Homogeneous quantum cascade lasers operating as terahertz frequency combs over their entire operational regime. A. Di Gaspare, L. Viti, H. E. Beere, D. D. Ritchie, and M. S. Vitiello. Nanophotonics 10, 181-186 (2021).
[4] Toward new frontiers for terahertz quantum cascade laser frequency combs. M. S. Vitiello, L. Consolino, M. Inguscio, and P. De Natale. Nanophotonics 10, 187-194 (2021).
[5] Quantum cascade laser based hybrid dual comb spectrometer. L. Consolino, M. Nafa, M. De Regis, F. Cappelli, K. Garrasi, F. P. Mezzapesa, L. Li, A. G. Davies, E. H. Linfield, M. S. Vitiello, S. Bartalini, and P. De Natale. Springer Nature Communications Physics 3, 1-9 (2020).

Self-catalyzed InSb/InAs Quantum Dot Nanowires

The nanowire geometry provides an excellent platform for the growth of lattice-mismatched materials in defect-free heterostructures. The most widespread approach for realizing axial nanowire heterostructures is the Au-assisted growth. However, Au incorporation may degrade their electrical and optical properties. Therefore, self-catalyzed or catalyst-free approaches are desirable. Here we show our study on the growth mechanism of InSb segments on top of catalyst-free InAs nanowire stems and the subsequent self-catalyzed InAs top-segment growth. Defect-free InSb quantum dots with controlled dimensions into InAs nanowires were finally demonstrated.

The growth of quantum dots (QDs) in nanowires (NWs) offers additional features over Stranski-Krastanow QDs, for example providing a tool for the manipulation of single QD. Because of its small bandgap, low-effective masses, high electron mobility, and large thermo-power figure of merit, indium antimony (InSb) is an attractive material. In this contribution, we demonstrate for the first time the successful growth of defect-free InSb QDs embedded into InAs NWs on Si (111) substrates by chemical beam epitaxy. In the first step, the growth of self-catalyzed InSb segments onto catalyst-free InAs NWs has been thoroughly investigated as a function of the In and Sb line pressures, and growth time (Fig. 1). We found that the radial growth of the InSb segment is not a consequence of the droplet inflation but is rather due to the vapor-solid (VS) radial growth on the NW sidewalls. At the same time, the presence of the In droplet on the NW top is absolutely required to maintain the axial growth. The growth kinetics of the InSb segment and of the In droplets on their tops have been explained and quantified within a theoretical model containing no free parameters [1].

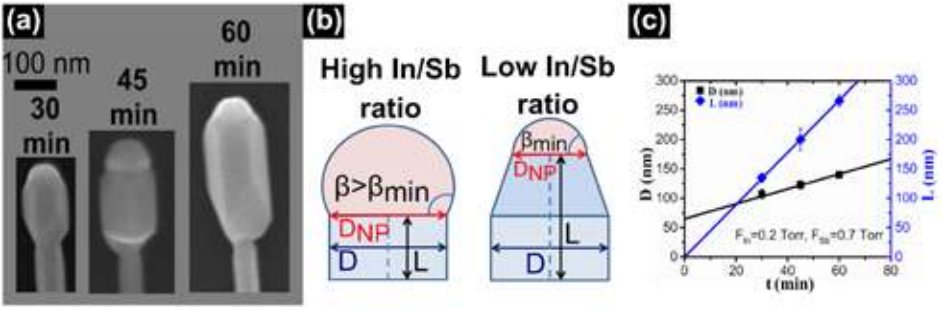

Fig. 1
(a) SEM images of InAs/InSb axial heterostructured NWs, obtained for 30, 45, and 60 min of InSb growth time. (b) Illustration of vertical (for $\beta > \beta_{min}$) or tapered (at $\beta = \beta_{min}$) NW geometry, with $\beta_{min} \approx 79°$ as the small stable angle determined by the surface energetics. (c) Time evolution of the diameter (D) and length (L) of InSb segments. The lines in (c) are theoretical fits to the experimental data (symbols).

In the second step, we grew self-catalyzed InSb/InAs QD NWs. A systematic variation of the growth parameters for the InAs top segment has been investigated and the resulting nanowire morphology analyzed. We found that the axial and radial growth rates decrease with increasing InAs growth temperature. Furthermore, both the axial and radial growth rates of InAs are As-limited in the self-catalyzed regime. Finally, the time evolution of the diameter along the entire length of the NWs allowed us to understand that there are two In diffusion paths contributing to the radial InAs growth, and that the interplay of these two mechanisms together with the total length of the nanowires determines the final shape and morphology of the nanowires (Fig. 2). Our study provides valuable guidelines for the realization of InSb/InAs QD NWs with the desired dimensions and morphology for device applications [2].

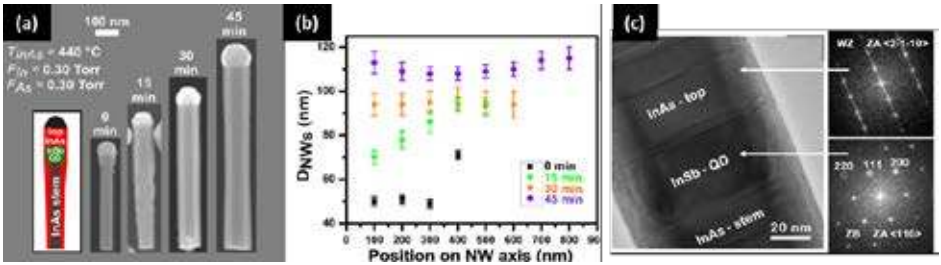

Fig. 2
(a) SEM images of representative InSb/InAs QD NWs, obtained with fixed line pressures (F_{In} = 0.30 Torr, F_{As} = 0.30 Torr) and growth temperature (T_{InAs} = 440 ± 5 °C), while the growth time of InAs top segments varies from 15 min to 45 min as indicated in each panel. The first NW at t = 0 min represents the InAs/InSb NW grown at 410 ± 5 °C. (b) NW diameter as a function of position along the length of NW, for samples of the same time series shown in panel (a). (c) High-resolution TEM image of the optimized InSb/InAs QD NW. The fast Fourier transform (FFT) analysis shown on the bottom right confirms the defect-free zinc blende structure of the QD.

Contact persons
Valentina Zannier (valentina.zannier@nano.cnr.it)
Lucia Sorba (lucia.sorba@nano.cnr.it)

References
[1] Growth of Self-Catalyzed InAs/InSb Axial Heterostructured Nanowires: Experiment and Theory. O. Arif, V. Zannier, V. G. Dubrovskii, I. V. Shtrom, F. Beltram, and L. Sorba. Nanomaterials 10, 494 (2020).
[2] Self-Catalyzed InSb/InAs Quantum Dot Nanowires. O. Arif, V. Zannier, F. Rossi, D. Ercolani, F. Beltram, and L. Sorba. Nanomaterials 11, 179 (2021).

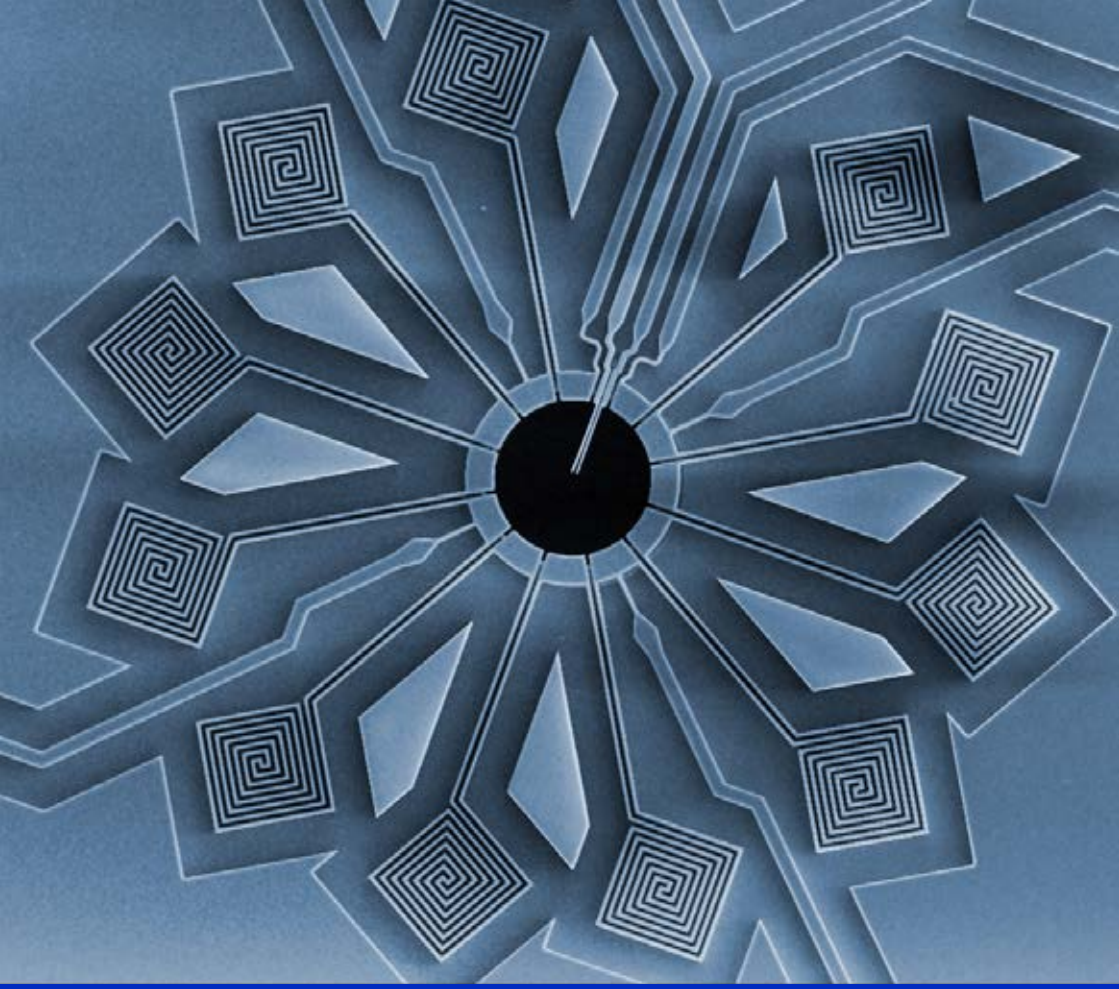

Highlights
-
Surfaces and interfaces: nanofabrication, imaging, and spectroscopy

Introduction to Surfaces and interfaces: nanofabrication, imaging, and spectroscopy

The thematic area concerning "**Surfaces and Interfaces: nanofabrication, imaging, and spectroscopy**" is focused on the use of nanotechnologies to realize outperforming materials and devices for **energy harvesting and storage, sensing and nanomechanics**. The materials investigated are in most cases prepared in the laboratories of the Institute, exploiting facilities for the physical vapor deposition methods, like molecular beam epitaxy, sputter deposition also combined with inert gas-aggregation, or by electrospinning, and employing advanced fabrication techniques like e-beam lithography and focused ion beam. The classes of materials investigated range from oxides to 2-dimensional materials, from fibers to plasmonic nanostructures. Material properties and devices are investigated with several advanced spectroscopic techniques in the laboratories and at synchrotron radiation facilities, with more and more importance given to the active control and the ability to tune the response of the materials in in-operando conditions. For the assessment of morphology at high-resolution scanning-probe microscopes and transmission electron microscopes are used. Furthermore, the use of MEMS realized in our labs as sorter for the TEM has allowed the mapping of electron wavefunctions, making the state decomposition visible and pushing the TEM towards a quantum instrument. Time-resolved studies by ultrafast spectroscopies allow to follow the dynamics of electronic and plasmonic excitations at the femtosecond time scale and to identify the corresponding decay channels.

A research topic highly investigated for energy harvesting and photocatalysis is plasmonics. Metal nanoparticles have been extensively studied for this purpose, however the excitation dynamics of plasmons can still reveal fundamental details for the understanding of the mechanisms that can enhance photovoltaics performance. Coupling metals with reducible oxides, either in form of nanoparticles or of dopants, have been explored as one

route to increase the reactivity of wide band gap materials in the visible range and towards hydrogen dissociation. Metal nanoparticles in transparent conductive oxides tune charge carrier concentration, while in hybrid perovskites solar cells they increase the optical path of solar radiation. Also in these cases the spectroscopic study of the electronic and optical properties and of the time-resolved dynamics of excitation/de-excitation processes like plasmon oscillations, hot electron generation, charge transfer, and polariton formation will open the way to a better understanding of the properties and to a more **efficient design of materials**.

2D materials are largely investigated for **sensing and storage**. Graphene functionalization can be exploited to improve its selective sensitivity towards target molecules. Different ways of defect engineering have been explored to implement it and the resulting responses have been assessed through spectroscopies. Graphene has also been used to prove that tuning of nanofriction can be obtained exploiting the film strain. Another 2D material is exfoliated black phosphorus that is particularly interesting for applications in electronic devices and energy storage because of its peculiar properties. Coupling black phosphorus layer with metal nanoparticles enhances its ambient stability, induces charge transfer and, as a consequence, n-type doping. To understand the role of metal nanoparticles, spectroscopy and microscopy have been integrated with first-principle calculations as an extremely important guide for the interpretation of the observed behavior and finally for optimal material design.

Another interesting class of materials for energy harvesting are **fibers** which can exhibit **piezoelectric and pyroelectric character**. The understanding of the behavior of polymers at a molecular level will help in designing new polymer-based generators.

Ultrafast dynamics of excited states in metal-oxide nanosystems for green solar photocatalysis

Transient excitation in plasmonic nanoparticles (NPs) can expand the activity of wide bandgap semiconductors in the visible range for application in solar photocatalysis. We have exploited the time-resolved x-ray absorption spectroscopy with free electron laser (FEL) to investigate the charge transfer from Ag NPs to CeO_2. Furthermore, the measurement of electron gas temperature by time-resolved UPS has shed light on the fs processes induced by UV pulses in plasmonic NPs, while small polaron formation in the oxide has been followed by transient absorption spectroscopy. The study of these excited states helps understanding and improving the plasmonic/semiconductor photocatalytic materials.

Wide bandgap semiconductors have been studied for application in green solar photocatalysis for years, with the drawback that they absorb in the UV. Coupling with plasmonic NPs can expand their activity to the visible range. We have embedded Ag NPs in a film of CeO_2 and we have exploited the chemical sensitivity of FEL time-resolved soft X-ray absorption spectroscopy (TRXAS) to investigate the transfer of hot electrons generated by plasmonic photoexcitation in the NPs to the oxide film. We have observed ultrafast changes (<200 fs) in the Ce $N_{4,5}$ absorption edge proving that the electron transfer to the Ce atoms occurs through a highly efficient electron-based mechanism [1] (Fig. 1).

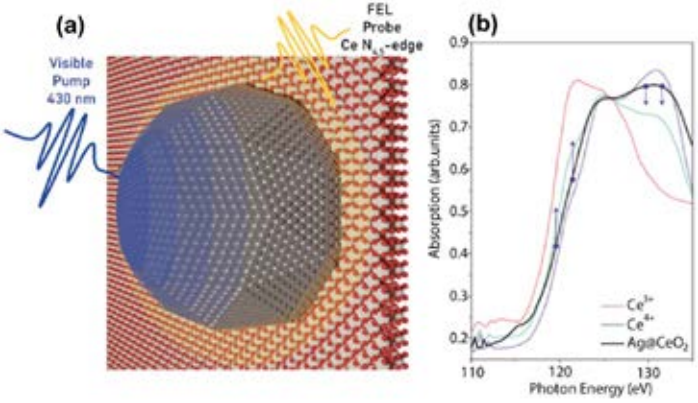

Fig. 1
(a) Schematic of the experimental configuration of Ag NP in CeO_2 film and (b) Ce $N_{4,5}$ XAS spectra before (black line) and after the pump excitation (green), compared to the reference spectra. Dots and arrows indicate the selected FEL energies used to probe the absorption variations.

One of the key points in hybrid plasmonic/semiconductor materials is the photoexcitation of plasmonic NPs. To understand the fs evolution of the photoexcitation we have measured the electronic temperature of Au NPs by means of ultrafast time-resolved photoemission spectroscopy excited by extreme-UV radiation pulses. [2] The electronic temperature is obtained by fitting high-resolution spectra at the Fermi edge and provides a direct picture of the ultrafast electron-gas dynamics (Fig. 2). These results have been discussed in the framework of the three-temperature model

Fig. 2
Photoexcitation by laser pump and HHG photoemission probing of Au NPs. As a consequence of the photo-excitation the Fermi edge is modified at a time scale below 1 ps. The temperature extracted from Fermi edge fit is interpreted in the framework of the three-temperature model.

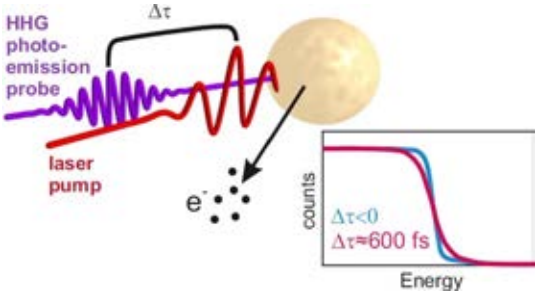

of fs processes in laterally-confined systems and help understanding the role of hot electrons in technological applications.
Finally, we have explored the dynamics of excited states in the oxide film, which determine the photocatalytic functionality of the material. Photoexcited CeO_2 exhibits a bleaching of the band edge absorbance in UV transient absorbance spectra, while a photoinduced absorbance feature is assigned to Ce 4f → Ce 5d transitions. In particular, we have observed a blue shift of the photoinduced absorbance signal that is assigned to the dynamic formation of small polarons with a characteristic time of 330 fs [3]. Additionally, combining steady-state and ultrafast transient absorption we have proposed a revised value for the optical gap of ceria (Eog = 4 eV), significantly larger than usually reported (Fig. 3).

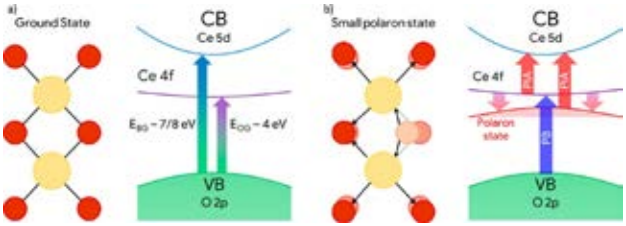

Fig. 3
(a) Ground and (b) photoexcited state of CeO_2 inducing the filling of the Ce 4f states. This produces a polarization that deforms the lattice, causing the formation of small polaron state (red). The photobleaching (PB) and photoinduced absorption (PIA) transient signals are highlighted with blue and red arrows.

Contact persons
Stefania Benedetti (stefania.benedetti@nano.cnr.it)
Paola Luches (paola.luches@nano.cnr.it)

References

[1] Ultrafast Dynamics of Plasmon-Mediated Charge Transfer in Ag@CeO2 studied by Free Electron Laser time-resolved X-ray Absorption Spectroscopy. J. S. Pelli Cresi, E. Principi, E. Spurio, D. Catone, P. O'Keeffe, S. Turchini, S. Benedetti, A. Vikatakavi, S. D'Addato, R. Mincigrucci, L. Foglia, G. Kurdi, I. P. Nikolov, G. de Ninno, C. Masciovecchio, J. Kopula Kesavan, F. Boscherini, and P. Luches. Nano Letters 21, 1729 (2021).
[2] Quantitative Ultrafast Electron-Temperature Dynamics in Photo-Excited Au Nanoparticles. M. Sygletou, S. Benedetti, M. Ferrera, G. M. Pierantozzi, R. Cucini, G. Della Valle, P. Carrara, A. De Vita, A. di Bona, P. Torelli, D. Catone, G. Panaccione, M. Canepa, and F. Bisio. Small 17, 2100050 (2021).
[3] Ultrafast Formation of Small Polarons and the Optical Gap in CeO2. J. S. Pelli Cresi, L. Di Mario, D. Catone, F. Martelli, A. Paladini, S. Turchini, S. D'Addato, P. Luches, and P. O'Keeffe. J. Phys. Chem. Lett. 11, 5686 (2020).

Electron microscopy for the quantum measurement of electron states by MEMS electron-optics elements

In this contribution we demonstrate how the new use of MEMS technology combined with artificial intelligence for automatic microscope control can change the way electron microscopy is carried out. We have been able to build and apply an electron OAM sorter for the first measurement of Orbital Angular Momentum but it can be useful also for, e.g., quantum state tomography measurement, arbitrary state measurement optimisation, spiral phase plates and fast/ultrafast microscopy measurements.

The complexity of an electron microscope has been steadily increasing with aberration correctors, monochromators and energy filters, and this allows microscopists to reach 20pm resolution, 5 meV energy resolution, and even time resolution at femtosecond time scale.
However, a new generation of electron optics based on MEMS and miniaturized phase plates is emerging and the group of microscopy at Cnr Nano is playing a big part in it. Through electron optical components, based on microelectromechanical systems technology, it is now possible to generate vortex beams [1], orbital angular momentum (OAM) analysers [2], and many more ideas are still emerging [3]. This new electron optics is flexibly tunable and allows for phase effects that could not be created in the past.
As the instrumental research stretches beyond the standard use of the microscope, more challenges are found for real operations and this complexity is the bottleneck of new instrumental developments.

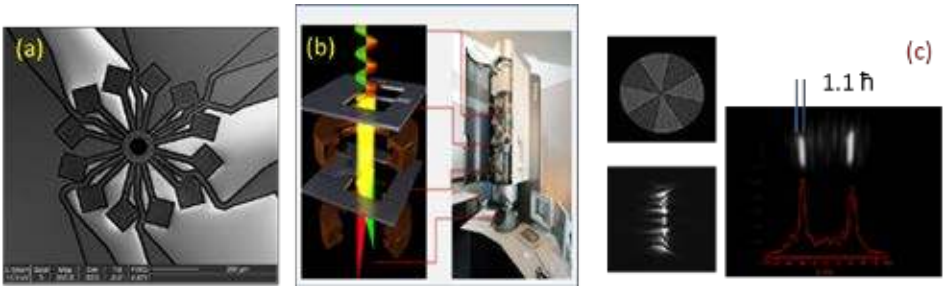

Fig. 1
(a) Example of our MEMS device for electron optics, (b) configuration of the OAM sorter in a microscope, (c) example of experimental OAM sorting with near nominal OAM resolution.

A natural solution to this problem is using Artificial Intelligence (AI). We are pioneering the use of artificial neural networks (ANN) [4], a class of AIs able to autonomously learn from a large set of training examples, to control electron optical devices within a transmission electron microscope.
The combination of AI and innovative optics is the instrument for very innovative measurements with electrons because the new optics require an unconventional control and a continuous feedback to fight potential instability.
The OAM sorter, based on 2 coupled MEMS phase plates, introduces a conformal mapping of the electron wavefunction and makes the state decomposition directly visible as spectrum on the detector. This is an optimisation in terms of measurement as in principle only one electron is needed to measure the state of a vortex beam and gives a feeling of a "quantum" measurement. However we will aim to make the electron microscope even more a quantum instrument by measuring the density matrix of specific excitation taking advantage of the discrete character of the OAM degree of freedom.

Contact person
Vincenzo Grillo (vincenzo.gillo@nano.cnr.it)

References

[1] Generation of electron vortices using nonexact electric fields. A. H. Tavabi, H. Larocque, P.-H. Lu, M. Duchamp, V. Grillo, E. Karimi, R. E. Dunin-Borkowski, and G. Pozzi. Phys. Rev. Research 2, 013185 (2020).
[2] Experimental Demonstration of an Electrostatic Orbital Angular Momentum Sorter for Electron Beams. A. H. Tavabi, P. Rosi, E. Rotunno, A. Roncaglia, L. Belsito, S. Frabboni, G. Pozzi, G. C. Gazzadi, P. H. Lu, R. Nijland, M. Ghosh, P. Tiemeijer, E. Karimi, R. E. Dunin-Borkowski, and V. Grillo. Phys. Rev. Lett. 126, 094802 (2021).
[3] Arbitrary Conformal Transformations of Wave Functions. G. Ruffato, E. Rotunno, L. M. C. Giberti, and V. Grillo. Phys. Rev. Applied 15, 054028 (2021).
[4] Alignment of electron optical beam shaping elements using a convolutional neural network. E. Rotunno, A. H. Tavabi, P. Rosi, S. Frabboni, P. Tiemeijer, R. E. Dunin-Borkowski, and V. Grillo. Ultramicroscopy 228, 113338 (2021).

Understanding hydrogen dissociation by doped oxides

An accurate atomic scale description of the interaction between hydrogen and oxide surfaces is important in view of designing efficient and non-critical catalysts, alternative to platinum, for hydrogenation reactions or fuel cells electrodes. The mechanisms for H_2 activation on pure and metal-doped CeO_2(111) surfaces have been investigated by comparing experimental studies by x-ray photoemission spectroscopy and scanning tunneling microscopy with density functional theory simulations. The study provides new insights on the promotional effect of low-concentration metal ions on H_2 dissociation.

Electrochemical devices for sustainable H_2 production and conversion largely employ catalysts based on platinum, a rare and expensive element. The increasing interest towards H_2 as a fuel has stimulated intense research efforts to identify alternative non-critical materials for H_2-related applications. Catalysts based on reducible oxides, among which CeO_2, have a high potential due to their ability to store and release oxygen depending on the external conditions. Reducibility may be increased by introducing low concentrations of cations having a lower valence than cerium.
We have investigated the mechanism of H_2 activation on Ag-modified cerium oxide surfaces. The study is performed on thin epitaxial cerium oxide films, analyzed by X-ray photoemission spectroscopy (XPS) to assess the changes of the Ag oxidation state and of the concentration of Ce^{3+} ions, O vacancies, and hydroxyl groups on the surface during thermal reduction cycles in vacuum and in H_2.
The results are interpreted using density functional theory (DFT) calculations, which showed that the presence of the Ag dopant reduces the barrier of H_2 dissociation on the cerium oxide surface, explaining the larger concentration of OH groups observed on the Ag-modified surface as compared to the pure cerium oxide surface at low temperature (Fig. 1 b). The lower concentration of reduced Ce^{3+} ions in Ag-modified cerium oxide in H_2 (Fig. 1 a) is explained in terms of a change of the oxidation state of Ag, which acquires some of the extra surface electrons left by the oxygen vacancies and the adsorbed hydrogen atoms, as confirmed by XPS data. The calculations also show that the presence of Ag decreases the activation barrier for surface diffusion of adsorbed H atoms, which is the rate limiting process for water formation, thus suggesting a larger rate of water formation on the Ag-modified than on the pristine surface at high temperature (Fig. 1d). This prediction is confirmed by the higher concentration of surface oxygen vacancies and lower concentration of OH groups on the Ag-modified CeO_2 surface at high T observed in the experiments (Fig. 1b,c).

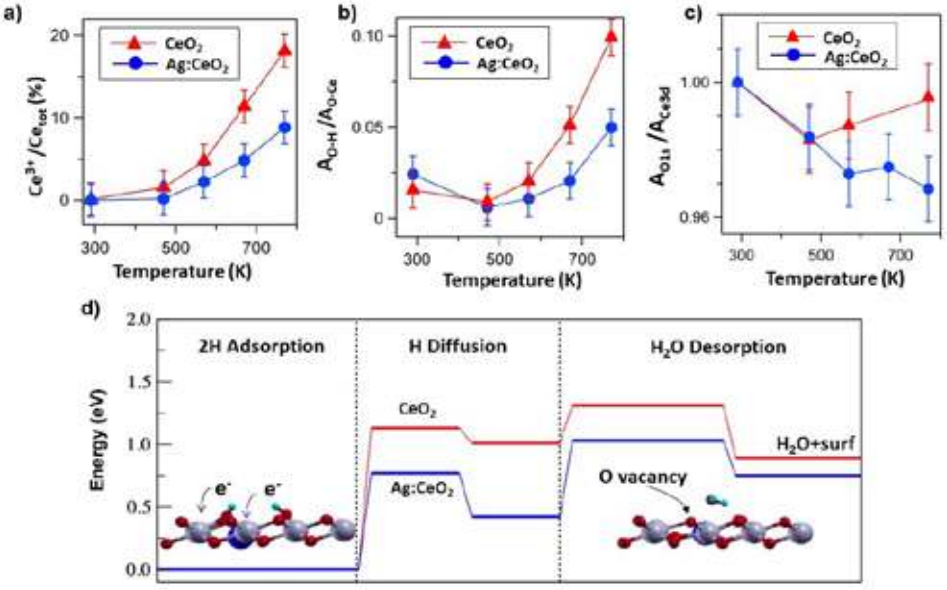

Fig. 1
a) Ce^{3+} concentration, b) O-H surface concentration, and c) O 1s intensity as a function of temperature, derived from XPS spectra acquired on a pure and on a Ag:CeO_2 film during thermal treatments in H_2. Minimum energy path of hydrogen-induced reduction of the pure CeO_2 surface and of the Ag:CeO_2 surface at T=0K evaluated by DFT.

Contact persons
Paola Luches (paola.luches@nano.cnr.it)
Stefania Benedetti (stefania.benedetti@nano.cnr.it)

Reference
[1] Surface Reactivity of Ag-Modified Ceria to Hydrogen: A Combined Experimental and Theoretical Investigation. S. Benedetti, G. Righi, P. Luches, S. D'Addato, R. Magri, and A. Selloni. ACS Appl. Mater. Interfaces 12, 27682 (2020).

Tunable Frictional Response of Induced Strained Graphene

In the nanoscale regime, one of the most plausible solutions to lower friction effects, reduce wear and protect surfaces, relies on coating them with ultrathin lamellar sheets, such as graphene monolayers. Nevertheless, the role of the substrate on which graphene is deposited is pivotal to modulate physical and electronic properties of the graphene film. In particular, strain induced by interaction with the substrate is one of the most interesting parameters to adapt, control and tune graphene features including tribological response. Here, we investigate the frictional response of graphene monolayer deposited on textured silicon substrates with different grooves density that generate different levels of strain.

A chemical vapor deposition (CVD)-grown single layer graphene has been deposited over the silicon dioxide textured surfaces by the wet transfer method. The substrate texturing consists of long parallel grooves equally spaced, from 40 to 250 nm, with a depth of a few nm. The height profile measurement of bare and covered surfaces reveals a higher degree of suspension for the substrate with the higher grooves density, sign that graphene over this kind of corrugations is partially suspended at the bottom of the grooves but clamped between two adjacent crests, resulting in a strain configuration. The strain level has been evaluated both theoretically, by using an analytical model and molecular dynamic simulations, and experimentally, by Raman spectroscopy. Finally the overall system has been analyzed by friction force microscopy (FFM) measurements. The FFM images comprise bare textured silicon regions and nearby graphene covered areas in a single acquisition. Due to the intrinsic anisotropy in the texture-induced strain in graphene, FFM measurements were performed in orthogonal (Fig. 1a) and parallel directions (Fig. 1c) relative to the groove axis. A significant reduction in the lateral force values (up to ten times) between bare and covered graphene for both orientations (Fig. 1b,d) was observed, confirming the excellent lubrication performance of single-layer graphene. On the other hand, the lateral force profile (data not shown here) of the graphene covered region is strongly dependent on the scan direction, being periodically modulated when scanning orthogonal to the grooves axis and almost flat when scanning parallel to the grooves axis. The anisotropic graphene response was furtherly demonstrated by load dependence friction curves obtained by orthogonal- and parallel-sliding movements (Fig. 1e). The difference in shear stress evaluated from these curves (Fig. 2) shows a preferential scanning direction parallel to the grooves axis. This indicates that the anisotropic strain distribution in the graphene monolayer induced from the textured surface plays a pivotal role in regulating the friction force.

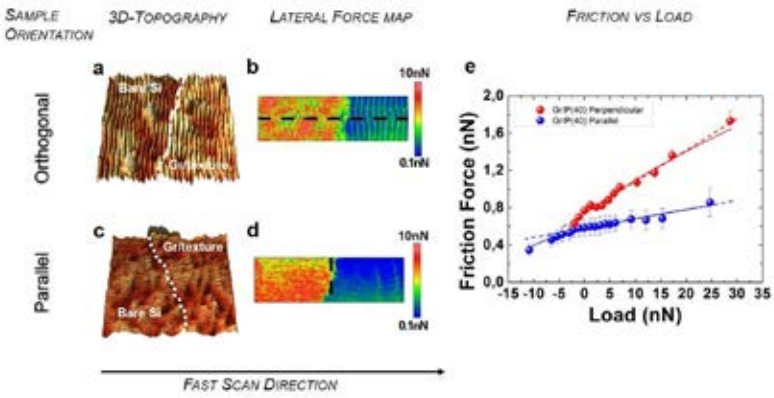

Fig. 1
a) Topography image (1.0 × 1.0 μm²) and b) lateral force map (1.0 × 0.3 μm²) measured on GrP40 sample at applied normal load ≈30 nN for grooves axis aligned orthogonal to the fast scan direction. The white dashed line in topography profiles represents the interface between the bare and graphene covered region. c) Topography image (1.0 × 1.0 μm²) and d) lateral force map (1.0 × 0.3 μm²) with groove axis aligned parallel to the fast scan direction at applied normal load ≈ 25 nN. e) Load dependent friction force curves on the same sample with the grooves axis oriented parallel (blue) and perpendicular (red) to the fast scan direction on the graphene covered region. Continuous lines are the fitting curve from Derjaguin–Muller–Toporov model and dashed line is the linear fit.

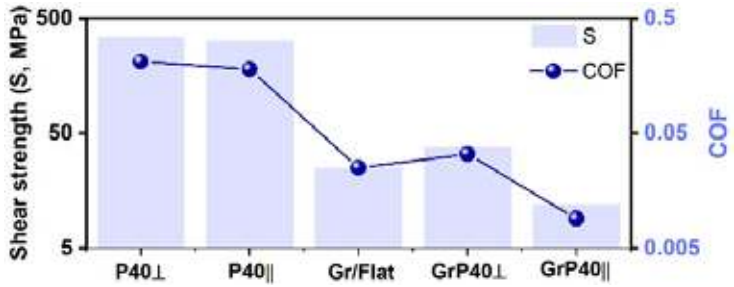

Fig. 2
Modulation in the shear strength (S, MPa) and coefficient of friction values at different scanning directions. Graphene on a flat surface lies intermediate between values obtained by scanning parallel (|||) and perpendicular (⊥) to the groove axis.

Contact person
Guido Paolicelli (guido.paolicelli@nano.cnr.it)

Reference
[1] Graphene confers ultralow friction on nanogear cogs. A. Mescola, G. Paolicelli, S. P. Ogilvie, R. Guarino, J. G. McHugh, A. Rota, E. Iacob, E. Gnecco, S. Valeri, N. M. Pugno, V. Gadhamshetty, M. M. Rahman, P. Ajayan, A. B. Dalton, and M. Tripathi. Small 17, 2104487 (2021).

Polymeric piezoelectric and pyroelectric energy harvesting devices

Piezoelectric and pyroelectric energy harvesters are interesting for powering wireless devices and wearable/ implantable systems. In this work, we realized and investigated the properties of energy harvesters composed of polymeric fibers and films. We demonstrated that not only crystallinity but also surface chemistry is crucial for improving piezoelectric performance in polyvinylidene fluoride (PVDF) fibers, whereas in pyroelectric films the measured output voltages are found to be influenced by the voltmeter's resistance and capacitance.

Polymeric nanomaterials capable of converting either mechanical or thermal stresses into electricity are of great interest for the realization of sustainable energy sources. Among the potential candidates, polyvinylidene fluoride (PVDF) provides piezoelectric, pyroelectric, and ferroelectric features combined with high mechanical strength, thermal stability, and biocompatibility. In particular, the all-trans β phase of PVDF shows the highest piezoelectric and pyroelectric character. An enhancement of the β phase content can be obtained by processing the material through electrospinning, which is a high-throughput technology that generates polymeric fibers from a solution continuously extruded through a nozzle by means of an electric field (~100 kV/m). In this work, we highlighted that the β phase content in PVDF nanofibers depends on the voltage polarity and ambient relative humidity (RH%) (Fig. 1a) [1]. In particular, by reducing the RH% level from 60% to 30%, the wrinkled and porous fiber's morphology modifies into a smooth and uniform one. Also, a 2-fold enhancement of the β phase content was observed at higher RH%, while the larger piezoelectric d_{33} coefficient (5.5 pm·V^{-1}, Fig. 1b) was measured in fibers spun with humidity of 60% and negative voltage polarity by piezoresponse force microscopy (PFM) [1]. These fibers enabled the realization of devices generating a power density up to 0.60 μW·cm^{-2} (Fig. 1c). Temperature fluctuations (30–34°C) can additionally be converted into electrical energy by exploiting the pyroelectric effect of PVDF. The output generated voltages of a device based on a film of PVDF was measured by using voltmeters exhibiting different internal resistance (RV) and capacitance (CV) (Fig. 1d) [2]. Remarkably, the measured output voltage increased with the RV and for positive temperature fluctuation, voltage outputs show both positive and negative values (Fig. 1e). Assisted by theoretical modeling, we pointed out that such findings are due to the finite RV and CV which sustain 'leakage' charges to move between the electrodes and we suggested that the use of infinite RV and low CV voltmeters would provide the most correct output measurements.

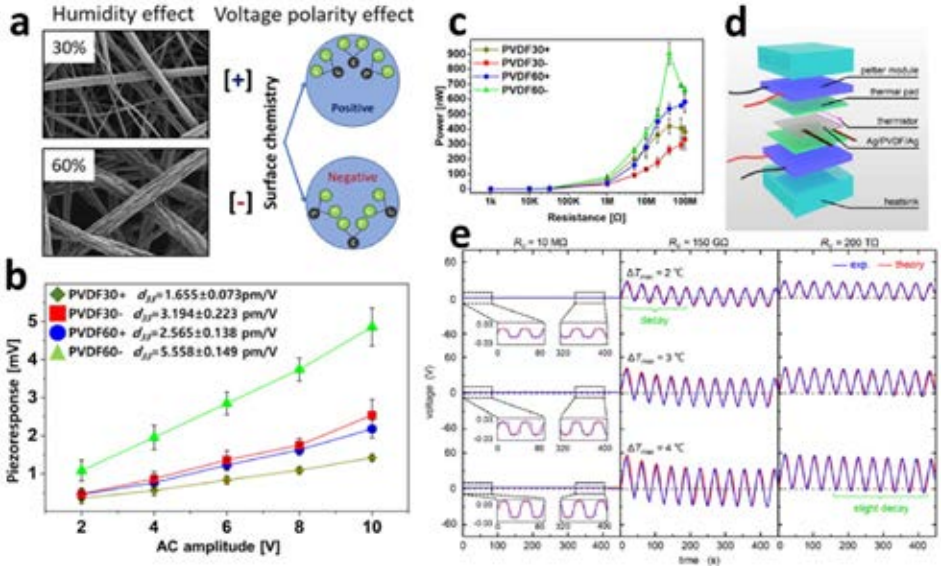

Fig. 1
a) SEM micrographs of PVDF fibers obtained at different ambient relative humidity levels and schematic of the voltage polarity (±) influence on the surface chemistry. b) Piezoresponse plot of single PVDF fibers as measured with PFM. c) Piezoelectric power output of different PVDF based devices tested across load resistances from 1k to 100 MΩ. Reproduced from ref. [1] under the terms of the CC-BY license. Copyright 2020 American Chemical Society. d) Schematic illustration of the pyroelectric device and the temperature controller used for the performance characterization. e) Experimental and theoretical comparison of the output voltage of pyroelectric devices as measured by three voltmeters with different inner resistances. Reproduced with permission from ref. [2] Copyright 2021, Elsevier Ltd.

Contact person
Luana Persano (luana.persano@nano.cnr.it)

References
[1] Enhanced Piezoelectricity of Electrospun Polyvinylidene Fluoride Fibers for Energy Harvesting. P. K. Szewczyk, A. Gradys, S. K. Kim, L. Persano, M. Marzec, A. Kryshtal, T. Busolo, A. Toncelli, D. Pisignano, A. Bernasik, S. Kar-Narayan, P. Sajkiewicz, and U. Stachewicz. ACS Appl. Mater. Interfaces 12, 13575 (2020).
[2] On the evaluation of output voltages for quantifying the performance of pyroelectric energy harvesters. Q. Li, S. Li, D. Pisignano, L. Persano, Y. Yang, and Y. Su. Nano Energy 86, 106045 (2021).

Surface properties and doping of few layer black phosphorus

A broad range of surface science techniques and ab initio simulations are employed to investigate and optimize the properties of exfoliated black phosphorus (bP). The treatment with Ni nanoparticles (NPs) allows to greatly improve the stability of few-layer bP flakes in ambient conditions. Copper deposition is demonstrated to induce charge transfer n-type doping of bP flakes. Exploiting the potential of a local surface investigation by scanning tunneling spectroscopy (STS), intriguing phenomena such as Coulomb blockade, and short-range doping are unveiled.

Among 2D materials, exfoliated black phosphorus (bP) has recently emerged because of its outstanding properties, i.e., modulation of the direct band gap, in-plane anisotropy, high charge-carrier mobility at room temperature, thus having a broad prospect for applications in electronic devices [1,2] and in energy storage. However, it shows higher chemical reactivity in comparison to other 2D materials, implying a lower stability. Moreover, the high concentration of P vacancies makes bP an intrinsically p-type material.

We here report on a relevant enhancement of ambient stability in bP when decorated with Ni NPs [3]. A combined characterization with TEM, Raman and x-ray spectroscopies provides quantitative insight of the oxidation process taking place at the bP surface with and without Ni NPs (work performed in collaboration with Cnr Iccom).

Furthermore, we explore surface charge transfer n-type doping of bP flakes by copper using Scanning Tunneling Microscopy (STM) and Spectroscopy (STS) at room temperature [4], see Fig. 1 a-c. STS reveals a gap opening at Cu islands, tentatively attributed to Coulomb blockade phenomena. Moreover, while n-type doping of bP by Cu is effectively demonstrated, line spectroscopy shows that it is very short-ranged, as shown in Fig. 1d. First-principles simulations give an atomistic understanding of these experimental evidences, allowing us to quantify the role of cluster size for an effective n-type doping of bP and showing that an electronic decoupling of the topmost bP layer from the underlying layers takes place in presence of the Cu cluster (Fig. 1e), consistent with the Coulomb blockade interpretation. Our results provide new routes to reach an ambient stability of bP and a novel microscopic understanding—difficult to retrieve by transport measurements—of the Cu doping of bP, which appears promising for the implementation of bP-based electronic applications.

The work on Cu doping of bP has been carried out within the project SURPHOS – Surface properties of few layer black phosphorus investigated by scanning tunneling microscopy (Cnr Nano SEED collaborative project).

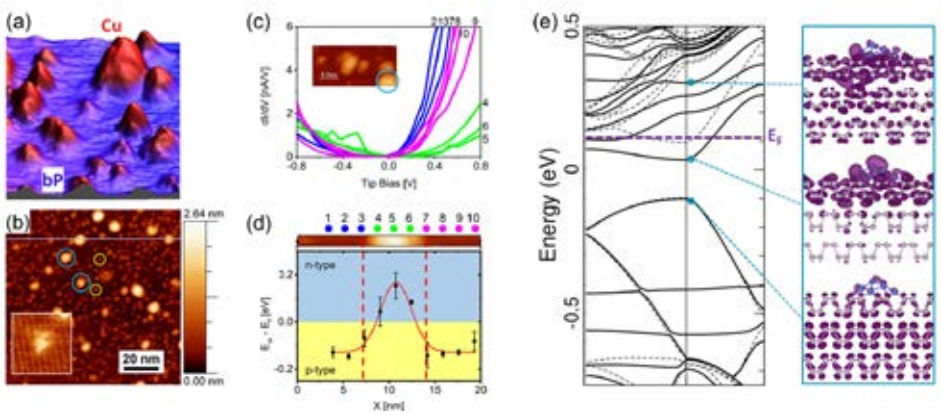

Fig. 1
(a,b) STM images of Cu islands on bP. (c) STS line spectroscopy across one island (blue circle in the inset). Numbers correspond to colored dots in panel d. (d) Midgap value of each spectrum with respect to the Fermi level, plotted as a function of lateral position. The plot field is colored with yellow and blue to indicate p-type and n-type doping regions, respectively. (e) Band structure of adsorbed Cu_n on 3-layer bP (solid line) as compared to pristine bP (dashed line), together with a few relevant Kohn–Sham squared wave functions showing the localization to the topmost bP layer of the states close to the Fermi level (EF).

Contact persons
Deborah Prezzi (deborah.prezzi@nano.cnr.it)
Stefan Heun (stefan.heun@nano.cnr.it)

References
[1] Ohmic contact engineering in few-layer black phosphorus: approaching the quantum limit. F. Telesio, G. Le Gal, M. Serrano-Ruiz, F. Prescimone, S. Toffanin, M. Peruzzini, and S. Heun. Nanotechnology 31, 334002 (2020).
[2] Nonclassical longitudinal magnetoresistance in anisotropic black phosphorus. F. Telesio, N. Hemsworth, W. Dickerson, M. Petrescu, V. Tayari, O. Yu, D. Graf, M. Serrano-Ruiz, M. Caporali, M. Peruzzini, M. Carrega, T. Szkopek, S. Heun, and G. Gervais. Phys. Status Solidi RRL 14, 1900347 (2020).
[3] Enhanced ambient stability of exfoliated black phosphorus by passivation with nickel nanoparticles. M. Caporali, M. Serrano-Ruiz, F. Telesio, S. Heun, A. Verdini, A. Cossaro, M. Dalmiglio, A. Goldoni, and M. Peruzzini. Nanotechnology 31, 275708 (2020).
[4] Black Phosphorus n-Type Doping by Cu: A Microscopic Surface Investigation. A.Kumar, F. Telesio, D. Prezzi, C. Cardoso, A. Catellani, S. Forti, C. Coletti, M. Serrano-Ruiz, M. Peruzzini, F. Beltram, and S. Heun. J. Phys Chem. C 24, 13477 (2021).

Deterministic Graphene organic functionalization: a controlled functionalization for energy storage and sensing

The outstanding properties of graphene rely on its perfect 2D hexagonal crystal. However, this perfection represents a limit in its use for sensing and storage applications, due to the weak interactions and chemical reactivity. Performance can be improved by increasing the useful surface in 3D arrangements or via functionalization. We achieved organic functionalization of graphene nanosheets and reduced graphene oxide. Next, we induced defects by electron irradiation, in order to control the functionalization. A deterministic functionalization at defect sites has thus been obtained, opening the way towards the controlled synthesis of graphene-based complex structures and devices at the nanoscale.

Organic functionalization of graphene represents a flexible solution for the realization of a platform selectively sensitive to target molecules or atoms, which provides a perspective for a large-scale use in sensing and storage applications. Among the possible routes for an organic functionalization, the use of cycloaddition reaction is one of the most appealing, due to its reversibility and the high controllability of the reaction. This research moves from the random functionalization of graphene, to optimize the reaction parameters, toward a high quality substrate and a fully controlled functionalization. In this framework, organic functionalization of graphene nanosheets (GNS) and reduced graphene oxide (RGO) is successfully performed via 1,3-dipolar cycloaddition of azomethine ylide in the liquid phase [1], and confirmed using various techniques.

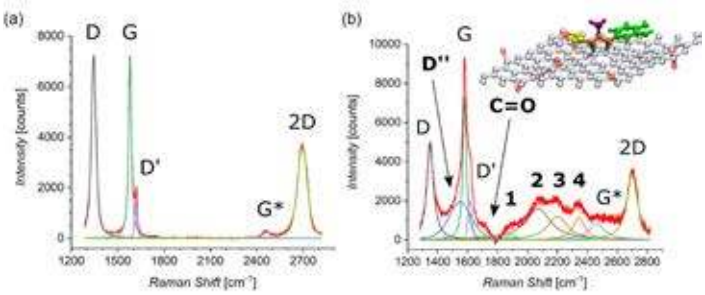

Fig. 1
Raman spectra of (a) pristine GNS and (b) functionalized GNS. The fit of each spectrum is shown and all peaks are labeled (the peaks that appear only after the functionalization of GNS by 1,3-DC of azomethine ylide in N,N-dimethylformamide (DMF) are in bold).

Among them, energy-dispersive X-ray spectroscopy allows to map the pyrrolidine ring of the azomethine ylide on the surface of functionalized graphene, while micro-Raman spectroscopy detects new features arising from the functionalization (Fig. 1), in agreement with the power spectrum obtained from ab initio molecular dynamics simulations. Moreover, XPS of functionalized graphene allows the quantitative elemental analysis and the estimation of the surface coverage, showing a higher degree of functionalization for RGO. This more reactive behavior originates from the localization of partial charges on its surface due to the presence of oxygen defects, as shown by the simula-

tion of the electrostatic features. This behavior suggests the use of defect engineering to control the functionalization (Fig. 2). Therefore, a further step is to induce defects by electron irradiation [L. Basta et al., Surfaces and Interfaces 28, 101694 (2022)] on a high quality exfoliated graphene in order to selectively functionalize the irradiated area with high lateral resolution, obtaining a deterministic functionalization [L. Basta et al., arXiv:2202.06609] (Fig. 3). Deterministic functionalization of graphene using 1,3-dipolar cycloaddition is shown to be a significant step towards the controlled synthesis of graphene-based complex structures and devices at the nanoscale.

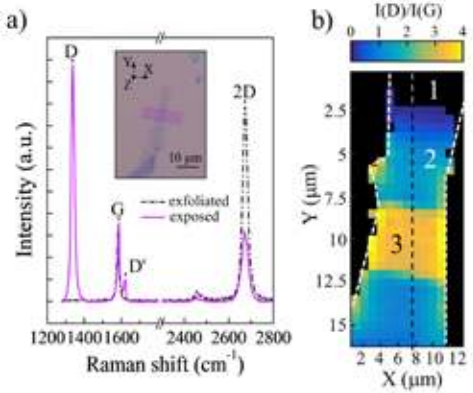

Fig. 2
a) Representative Raman spectrum of as-exfoliated (black dash-dotted curve) and e-beam exposed graphene (violet curve). Inset shows the optical microscopy image of the graphene flake, where the violet area indicates the exposed area. b) Two-dimensional spatial distribution of I(D)/I(G). The white dashed lines indicate the flake edges.

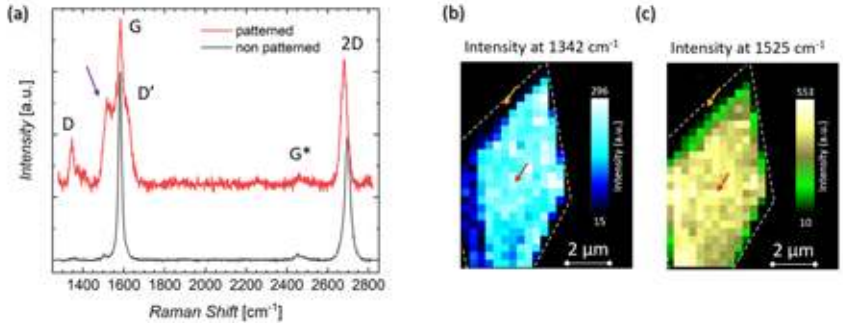

Fig. 3
(a) Raman spectra of a functionalized flake collected in the non-patterned (black line) and patterned (red line) areas of the flake (shifted in height). New Raman features are visible only in the spectrum of patterned functionalized graphene. The arrow indicates the peak used to obtain (c). Raman maps of (b) D peak intensity and (c) intensity at 1525 cm^{-1} collected on the same flake after the functionalization procedure (the white dashed line follows the edges of the flake).

Contact persons
Stefano Veronesi (stefano.veronesi@nano.cnr.it)
Stefan Heun (stefan.heun@nano.cnr.it)

Reference

[1] Covalent organic functionalization of graphene nanosheets and reduced graphene oxide via 1,3-dipolar cycloaddition of azomethine ylide. L. Basta, A. Moscardini, F. Fabbri, L. Bellucci, V. Tozzini, S. Rubini, A. Griesi, M. Gemmi, S. Heun, and S. Veronesi. Nanoscale Advances 3, 5841 (2021).

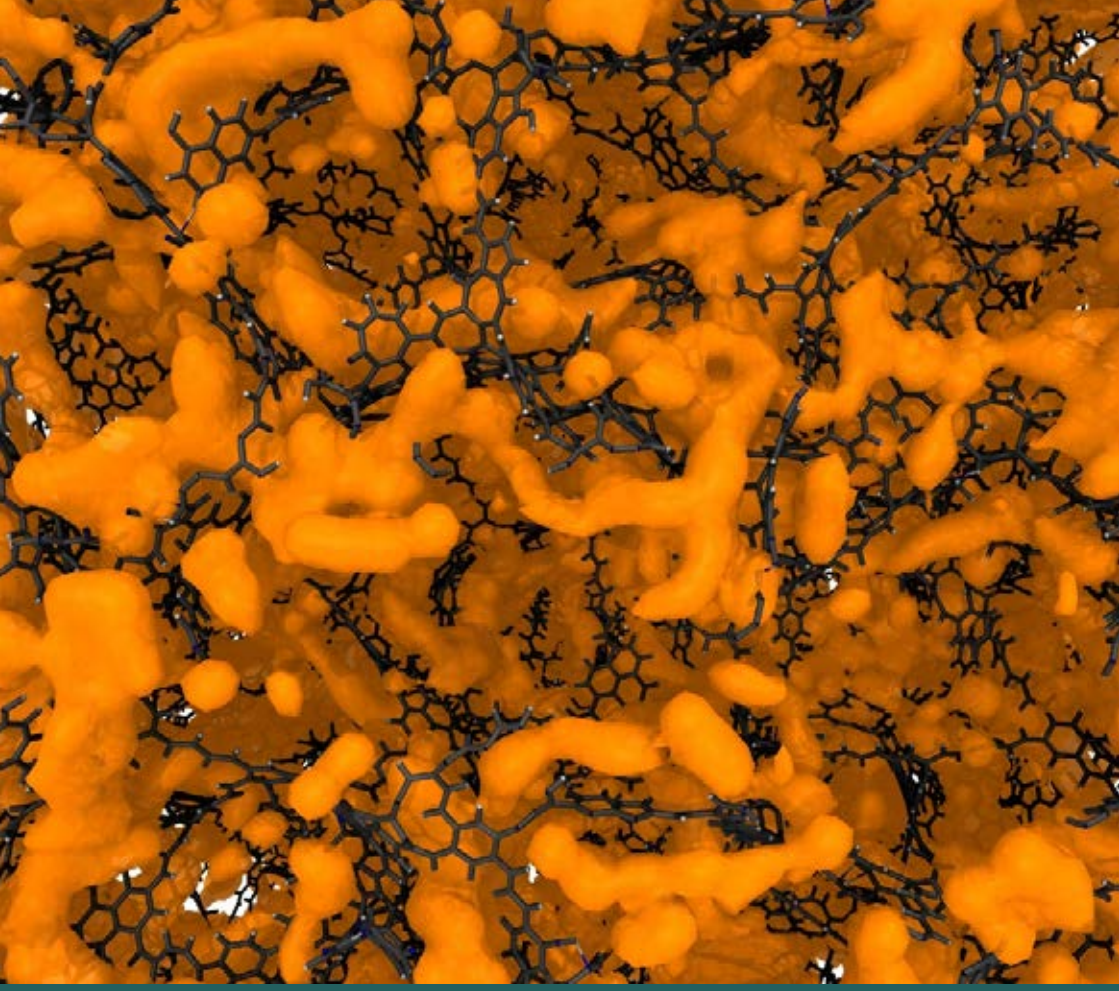

Highlights
-
Nanoscale theory modelling and computation

Introduction to Nanoscale theory modelling and computation

Theory modelling and simulations are an ever important part of the Cnr Nano research activities. Making use of the fast progresses in computer technology and new paradigms such as high-throughput or artificial intelligence, they allow to greatly accelerate the design and understanding of new materials and simulate complex and realistic devices, as well as understanding fundamental physics problems.

One aspect of these activities is the use of **state-of-the-art calculation methods and large scale simulations** to address cutting-edge scientific problems in the fields of nanoscience and nanomaterials, relevant in a wide range of applications, from environmental and energy problems, such as light harvesting and photocathalysis, to quantum technologies such as spintronics and high-density data storage. Another aspect is the study of fundamental physics problems such as **new states of matter**. This research area also contributes to the development of **new theory and algorithms**, made available to the whole scientific community through open source software and databases.

Ab-initio theoretical calculations are often able to draw insights on experimental measurements and at times are decisive in distinguishing between different physical interpretations. In a first principles calculations study, it was shown that MoS2 under pressure is unstable against the spontaneous generation of excitons. A previously observed Raman feature was now identified with the onset of an excitonic insulator phase, thus providing a direct spectroscopic fingerprint of this long-sought permanent Bose-Einstein condensate of excitons. In the field of light matter-interaction, it was possible to track an optically bright state and its abrupt transition into a dark state in molecular aggregates relevant for photovoltaics while **non-adiabatic dynamics simulations** were used to identify the source of this behaviour. First principles simulations in combination with scanning tunnelling microscopy were employed to investigate molecular motors on surfaces, in order to identify the role of the surface on the chemical processes at the basis of the molecular motion.

Either by using high-throughput techniques interfaced with atomistic approaches and statistical analysis, or machine learning applied to molecular dynamics using empirical reactive force fields, large scale simulations are an useful tool in the **design and optimisation of new materials and devices**. An example of this is the work on transition metal rocksalt crystals and superlattices with tunable optical properties in view of plasmonic and nano-optical applications. A further example is the design of nanoporous graphene scaffolds for environmental applications, done by determining **the correlation between final structural properties and synthesis parameters**. The third case is the design of a **multifunctional switch for molecular spintronics**, triggered both optically and magnetically, possibly due to a joint theoretical experimental study of molecular radicals anchored on gold nanoparticles.

The development of **new theory and algorithms** accompanies the progress of computer technology. Several theoretical innovations have been made in order to **extend the present density functional theory** methods to the treatment of stationary excited states and excitations in strongly correlated materials. Within many-body perturbation theory, contributions such as the new **multipole approximation** used within the GW approximation, significantly increase accuracy without aggravating the computational cost. Many of these developments have been included in open-source scientific software with a wide diffusion among the scientific community. Cnr Nano researchers have also contributed to a comprehensive overview of **electronic-structure methods for materials design**, discussing its recent history, new possibilities, and how innovations in the field are changing the entire research ecosystem.

Magnetic order and spinterface of metal-free molecular radicals

The field of organic radical thin-films has undergone an incredible boost in view of a plethora of promising applications that range from emerging quantum technologies to spintronics and high-density data storage devices, as confirmed by the increasing investments by electronics majors and ITC companies. Here, we present a joint theoretical experimental set of papers which investigate the electronic and magnetic properties of thin film composed of molecular radicals, with multiple spins and without transition metal elements.

Metal-free organic radicals are fascinating materials which combine stable magnetic moments and light chemical elements (C, N, B). Molecular radicals are promising materials that intersect with many different fields such as organic/molecular spintronics and electronics, organic magnetism, and quantum computing, not least because of their tremendous flexibility by chemical design. Among them, organic radicals have been recently proposed as molecular spin qubits. However, what happens with the spin of a metal-free molecule in the solid-state or in a metal/metal-oxide interface is largely unknown.
In this work we investigated the magnetic, electronic, and optical properties of metal-free radicals in the solid state (thin films) [1-2; Chem 8, 1 (2022)] and/or anchored to gold nanoparticles [3]. We demonstrated for the first time the possibility of having a long-range magnetic (antiferromagnetic) order in ultra-thin films (Fig. 1), which can be controlled during the evaporation growth; as well as the possibility to stabilize high-spin radicals (S=1/2, S=1, S=3/2) in thin films, which are stable in air and room temperature [1,2]. The simultaneous presence of permanent magnetic moment and high π-like aromatic rings results in highly-conductive magnetic systems that can be used for organic electronics; while the absence of heavy transition metals reduces the spin-orbit spin-flip and fosters long-living quantum states. Finally, the anchoring of molecular radicals on gold nanoparticles (Fig. 2) allowed the realization of an unprecedented stable, and highly reversible multifunctional switch triggered by both optical and magnetic stimuli, for molecular spintronics [NanoLett 22, 768 (2022)].
This work is based on extended collaborations among European (Univ. Tubingen, DE; Univ. Hamburg, DE; ICMAB-CSIC, ES) and US (Univ. Nebraska, NB) experimental groups. The entire theoretical study (simulation and modeling) is a full Cnr Nano outcome.

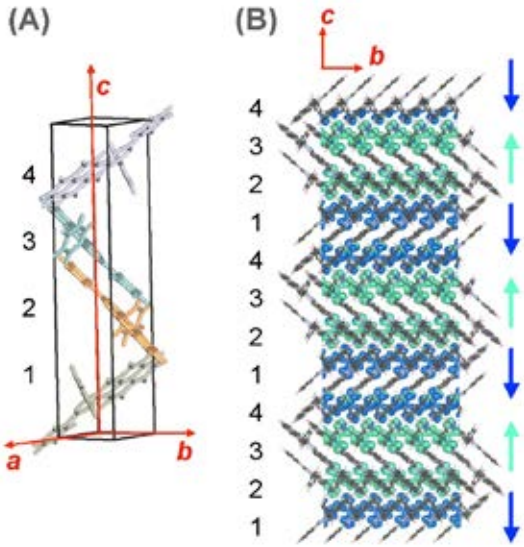

Fig. 1
(A) Primitive cell of monoclinic Blatter-pyr crystal. Labels 1-4 indicate the four molecules in the cell. (B) Side view of the 9 mm-thick film. Colored isosurfaces represent the charge spin-density plots for the antiferromagnetic phase. Green (blues) color indicates the majority (minority) spin-up (spin-down) orientations of single radicals. Picture adapted from [Chem 8, 1 (2022)].

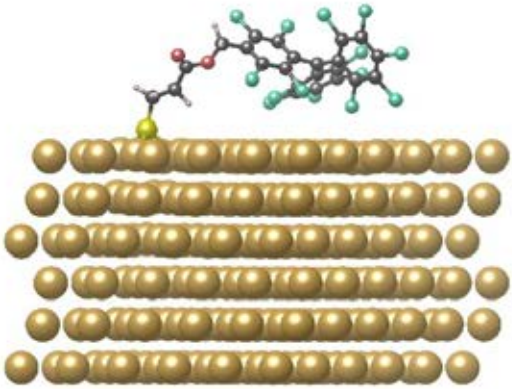

Fig. 2
Atomic structure surface molecular switch base on Au nanoparticles decorated with persistent perchlorotriphenylmethyl (PTM) radicals. Picture adapted from [NanoLett 22, 768 (2022)].

Contact person
Arrigo Calzolari (arrigo.calzolari@nano.cnr.it)

References
[1] Challenges in controlled thermal deposition of organic diradicals. T. Junghoefer, N. M. Gallagher, K. Kolanji, E. Giangrisostomi, R. Ovsyannikov, T. Chassé, M. Baumgarten, A. Rajca, A. Calzolari, and M. B. Casu. Chem. Mater. 33, 2019 (2021). Front cover.
[2] From radical to triradical thin film processes: the Blatter radical derivatives. A. Calzolari, A. Rajca, and M. B. Casu. J. Mater. Chem. C 9, 10787 (2021).

Plasmonic by design

By using high-throughput techniques, based on the combination of atomistic first principles calculations and statistical analysis, we designed and characterized a class of transition metal rocksalt crystals and superlattices with tunable optical properties in the visible and near-IR range. These systems are proposed as multifunctional materials for plasmonic and nano-optical applications, which combine tunable plasmonic properties to mechanical and chemical stability, easy growth, CMOS compatibility, and low costs. The atomistic approach used in this set of works allowed us to investigate the role of composition, stoichiometry and disorder on the plasmonic properties of these materials.

The manipulation of light on the deep subwavelength scale is essential for enhancing light-matter interactions and improving the performance of nanophotonic devices. In particular, hyperbolic metamaterials (HMMs) are highly anisotropic optical materials that behave as metals or as dielectrics depending on the direction of propagation of light. Their extraordinary optical properties made HMMs essential for a plethora of applications, ranging from aerospace to automotive, from wireless to medical and IoT. All these applications rely on the delicate balance between localization and loss of electronic excitations upon interaction with the impinging radiation. In this regard, the possibility to control and tune the optoelectronic properties of materials assumes a paramount relevance in the development of nanophotonics. Achieving the tunability of the electronic and optical properties of metal bulk and films is a difficult task. The coupling of optical properties with specific mechanical characteristics, chemical and thermal stability, CMOS compatibility, and low cost prevents the use of simple systems, such as noble metals. This calls for materials that show enhanced optical properties as well as tailorable mechanical and chemical properties.

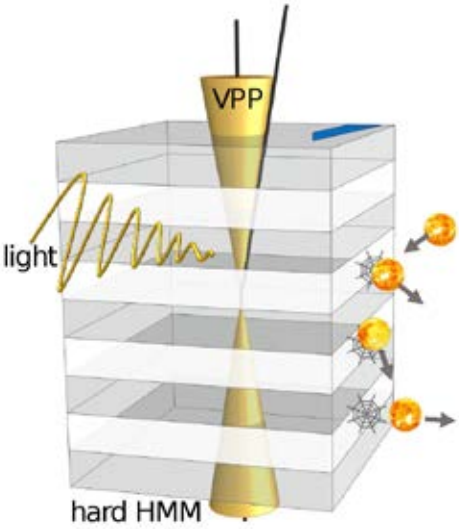

Fig. 1
Pictorial sketch of a rocksalt-based superlattice acting as mechanically hard hyperbolic metamaterial. The yellow cone identifies the excitation of a volume-plasmon polariton (VPP) along the stack upon proper light excitation. Picture adapted from Ref. [2]

Here, we adopted massive high-throughput techniques, based on density functional theory, to design and characterize tunable plasmonic materials that can be used as optical HMMS in the near-IR and visible range. Starting from simple transition-metal crystals (such as nitrides and carbides), we [1] investigate the role of composition, off-stoichiometry, and structural disorder in TiN_x compounds, and [2] we provide an efficient strategy to fine engineering stable, easy-to-grow HMM superlattices, with selected optical and mechanical hardness (both ultrasoft and hard materials), see Fig. 1. Once validated by the experiments, this new class of metamaterials may foster previously unexplored optical/mechanical applications in extreme conditions, e.g., in the fields of aerospace, satellites, and security systems.

Contact persons
Alessandra Catellani (alessandra.catellani@nano.cnr.it)
Arrigo Calzolari (arrigo.calzolari@nano.cnr.it)

References
[1] Tailoring the plasmonic properties of metals: the case of substoichiometric titanium nitride. A. Catellani, P. D'Amico, and A. Calzolari. Phys. Rev. Mater. 4, 015201 (2020).
[2] Hyperbolic metamaterials with extreme mechanical hardness. A. Calzolari, A. Catellani, M. Buongiorno Nardelli, and M. Fornari. Adv. Opt. Mater. 9, 2001904 (2021). Front Cover.

Electronic-structure methods and High Performance Computing for materials design

Electronic-structure simulations are an extensive part of the design and understanding of new materials and can greatly accelerate their identification, characterization, and optimization. The fast progress on computer technology requires corresponding advances in theory and algorithms, with special focus on accuracy and efficiency. To this purpose we have contributed to the development of new electronic-structure methods, both at the density functional theory and the many-body perturbation theory levels. These developments have been included in open-source codes with a wide diffusion among solid state physics and materials science researchers, in particular, Quantum Espresso and Yambo.

For the past twenty years, first-principles simulations have outgrown their initial core rooted in condensed-matter physics and quantum chemistry, becoming powerful and widely used tools. Significantly, applications of electronic-structure methods now range from nanotechnology to planetary science, from metallurgy to quantum materials. Their complexity and diversity have become vast enough to benefit from a comprehensive overview.
Review [1] outlines the framework of density functional theory, Green's function methods and many-body perturbation theory. It discusses their abilities to deliver predictions under realistic and ever-more complex conditions and highlights how physics-driven or data-driven approaches are changing the entire research ecosystem, through the use of high-throughput or artificial intelligence.

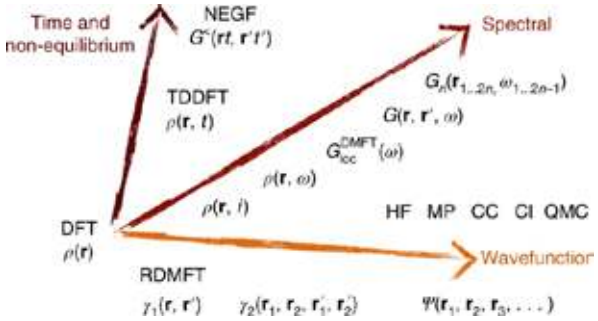

Fig. 1
The complex landscape of electronic-structure methods is captured here grouping hierarchies of methods that progressively extend scope and accuracy while increasing cost and complexity. From Ref. [1].

In parallel, we have developed new electronic-structure methods, included in wide diffusion open-source codes. Article [2] presents the ongoing efforts to port this open-source distribution of computer codes, renowned for its performance on a wide range of hardware architectures, onto heterogeneous architectures based on GPU accelerators, coupling exceptional performances to acceptable energy consumptions.

Within many-body perturbation theory, we are working on several aspects of the so-called GW approximation. One example is the new multipole approximation (MPA) [3], implemented within the YAMBO code, which gives a simplified yet accurate description of W and evaluation of the GW self-energy. The MPA technique delivers an accuracy comparable with much more computationally costly methods. Other developments were made in order to increase the accuracy using lower convergence parameters for 2D semiconductors, or to treat the frequency dependence, introducing an algorithmic inversion method that can be applied to dynamical potentials expanded as sum-over-poles, used in many advanced electronic-structure methods.

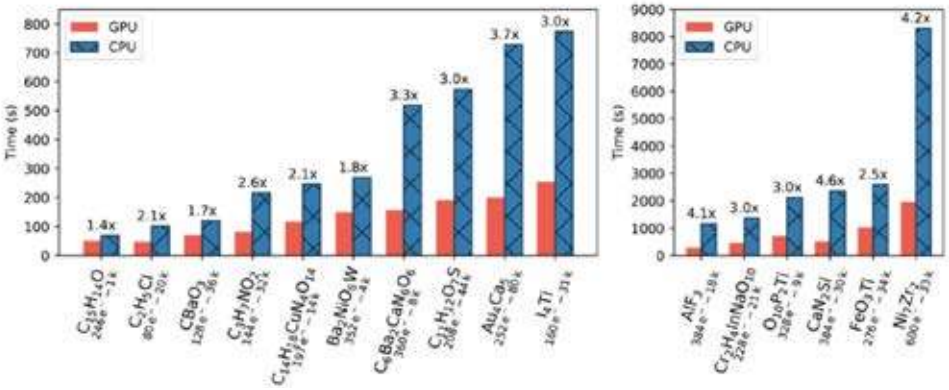

Fig. 2
Collection of benchmarks performed with Quantum ESPRESSO v. 6.5 and QE-GPU v. 6.5 on an 18-core Intel(R) Xeon(R) E5-2697 v4 @ 2.30 GHz or the same CPU plus a NVIDIA V100 card. From Ref. [2].

Contact person
Andrea Ferretti (andrea.ferretti@nano.cnr.it)

References
[1] Electronic-structure methods for materials design. N. Marzari, A. Ferretti, and C. Wolverton. Nature Materials 20, 736 (2021).
[2] Quantum ESPRESSO toward the exascale. P. Giannozzi, O. Baseggio, P. Bonfà, D. Brunato, R. Car, I. Carnimeo, C. Cavazzoni, S. de Gironcoli, P. Delugas, F. Ferrari Ruffino, A. Ferretti, N. Marzari, I. Timrov, A. Urru, and S. Baroni. J. Chem. Phys. 152, 154105 (2020).
[3] Frequency dependence in GW made simple using a multipole approximation. D. A. Leon, C. Cardoso, T. Chiarotti, D. Varsano, E. Molinari, and A. Ferretti. Phys. Rev. B 104, 115157 (2021).

Understanding and predicting excitations in materials via easily computable quantum mechanics

Developing more efficient photovoltaics, understanding biochemical processes, and harnessing quantum electronics – just to mention a few notable examples – require the study of quantum excitations of matter at the atomistic scale. On the one hand, in order to make this problem solvable with the available computational resources, the original problem must be reformulated and approximated. On the other hand, for the results to be quantitatively significant, they should be sufficiently accurate. In support of such an endeavor, we have put forward several theoretical innovations that extend the present density functional theory methods to the treatment of stationary excited states, excitations in strongly correlated materials, and the calculation of the electronic gap for arrays of quantum dots.

Density functional theory (DFT) is the workhorse of computational materials science, but it works only for non-excited states. In [1,2] we show how, via auxiliary mixed states, standard DFT methods can alternatively be extended to work also for stationary excited states. The results obtained for single- and (the challenging case of) double-excitations demonstrate that our new approach is competitive against prominent, yet computationally more expensive, alternatives. Fig. 1 outlines the key elements and the main logical steps of the approach.

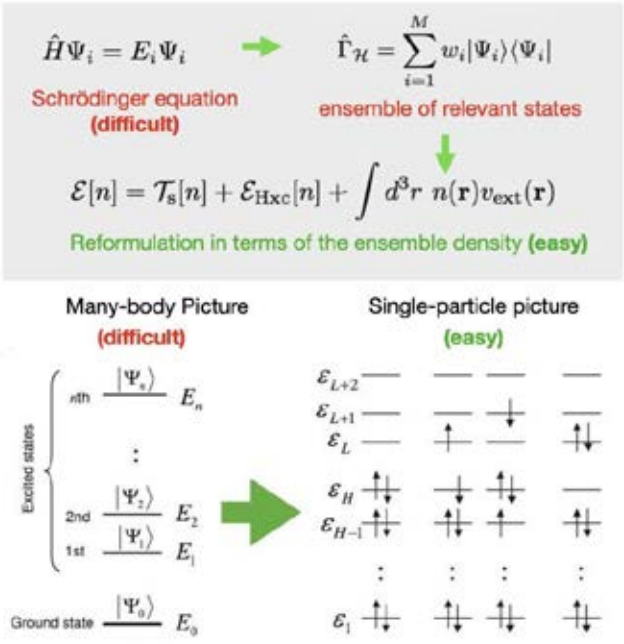

Fig. 1
Ensemble density functional theory [1,2] and, analogously, the newly proposed ensemble reduced density matrix functional theory [3] allow us to reformulate the initial (difficult) problem of solving the Schrödinger equation for an ensemble of many-body excitations into a (much easier) problem of searching for a minimum of the ensemble energy by only dealing with single-particle quantities.

Accurately tackling strongly correlated materials remains a difficult task via DFT methods – it is especially true in the case of excitations. In [3] we propose a solution to this challenge by first pointing out, and then building, on a Pauli-like exclusion principle for mixed states. In this approach, one must switch from the functional of the ensemble particle density to the functionals of the ensemble one-body reduced density; the rest of the logical steps are analogous to the ones depicted in Fig. 1 for ensemble DFT.

Arrays of quantum dots can be used to engineer electronic devices with tailored properties. The (so-called) fundamental gaps concern excitations involving exchange of particles, such as the exchange of electrons through a transistor from/to the rest of the circuit. We then show how to determine the fundamental gaps for arrays of quantum dots by unprecedentedly agile computations [4]. Fig. 2 sketches the system we have considered along with the corresponding energy levels.

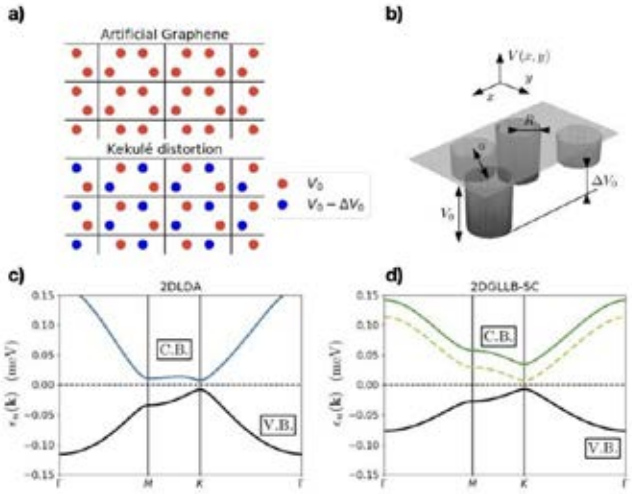

Fig. 2
a) Periodic array of quantum dots in a graphene-like configuration. Electrons can move throughout the array or get confined in the quantum dots. b) Distortions can be introduced by tailoring the confinements realized via the quantum dots. c) Energy levels for a Kekulé-distorted graphene-like array obtained using the local-density approximation (2DLDA). d) Energy levels form our new approach, (2DGLLB-SC). The energy gaps, that appear on introducing distortions in the confinements, are greatly underestimated in 2DLDA; more realistic values are obtained via our approach, yet keeping calculations agile [4].

Contact person
Stefano Pittalis (stefano.pittalis@nano.cnr.it)

References

[1] Ensemble density-functional theory: Insight from the fluctuation-dissipation theorem. T. Gould, G. Stefanucci, and S. Pittalis. Phys. Rev. Lett. 125, 233001 (2020).
[2] Double Excitations from Ensemble Density Functionals: Theory and Approximations. T. Gould, L. Kronik, and S. Pittalis. Phys. Rev. A 104, 022803 (2021).
[3] Ensemble reduced density matrix functional theory for excited states and hierarchical generalization of Pauli's exclusion principle. C. Schilling and S. Pittalis. Phys. Rev. Lett. 127, 023001 (2021).
[4] Density-functional approach to the band gaps of finite and periodic two-dimensional systems. A. Guandalini, A. Ruini, E. Räsänen, C. A. Rozzi, and S. Pittalis. Phys. Rev. B 104, 085110 (2021).

Molecular motors at surfaces: insights from first-principles simulations

First principles simulations based on Density Functional Theory (DFT) are employed to investigate adsorption and stability of molecular motors (MMs) at metallic and semiconducting surfaces, in combination with Scanning Tunneling Microscopy (STM) studies. Charge transfer effects as well as local modifications of the potential energy landscape of the MM states are identified as key aspects of the role of the surface on the chemical processes at the basis of the molecular motion.

Molecular motors (MMs) are able to convert electrical, optical, or chemical energy into controlled motion. Usually active in biological matter, these processes are mimicked by artificial MM in solution, which have seen enormous developments during the last decades. However, a fundamental application of MMs is in molecular machines used for the transport of material along a given path, which cannot be realized with freely-floating molecules. While a surface is thus essential, offering the advantage to constrain the motion in 2d, molecule-surface interaction can inhibit molecular motion either via strong adsorption, or by quenching electronic states required for the chemical process. All of these difficulties make MMs only scarcely studied at surfaces.

We have investigated the structural and electronic properties of a unidirectional Feringa motor (Fig. 1a) adsorbed on prototypical metallic and wide-gap semiconducting surfaces, i.e., Cu(111) and rutile TiO_2(110), by employing DFT simulations. On both surfaces, atomic-scale configuration and adsorption geometry are univocally identified by combining STM studies (*) with total energy DFT calculations and STM image simulations. On TiO_2 (Fig. 1b), our simulations reveal that, despite the weak interaction, the MM transfers charge to the surface, and this turns out to affect adsorption stability. Moreover, they show that small polarons, introduced by surface hydroxyls, can act as adsorption traps for the MMs [1]. On Cu(111) (Fig. 1c), we demonstrate that the presence of the metal surface strongly distorts the potential energy landscape of the MM states, leading to the stabilization of one of the intermediate states that are involved in the helix inversion as part of the motor rotary cycle, which becomes the preferred adsorption geometry at room temperature. These results represent important, though still preliminary, steps towards the long-term goal of fully taking advantage of the surface itself to steer and, ultimately, control the molecular motion.

(*) These works were performed in collaboration with the group of Prof. Leonhard Grill (Graz University).

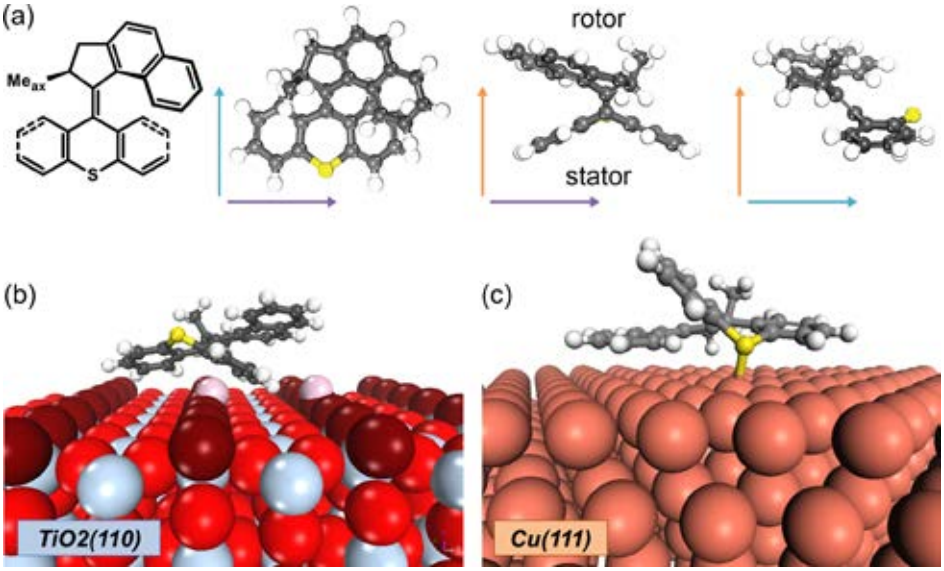

Fig. 1
(a) Chemical structure and calculated gas-phase geometry of the studied molecular motor (MM) viewed from different angles (gray, carbon; yellow, sulfur; white, hydrogen). (b) Perspective view of the MM trapped at hydroxyl groups on the TiO_2(110) surface. (c) Perspective view of the MM adsorbed at the Cu(111) surface.

Contact person
Deborah Prezzi (deborah.prezzi@nano.cnr.it)

Reference
[1] Adsorption and Motion of Single Molecular Motors on TiO2(110). P. Jacobson, D. Prezzi, D. Liu, M. Schied, J. M. Tour, S. Corni, A. Calzolari, E. Molinari, and L. Grill. J. Phys. Chem. C 124, 24776 (2020).

Two-dimensional materials as excitonic insulators

In a series of papers we report theoretical and experimental evidence that monolayer WTe_2 and bulk MoS_2 under pressure host the long-sought excitonic insulator phase. This is a permanent Bose-Einstein condensate of excitons - electron-hole pairs bound by Coulomb attraction – that spontaneously form at thermodynamic equilibrium.

We claim that MoS_2 under pressure [1] and monolayer WTe_2 [2] are "excitonic insulators" (EIs). The long-sought EI is a permanent Bose-Einstein condensate of excitons, electron–hole pairs bound by Coulomb interaction, which form in the absence of optical excitation. A surge of experimental claims has recently addressed layered materials, because of reduced Coulomb screening. However, the transition to the putative EI is ubiquitously accompanied by the softening of a phonon inducing a structural change; therefore it remains unclear whether the observed phase is genuinely excitonic or instead stabilized by electron–phonon interaction.
Our first principles calculations [1] show that, for a range of applied pressure, MoS_2 is unstable against the spontaneous generation of excitons but stable against lattice distortion. We predict that the EI is an antiferroelectric, electronic density wave. At the onset of the EI phase, those optical phonons that share the exciton momentum provide a unique Raman fingerprint for the EI formation. We identify such a fingerprint in a Raman feature that was previously observed experimentally, thus providing direct spectroscopic confirmation of an EI phase in bulk MoS_2 above 30 GPa.
Furthermore, we present theoretical [2] and experimental evidence [Nature Physics 18, 94 (2022)] that the two-dimensional bulk of monolayer WTe_2 contains excitons that spontaneously form in thermal equilibrium. On cooling from room temperature to 100 K, the conductivity develops a V-shaped dependence on the electrostatic doping, while the chemical potential develops a step at the neutral point. These features are much sharper than possible in an independent-electron picture, but they can be accounted for if electrons and holes interact strongly and are paired in equilibrium. Our calculations from first principles show that the exciton binding energy is larger than 100 meV and the radius as small as 4 nm, explaining their formation at high temperature and doping levels. Below 100 K, a more strongly insulating behavior is seen, suggesting that a charge-ordered state forms. The observed absence of charge density waves in this state is surprisingly within an excitonic insulator picture, but we show that it can be explained by the symmetries of the exciton wavefunction. Therefore, in addition to being a topological insulator, monolayer WTe_2 exhibits strong correlations over a wide temperature range.

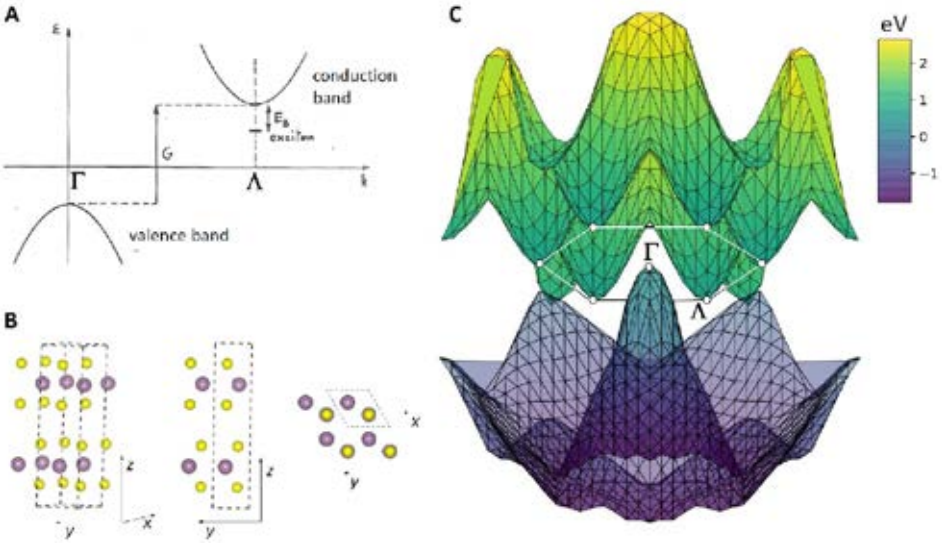

Fig. 1
Indirect-gap MoS_2 as a candidate excitonic insulator. (A) Sketch of the excitonic insulator instability, adapted from Walter Kohn's original proposal. An exciton binds an electron at the conduction band bottom, located at Λ in **k** space, with a hole at the valence band top at Γ. If the exciton binding energy, E_b, is larger than the indirect gap, G, then the system is unstable against the spontaneous generation of excitons. The reconstructed many-body ground state—a condensate of excitons at thermodynamic equilibrium—is the excitonic insulator. (B) Model of the $2H_c$ crystal structure from different views. The violet (yellow) color labels Mo (S) atoms. The dashed frame appearing in side and top views is the unit cell of the layered structure, with *a* and *c* being the in- and out-of-plane lattice constants, respectively. (C) Lowest conduction and topmost valence energy band as a function of wave vector in the k_z =0 plane, as obtained from first-principles many-body perturbation theory (GW) at a pressure of 34 GPa. After Ref. [1].

Contact persons
Massimo Rontani (massimo.rontani@nano.cnr.it)
Daniele Varsano (daniele.varsano@nano.cnr.it)

References
[1] Evidence of ideal excitonic insulator in bulk MoS2 under pressure. S. Ataei, D. Varsano, E. Molinari, and M. Rontani. PNAS 118, e2010110118 (2021).
[2] A monolayer transition metal dichalcogenide as a topological excitonic insulator. D. Varsano, M. Palummo, E. Molinari, and M. Rontani. Nature Nanotechnology 15, 367 (2020).

Intermolecular conical intersections in photovoltaic polimer aggregates

Conical intersections of multidimensional potential energy surfaces are ubiquitous in nature and control pathways of many photo-initiated intramolecular processes. Here, using ultrafast two-dimensional electronic spectroscopy, we tracked the coherent motion of a vibrational wave packet on an optically bright state and its abrupt transition into a dark state after only 40 fs in molecular aggregates relevant for photovoltaics. Non-adiabatic dynamics simulations identify an intermolecular conical intersection as the source of this dynamics. Our results indicate that intermolecular conical intersections may effectively steer energy pathways in functional nanostructures for optoelectronics.

We investigated thin films of solution-processable acceptor–donor–acceptor (ADA) oligomers consisting of two terminal dicyanovinyl groups as acceptor and a central dithienopyrrole-thiophene unit as donor. These oligomers have recently emerged as efficient photoactive materials in different applications such as organic photovoltaics, light-emission, sensors, and transistors.

The thin films were excited by broad-band 8-fs pulses centered around the low-energy excitation at 1.9 eV. At early waiting times, T < 20 fs, the two-dimensional electronic spectroscopy spectra of the aggregate thin film show a well-defined grid-like peak pattern that reflects the impulsive optical excitation of coherent vibrational wave packets. After T ≈ 45 fs, the 2DES maps are fundamentally different, as a much broader diagonal peak around 1.94 eV is seen.

This observation is rationalized by non-adiabatic simulations of the dynamics of the optically excited wave packet initiated in the Franck–Condon region. The ensemble average over semiclassical trajectories of the nuclear motion shows that the relative energy difference $\Delta E_{2,1}$ between the S_2 (bright) and S_1 (dark) states initially decays monotonically until, suddenly, it rapidly increases. The steep increase in $\Delta E_{2,1}$ is a direct signature of the unidirectional, non-adiabatic population transfer from S_2 to S_1 and strong evidence for an intermolecular conical intersection connecting them. After the crossing, large-amplitude oscillations of $\Delta E_{2,1}$ initiate.

The time evolution of the electronic transition density matrix reflects the spatial distribution of the optically excited wavefunction. As long as the system is in the S_2

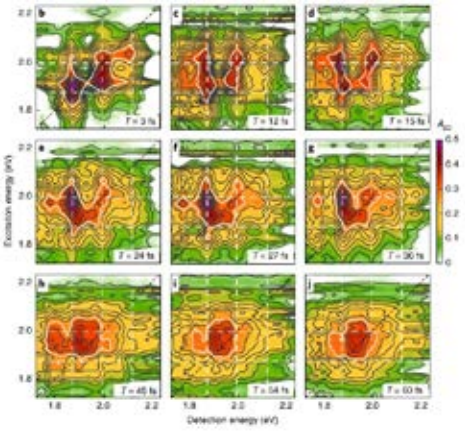

Fig. 1
Snapshots of two-dimensional electronic spectroscopy spectra of ADA oligomer aggregates. The maps show a grid-like peak pattern revealing coherent vibrational wave packet motion on the S_2 state with a roughly 30-fs period (white dashed lines). At T ≈ 45 fs, the grid pattern disappears and the 2DES spectra become essentially featureless.

state, rapid periodic oscillations of very small transition density fractions between the oligomer units are seen. The excitation remains, however, delocalized over the entire dimer. On transition to S_1, both the amplitude and period of these transition density oscillations dramatically increase, indicating an abrupt change of the potential energy surface. We find that this transition initiates a dynamic localization process of the electronic density on one of the oligomers, followed by pronounced oscillations of the transition density between the two units.

In dichloro-methane solution the aggregation of the oligomers is completely suppressed, and none of these features is observed.

Our results show that, in this system, intermolecular conical intersections control the transition from a coherently moving vibronic wave packet, spatially delocalized across several oligomer units, towards a localized trapped exciton, whose transport proceeds by classical diffusive hopping. Controlling these initial coherent dynamics thus provides new opportunities for steering the flow of energy and charges and their pathways on the nanoscale in functional assemblies.

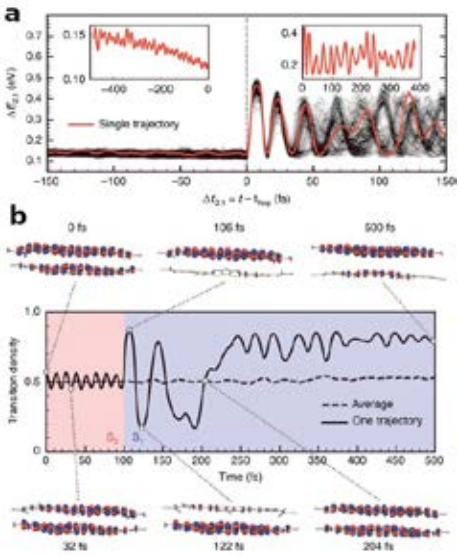

Fig. 2
Non-adiabatic excited-state molecular dynamics simulations of an ADA oligomer dimer. a) Dynamics of the electronic energy gap $\Delta E_{2,1}$ between S_1 and S_2 states for all trajectories (black) and an exemplary one (red, insets). b) Transition density dynamics on one oligomer unit for (solid) an exemplary trajectory and (dashed) the ensemble average. Snapshots of the orbital plots at selected times show the initial spatial delocalization of the transition density.

Contact person
Carlo Andrea Rozzi (carloandrea.rozzi@nano.cnr.it)

References

[1] Intermolecular conical intersections in molecular aggregates. A. De Sio, E. Sommer, X. T. Nguyen, L. Groß, D. Popović, B. T. Nebgen, S. Fernandez-Alberti, S. Pittalis, C. A. Rozzi, E. Molinari, E. Mena-Osteritz, P. Bäuerle, T. Frauenheim, S. Tretiak, and C. Lienau. Nat. Nanotechnol. 16, 63-68 (2021).

[2] Roadmap on bio-nano-photonics. E. Herkert, N. Slesiona, M. E. Recchia, T. Deckert, M. F. Garcia-Parajo, E. M. Fantuzzi, A. Pruccoli, I. C. Ragupathy, D. Gudavičius, H. Rigneault, J. Majer, A. Zumbusch, E. Munger, S. Brasselet, A. T. Jones, P. Watson, S. A. Boppart, V. Singh, S. Borkar, F. E. Quintela Rodriguez, W. Langbein, V. Petropoulos, N. F. van Hulst, M. Maiuri, G. Cerullo, D. Brida, F. Troiani, C. A. Rozzi, E. Molinari, M. Vengris, and P. Borri. J. Opt. 23, 073001 (2021).

[3] Octopus, a computational framework for exploring light-driven phenomena and quantum dynamics in extended and finite systems. N. Tancogne-Dejean, M. J. T. Oliveira, X. Andrade, H. Appel, C. H. Borca, G. Le Breton, F. Buchhol, A. Castro, S. Corni, A. A. Correa, U. De Giovannini, A. Delgado, F. G. Eich, J. Flick, G. Gil, A. Gomez, N. Helbig, H. Hübener, R. Jestädt, J. Jornet-Somoza, A. H. Larsen, I. V. Lebedeva, M. Lüders, M. A. L. Marques, S. T. Ohlmann, S. Pipolo, M. Rampp, C. A. Rozzi, D. A. Strubbe, S. A. Sato, C. Schäfer, I. Theophilou, A. Welden, and A. Rubio. J. Chem. Phys. 152, 124119 (2020).

[4] Nonlinear light absorption in many-electron systems excited by an instantaneous electric field: a non-perturbative approach. A. Guandalini, C. Cocchi, S. Pittalis, A. Ruini, and C. A. Rozzi. Phys. Chem. Chem. Phys. 23, 10059 (2021).

Designing nanoporous graphene scaffolds for environmental applications

Among the extraordinary properties of graphene, its huge surface-to-mass ratio (SSA) is the most interesting for environmental applications. These include the development of materials to be used both in the clean energy cycle (adsorbers of hydrogen or electrolytes for batteries and supercapacitors) and in pollution prevention (filters and CO_2 sorters). However, in all of these cases, the large SSA must be declined into 3D structures, to obtain graphene based materials with finely tuned structural properties (e.g., porosity and density). In the last years, we devoted an effort to the design and optimization of these materials by means of advanced modeling techniques and simulations.

3D materials based on graphene can be built following essentially two routes. One is the bottom-up approach, by controlled functionalization and assembly of graphene sheets separated by molecular pillars. This ideally leads to regular scaffolds with predetermined structural properties and the possibility of endowing the system with a number of functional properties [1]. This route is however limited by its complexity, requiring the full control of the sheets' nano-scale chemical functionalization and assembly. Conversely, the top-down approach consisting in the condensation of a suspension of graphene flakes, easily returns cheap 3D graphene nanoporous scaffolds, but with disordered and not easily controllable structure.
To help drive the synthesis of 3D nanoporous scaffolds and quantify the relationships between structure and functionality, we developed and implemented an algorithm capable of generating realistic computer models (Fig. 1a-d) with pre-determined porosity, density and SSA (Fig. 1e) [2]. Our algorithm combines molecular dynamics using different advanced empirical reactive force fields with stochastic algorithms to generate the seed structures mimicking the steps of the synthesis. As a consequence, we obtained a relationship between the final structure properties and the synthesis parameters which could be used to optimize the production.

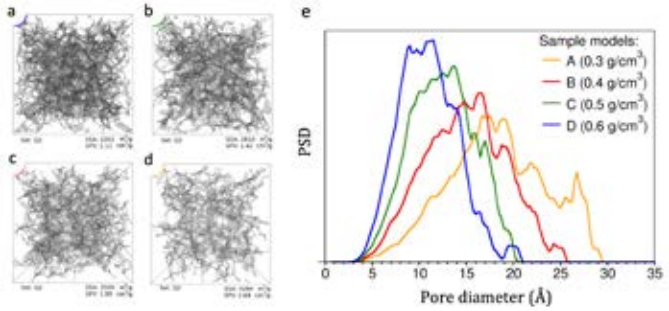

Fig. 1
Models of nanoporous 3D graphene at different porosity and accessible surface (a-d, structural parameters reported in the legend, scaffold structure represented in ball&stick, in black), and (e) their structural characterization in terms of density and pore size distribution (PSD).

We subsequently built a large database of structures (~103) and characterized them vs H_2 adsorption (Fig. 2a–d). With the aid of machine learning algorithms, we derive a quantitative relationship between structure and adsorption, and show that it depends both on the SSA and on the ratio between surface and edges, in turn due to the presence of perforations or other defects (Fig. 2e). Because the affinity of edges to different elements is variable, these results can be used not only to optimize the structural properties of these materials for H_2 adsorption, but also to create highly selective materials for other fluids, for optimized filtering and gas sequestration.

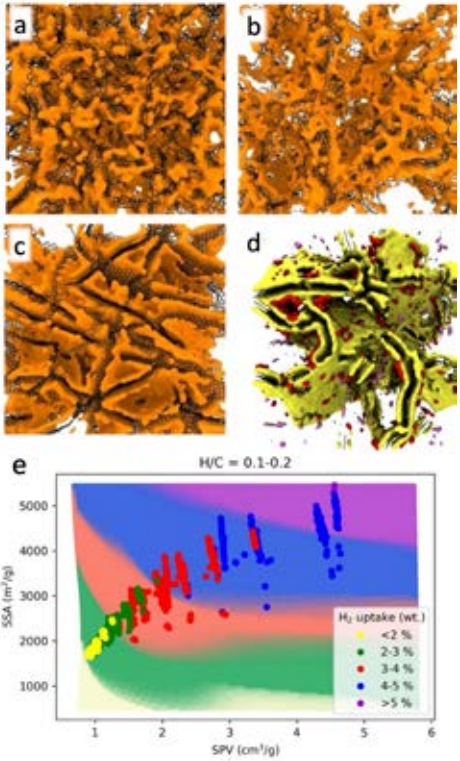

Fig. 2
(a-d) Hydrogen adsorption in selected nanoporous scaffolds with increasing porosity as in Fig. 1. The adsorbed H_2 space distribution is represented as iso-density surfaces in orange. The accumulation on the scaffold surfaces (in black as in Fig. 1), on edges and in interstitial is clearly visible, especially in c and d. In d, we show that H_2 can accommodate in layers, represented in different colors, the first one in yellow uniformly covering the scaffold, the second in red fragmented and concentrated in interstitials (free molecules are also present in the void areas, in magenta). (e) Machine learning analysis and prediction of H_2 uptake as a function of structural parameters SSA and specific pore volume (SPV).

Contact persons
Valentina Tozzini (valentina.tozzini@nano.cnr.it)
Luca Bellucci (luca.bellucci@nano.cnr.it)

References
[1] Engineering 3D Graphene-Based Materials: State of the Art and Perspectives. L. Bellucci and V. Tozzini. Molecules 25, 339 (2020).
[2] In Silico design, building and gas adsorption of nano-porous graphene scaffolds. L. Bellucci, F. Delfino, and V. Tozzini. Nanotechnology 32, 045704 (2021).

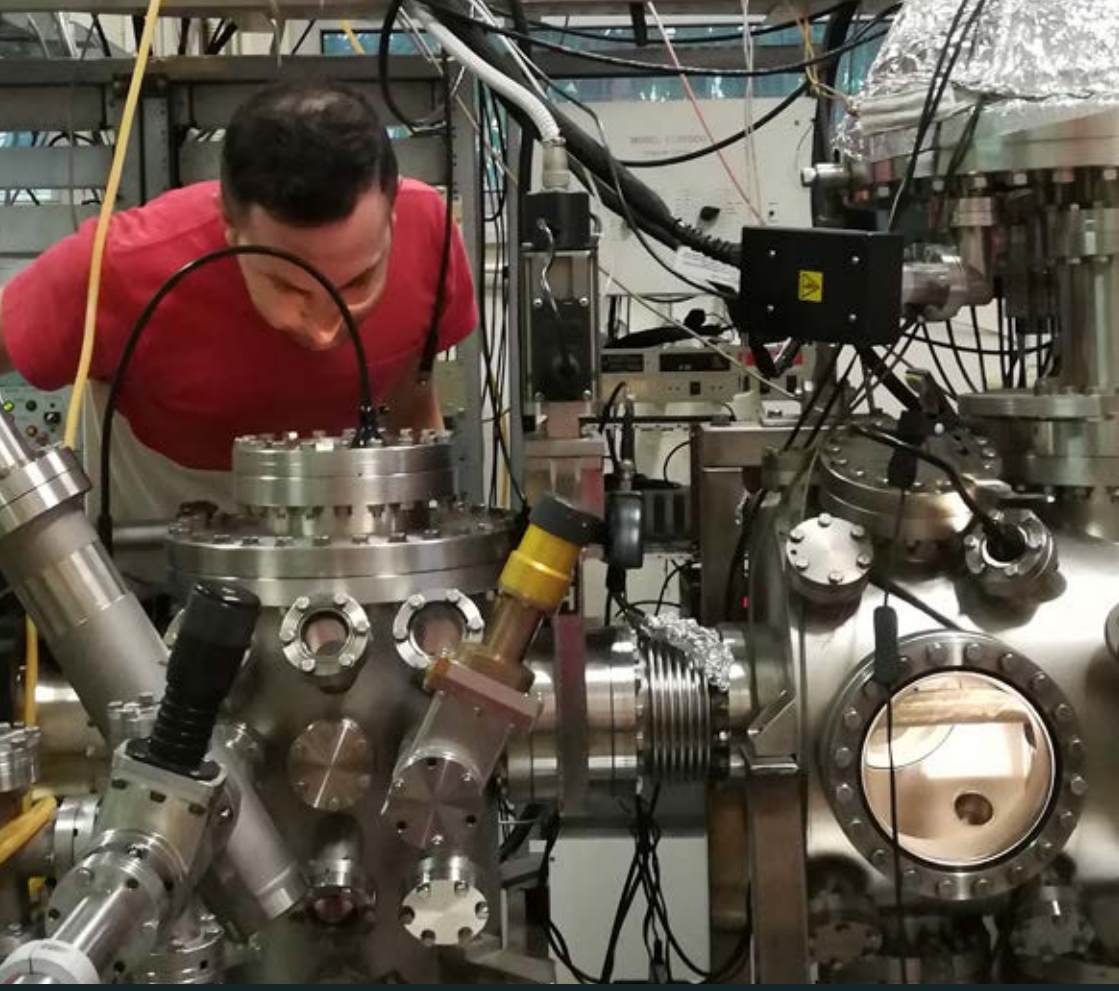

Projects and grants

Cnr Nano research activity is mainly supported by funding obtained through competitive calls at different levels, from international to local. Projects running in 2020-2021 are listed below with the following details: acronym, project name, call details, project ID, coordinator, Cnr Nano principal investigator (if different), dates, website (if available). A short abstract is given for European-funded projects.
For further information, please contact the project's Cnr Nano principal investigator.

European projects

AndQC. Andreev qubits for scalable quantum computation. H2020-FETOPEN-2018-2020-01; GA 828948. Chalmers Tekniska Hoegshkola AB, SE (A. Geresdi); Cnr Nano Pisa (L. Sorba). 2019-2023.
www.andqc.eu

Abstract. The goal is to establish the foundations of a radically new solid-state platform for scalable quantum computation, based on Andreev qubits. This platform is implemented by utilizing the discrete superconducting quasiparticle levels (Andreev levels) that appear in weak links between superconductors. Each Andreev level can be occupied by zero, one, or two electrons. The even occupation manifold gives rise to the first type of Andreev qubit. We will characterize and mitigate the factors limiting the coherence of this qubit to promote these proofs of concept experiments towards a practical technology. The odd occupation state gives rise to a second type of qubit, the Andreev spin qubit, with an unprecedented functionality: a direct coupling between a single localized spin and the supercurrent across the weak link. Further harnessing the odd occupation state, we will investigate the so far unexplored scheme of fermionic quantum computation, with the potential of efficiently simulating electron systems in complex molecules and novel materials. The recent scientific breakthrough by the Copenhagen node of depositing of superconductors with clean interfaces on semiconductor nanostructures opened a realistic path to implement the Andreev qubit technology. In these devices, we can tune the qubit frequency by electrostatic gating. We will demonstrate single- and two-qubit control of Andreev qubits, and benchmark the results against established scalable solid-state quantum technologies, in particular semiconductor spin qubits and superconducting quantum circuits.

BIG MAP. Battery interface Genome – Materials Acceleration Platform. H2020-LC-BAT-2020-3; GA 957189. Technical University of Denmark – DTU, DK (T. Wegge); Cnr Nano Modena (E. Molinari). 2020-2023.
www.big-map.eu

Abstract. Energy production and transport are evolving rapidly to meet today's growing demand and environmental goals. However, low-cost and high-performance solutions are lacking when it comes to energy storage. To address the absence of innovative battery technologies, the EU-funded BIG-MAP project aims to develop a modular, closed-loop infrastructure and methodology to bridge physical insights and data-driven approaches. To this end, it will cohesively integrate machine learning, computer simulations and AI-orchestrated experiments and synthesis to accelerate the discovery and optimisation of sustainable battery materials. The project will play a role in the creation of a versatile and chemistry-neutral European Materials Acceleration Platform that can significantly increase the rate of discovery of new battery materials and interfaces.

BIOIMD. Bioresorbable self-powered implantable device. H2020-MSCA-IF-2019; GA 896811. Cnr Nano Pisa (L. Persano). 2021-2023.

Abstract. Novel implantable medical devices (IMDs) allow the monitoring or detection of diseases inside the human body, yet the challenge is that these devices need to be supplied with continuous power. The implantable batteries suffer from limited lifetime and maintenance problems, and they require periodic replacement through surgery. Scavenging energy from biomechanical sources using piezoelectric devices presents a smart strategy since they can harvest electric supply from the inexhaustible motions of organs such as the heart, lungs, and diaphragm. The focus of the EU-funded BIO-IMD project is to develop high-performance piezoelectric polymer-based biodegradable IMDs which can be accommodated by the body and finally resorbed without any toxicity.

EU-SUPER. Superconducting Magnetic RAM for Next Generation of Supercomputers. H2020-MSCA-IF-2017; GA 796603. Cnr Nano Pisa (F. Giazotto). 2018-2020.

Abstract. The ongoing demand for computing-power and data-storage is quickly approaching the physical limits of conventional silicon-based electronics. To overcome this limit different approaches beyond conventional complementary metal-oxide-semiconductor (CMOS) technology are nowadays under investigation. On one hand, quantum computers, based on non-classical superposition of logic units (bit), offer bright perspectives. On the other hand, energy-efficient superconducting circuits based on Josephson junctions have already demonstrated a computational speed two orders of magnitude larger than conventional CMOS-based ones. The complete implementation of a supercomputer based on this technology is currently limited by the lack of memories operating at cryogenic temperatures, i.e. in close contact and compatible with the superconducting processor.
Starting from the growth of thin films of FI/S bilayers, the first objective of this project will be the design of new architectures to control the magnetic configuration of the FI/S interfaces. The successful miniaturization and patterning of these materials will enable the realization of a prototype of FI/S-based superconducting magnetic-RAM (SMRAM), thus providing the missing building block towards the implementation of the superconducting computer. The last objective of the project is to demonstrate the scalability (including all the write and read protocols) to make the SMRAM technology ready for the large-scale market.

EXTREME-IR. Extreme Optical Nonlinearities in 2D materials for Far-Infrared Photonics. H2020-FETOPEN-2018-2020; GA 896811. CNRS, FR (Sukhdeep Dhillon); Cnr Nano Pisa (M. S. Vitiello). 2021-2025. *http://extreme-ir.eu/*

Abstract. Generating light across the mid-infrared and terahertz regions of the spectrum has opened up a plethora of sensing applications and enabled the study of fundamental light-matter interactions. Quantum cascade lasers, which have recently moved

from laboratory curiosity to industrial mainstay, have largely increased the range of practical applications. Despite their potential, they are limited in their ability to fill the far-infrared gap, namely the frequency region between 5 and 12 THz. The EXTREME-IR project aims to overcome this barrier by pioneering a radically new platform that exploits nonlinear optics in 2D materials to realise compact and coherent far-infrared sources.

GENESIS. GatE-coNtrollEd Superconducting TransIStors. H2020-FETOPEN-2018-2019-2020-4; GA 101034849. Cnr Nano Pisa (F. Giazotto). 2021-2022.

Abstract. As global internet traffic continues to increase, existing telecommunications (TLC) infrastructures face technological restrictions due to their speed and the enormous amount of data processed at network nodes. Although improved transmission bitrate (Tb/s) will be achieved using microwave (GHz) or terahertz (THz), data sorting-related radio frequency signals will become more difficult. The EU-funded GENESIS project will propose a new paradigm for electronics in which the basic building blocks rely on gate-controlled superconducting transistors solving the TCL infrastructure problem. The project will assess the expected superior performances for superconducting devices. It will perform a stakeholder analysis to confirm the system's functionalities as well as crucial requirements for the technology's integration into selected application scenarios, and also carry out a Freedom to Operate analysis.

GRANT (ATTRACT Seed project). GRaphene Golay micro-cell Arrays for a color-seNsitive TeraHertz imaging sensor. H2020-INFRAINNOV-2017-1; GA 777222. Cnr Iom (M. Lazzarino); Cnr Nano Pisa (A. Pitanti). 2019-2020.
https://attract-eu.com/selected-projects/graphene-golay-micro-cell-arrays-for-a-color-sensitive-terahertz-imaging-sensor-grant

Abstract. Grant project aims at the realization of Golay micro-cells based on graphene suspended membranes. The pressure change in the cell due to the absorption of THz radiation will extremely push the ultralight membranes, improving the system detection sensitivity. Furthermore, a proper pattering of one cell side using metallic metasurfaces will enable selective absorption and the use of the micro-cells in color-sensitive arrays, building the base for an improved THz detection technology.

Graphene Flagship Core Project 2. H2020-SGA-FET-GRAPHENE-2017; GA 785219. Chalmers Tekniska Hoegskola AB, SE (J. Kinaret); Cnr Nano Pisa (V. Tozzini and M. S. Vitiello). 2018-2020.
www.grapheneflagship.eu

Abstract. The progress of the flagship follows the general plans set out in the Framework Partnership Agreement, and the second core project represents an additional step towards higher technology and manufacturing readiness levels. The Flagship is built upon the concept of value chains, one of which is along the axis of materials-compo-

nents-systems; the ramp-up phase placed substantial resources on the development of materials production technologies, the first core project moved to emphasise components, and the second core project will move further towards integrating components in larger systems. This evolution is manifested, e.g., in the introduction of six market-motivated spearhead projects during the Core 2 project.
Within the Optoelectronics work package, Cnr Nano is involved in the development of graphene high-speed photodetectors at THz frequencies, and saturable absorbers exploiting graphene, and graphene THz modulators. Within the energy storage work package, it is involved in computer modeling and design of graphene-based nano-porous materials to be used as smart electrodes in supercapacitors and batteries.

INTERSECT. Interoperable Material-to-Device simulation box for disruptive electronics. H2020-NMBP-TO-IND-2018; GA 814487. Cnr Nano Modena (A. Calzolari). 2019-2022.
www.intersect-project.eu

Abstract. INTERSECT wants to leverage European leadership in materials' modelling software and infrastructure to provide industry-ready integrated solutions that are fully compliant with a vision of semantic interoperability driven by standardized ontologies. The resulting IM2D framework - an interoperable material-to-device simulation platform - will integrate some of the most used open-source materials modelling codes (Quantum ESPRESSO and SIESTA) with models and modelling software for emerging devices via the SimPhony infrastructure for semantic interoperability and ontologies, powered by the AiiDA workflow engine, and its data-on-demand capabilities and apps interface. API-compliance with established standards will allow pipelines to and from public repositories, and embedding into the front-end of materials hubs, such as MarketPlace, while testing, validation, and standardization will take place together with the industrial partners. INTERSECT will drive the uptake of materials modelling software in industry, bridging the gap between academic innovation and industrial novel production, with a goal of accelerating by one order of magnitude the process of materials' selection and device design and deployment.

IQubits. Integrated Qubits Towards Future High-Temperature Silicon Quantum Computing Hardware Technologies. H2020-FETOPEN-2018-2019-2020-01; GA 829005. Aarhus Universitet, DK (D. Zito); Cnr Nano Modena (F. Troiani). 2019-2023.
www.iqubits.eu

Abstract. The objectives of the interdisciplinary project IQubits are to (i) develop and demonstrate experimentally high-temperature (high-T) Si and SiGe electron/hole-spin qubits and qubit integrated circuits (ICs) in commercial 22nm Fully-Depleted Silicon-on-Insulator (FDSOI) CMOS foundry technology as the enabling fundamental building blocks of quantum computing technologies, (ii) verify the scalability of these qubits to 10nm dimensions through fabrication experiments and (iii) prove through atomistic simulations that, at 2nm dimensions, they are suitable for 300K operation. The

proposed 22nm FDSOI qubit ICs consist of coupled quantum-dot electron and hole spin qubits, placed in the atomic-scale channel of multi-gate n- and p-MOSFETs, and of 60-240GHz spin control/readout circuits integrated on the same die in state-of-the-art FDSOI CMOS foundry technology. To assess the impact of future CMOS scaling, more aggressively scaled Si-channel SOI and nitride-channel qubit structures will also be designed and fabricated in two experimental processes with 10nm gate half pitch. The latter will be developed in this project. The plan is for the III-nitrides (III-N) qubits to be ultimately grown on a SOI wafer, to be compatible with CMOS.

LESGO. Light to Store chemical Energy in reduced Graphene Oxide for electricity generation. FETPROACT-EIC-05-2019; GA 952068. ICFO, ES (J. Martorell); Cnr Nano Pisa (V. Tozzini). 2020-2023.
https://lesgo-project.eu/

Abstract. Electricity generation based on renewables is unpredictable, but hydrogen (H2) could be a promising energy storage route. Since over 95% of H2 comes from breaking the carbon-hydrogen bond in hydrocarbons, storing hydrogen bound to carbon may provide a long-term solution. However, extracting hydrogen from liquid hydrocarbons includes CO2 emissions. To address this problem, the EU-funded LESGO project aims to store energy in the C-H bond of reduced graphene oxide (rGO-H). The advantages of rGO-H include safe storage, easy transportation, an energy density over 100 times larger than that of H2 gas and no CO2 emissions in the electricity generation process. The project will promote an affordable and eco-friendly means of supplying electrical power on demand where required.

MaX. Materials design at the exascale. H2020-EINFRA-2015-1; GA 676598. Cnr Nano Modena (E. Molinari). 2015-2018. Materials design at the exascale. European Centre of Excellence in materials modelling, simulations, and design. H2020-INFRAEDI-2018-1; GA 824143. Cnr Nano Modena (E. Molinari). 2018-2021.
www.max-centre.eu

Abstract. MaX aims at allowing the pre-exascale and exascale computers expected in Europe in the 2020's to meet the demands from a large and growing base of researchers committed to materials discovery and design. This goal will be achieved by: i) an innovative software development model, based on the concept of separation of concerns, that will enable performance of the community codes on heterogeneous hardware architectures, without disrupting their internal structure, the richness of their simulation capabilities, and their distributed and open development model. In this way, the most important community codes for quantum mechanical materials modelling will be ready for pre-exascale machines by the completion of MaX programme, and prepared to be ported to new architectures as they will become available; ii) an integrated ecosystem enabling the convergence of HPC and HTPC, that will allow steering the millions to hundreds of millions of simulations that are needed to optimise the properties and performances of a material or a device, with robust and reproducible workflows, all con-

tributing to an ever growing repository of curated data; iii) a new approach to scientific computing in which hardware and software are co-designed and co-developed taking into mutual account the constraints and goals; iv) innovative measures for easy access to materials science applications, for engaging academic and industrial communities and fostering a broader and diverse pool of well trained users and developers.

MINEON. MINiaturized Electron Optics for Nano-controlled beams. H2020-FETOPEN-2018-2020 Launchpad; GA 101035013. Cnr Nano Modena (V. Grillo). 2021-2022.
www.mineon.eu

Abstract. Novel electron beam shaping enhances functionality in compact electron microscopy system. The evolution of technologies in virtually all fields follows a similar route, packing ever greater functionality into increasingly compact designs that simultaneously expand access due to portability and space requirements. Much as computers have evolved from mainframes to minicomputers, personal computers and now laptops, the same evolution is happening with technologies that enable us to visualise and control materials' properties down to atomic resolution. The EU-funded MINEON project is perfecting the next evolutionary leap for electron microscopy. The team is laying the foundations for commercialisation of its revolutionary electron microscopy plug-in components harnessing electron beam shaping based on miniaturised micro-electromechanical systems technology.

MIR-BOSE. Mid- and far-IR optoelectronic devices based on Bose-Einstein condensation. H2020-FETOPEN-1-2016-2017; GA 737017. Université Paris Sud, FR (R. Colombelli); Cnr Nano Pisa (M. S. Vitiello). 2017-2023.
www.mir-bose.eu

Abstract. The MIR-BOSE project will demonstrate disruptive optoelectronic devices operating in the strong coupling regime between light and matter. In particular: the first bosonic lasers operating in the mid-IR and THz frequency ranges of the electromagnetic spectrum. Second, a new concept of inverse-Q-switching leading to the generation of high power pulses in the mid-IR ranges, overcoming severe bottlenecks in current technology. Finally, non-classical/quantum light sources and devices based on ultra-fast modulation of the light-matter interaction, generating squeezed states of light in the mid-IR/THz spectral range for quantum optics applications. These new sources will have a major impact on a wide range of technologies and applications in the mid-IR and THz frequency ranges, being advantageous compared to current commercial solutions.

OPENMODEL. Integrated Open Access Materials Modelling Innovation Platform for Europe. H2020-NMBP-TO-IND-2018-2020; GA 953167. Fraunhofer IFAM, DE (W. Leite Cavalcanti); Cnr Nano Modena (A. Calzolari). 2021-2025.
open-model.eu

Abstract. OpenModel – Integrated Open Access Materials Modelling Innovation Platform for Europe. OpenModel aims to design, create, provide, and maintain a sustainable integrated open platform for innovation which delivers predictable, validated, and traceable simulation workflows integrating seamlessly third-party physics-based models, solvers, post-processors and databases. OpenModel thus bridges the gap from industry challenge via translation to actionable results that enable well informed business decisions. Six use cases (Success Stories) show the applicability to a wide range of materials and their related processing technologies and demonstrate how OpenModel facilitates setting up experiments, reducing error and enhancing development efficiency.

PHENOMEN. All-Photonic Circuits enabled by opto-mechanics. H2020-FETOPEN-2014-2015-RIA; GA 713450. ICN2, ES (C. Sotomayor Torres); Cnr Nano Pisa (A. Pitanti). 2016-2019.
www.phenomen-project.eu

Abstract. Phenomen aims at building a phononic chip platform, where coherent vibrations above 1 GHz can be generated, routed and detected via optomechanical devices operating at room temperature. Adding novel functionalities in phonon processing such as switching and modulation, the technology developed in Phenomen will enable the coupling of different physical (quantum) systems towards the realization of the ultimate hybrid platform, where photons, electrons, and phonons can be interchangeably used for information manipulation and control.

Q-SORT. Quantum sorter. H2020-FETOPEN-1-2016-2017; GA 766970. Cnr Nano Modena (V. Grillo). 2017-2021.
www.qsort.eu

Abstract. Q-SORT introduces a revolutionary concept whereby the transmission electron microscope (TEM) is employed as a so-called Quantum Sorter, i.e., a device that can pick out and display detailed information about electron quantum states. This in turn provides researchers with precious new information about the sample being examined. The project -which includes applications in physics, biology, and biochemistry- is expected to have a wide-ranging impact due to the ubiquitous adoption of TEM and STEM across many disciplines. Q-SORT also has foundational value in physics as it fosters its own kind of sparse-sensing approach to TEM, advancing the field in the direction of quantum measurement.

SMART-electron. Ultrafast all-optical spatio-temporal electron modulators: opening frontiers in electron microscopy. H2020 FETOPEN 2018-2020; GA 964591. University of Milan – Bicocca (G. Vanacore); Cnr Nano Modena (V. Grillo). 2021-2025.
www.smartelectron.eu

Abstract. SMART-electron aims at developing an innovative technological platform for designing, realizing and operating all-optical rapidly programmable phase masks for electrons. SMART-electron will introduce a new paradigm where properly synthesized ultrafast electromagnetic fields will be used for engineering the phase space of a free-electron wave function. This will allow us to achieve unprecedented space/time/energy/momentum shaping of electron matter waves, thus surpassing conventional passive monolithic schemes, and revolutionizing the way materials are investigated in electron microscopy.

SPRINT. Ultra-short pulse laser resonators in the Terahertz. H2020-ERC-CoG-2015; GA 681379. Cnr Nano Pisa (M. S. Vitiello). 2016-2021.

Abstract. Ultra-short light pulses with large instantaneous intensities can probe light-matter interaction phenomena, capture snapshots of molecular dynamics and drive high-speed communications. In a semiconductor laser, mode-locking is the primary way to generate ultrafast signals. Despite the intriguing perspectives, operation at Terahertz (THz) frequencies is facing fundamental limitations: engineering "ultrafast" THz semiconductor lasers from scratch or finding an integrated technology to shorten THz light pulses are currently two demanding routes. SPRINT aims to innovatively combine the ground-breaking quantum cascade laser (QCL) technology with graphene, to develop a new generation of passive mode-locked THz photonic laser resonators, combined with unexplored electronic nanodetectors for ultrafast THz sensing and imaging.

SUPERCONTACTS. Solid state diffusion for atomically sharp interfaces in semiconductor-superconductor hybrid structures. H2020-MSCA-IF-2020; GA 101022473. Cnr Nano Pisa (E. Strambini). 2021-2023.

Abstract. A matchmaker's delight strengthens the field of superconducting optoelectronics. Semiconductors, materials that literally 'semi-conduct' electricity, have revolutionised our lives with applications in everything from consumer electronics and solar cells to lasers. Integrating semiconductors with superconductors opens the door to limitless possibilities of device functionality and new applications including quantum processing, communication, and encryption. However, fine-tuning and optimising the actual physical interface between the two types of materials has been challenging due to lack of control. With the support of the Marie Skłodowska-Curie Actions programme, the SuperCONtacts project intends to overcome these limitations with a new fabrication technique that will lead to the realisation of atomically sharp superconductor–semiconductor interfaces.

SUPERGALAX. Highly sensitive detection of single microwave photons with coherent quantum network of superconducting qubits for searching galactic axions. Cnr Spin, IT (M. Lisitskiy); Cnr Nano Modena (M. Affronte). 2020-2023.
supergalax.eu

Abstract. Breakthrough method of detecting low-energy microwave photons. Detecting single photons at the microwave frequency range is important in the search for axion dark matter, quantum computing and metrology applications. The EU-funded SUPERGALAX project proposes a novel approach for the acquisition of extremely low-energy microwave signals. Researchers will fabricate and explore the dynamics of coherent quantum networks comprising a large amount of strongly interacting superconducting qubits – transmons and flux qubits. The team expect that the measurement sensitivity of their superconducting network detector will reach the Heisenberg limit – the standard limit on the precision with which a quantum measurement can be carried out. Manipulating and measuring individual photons at particularly low microwave frequencies will aid in the detection of hypothetical dark-matter axions, making information processing more efficient.

SUPERGATE. Gate Tuneable Superconducting Quantum Electronics. H2020-FETOPEN-2018-2020; GA 964398. University of Kostanz, DE (E. Scheer); Cnr Nano Pisa (F. Giazotto). 2021-2024.
www.supergate.uni-konstanz.de

Abstract. A new approach to superconducting logic gates could usher in a new age of supercomputing. Calculators were a major improvement over pencil and paper, but computers truly revolutionised our ability to do calculations, exponentially increasing the number and complexity of computations possible in a fraction of the time. Supercomputers relying on superconducting quantum logic gates have extended those possibilities. They are increasingly invaluable to numerous fields but are facing challenges in terms of enhancing performance while reducing energy consumption. The EU-funded SuperGate project will develop a new approach to superconducting logics that will enable the same or better performance while minimising current problems, ushering in the next evolution of supercomputers.

SUPERTED. Thermoelectric detector based on superconductor-ferromagnet heterostructures. H2020-FETOPEN-1-2016-2017; GA 800923. Jyvaskylan Yliopisto, FI (T. Heikkilä); Cnr Nano Pisa (F. Giazotto). 2018-2022.
superted-project.eu

Abstract. Superted proposes to study a new type of sensor based on the thermoelectric conversion of the radiation signal to electrically measurable one. This approach is based on the newly found giant thermoelectric effect taking place in superconductor/ferromagnet heterostructures. Utilizing this effect, the sensor pixels can be self-powered by the measured radiation, and therefore extra bias lines are not needed (patent pending

for the detector concept). Within the project, we aim to establish a proof of concept of this device by (i) fabricating such detector elements, and (ii) characterizing single pixels of thermoelectric detectors for X-ray and THz imaging via approaches that are scalable to large arrays.

SUPERTOP. Topologically protected states in double nanowire semiconductor hybrids. H2020 QuantERA ERA-NET Cofund in Quantum Technologies 2017. Budapest University of Technology and Economics, HU (S. Csonka); Cnr Nano Pisa (L. Sorba). 2018-2020.
dept.physics.bme.hu/Supertop/

Abstract. To realize fully topologically protected universal quantum computation, more exotic anyons, such as parafermions are required. Thus, the unambiguous demonstration of parafermion states will have a great impact on the development of universal quantum computation. The experimental realization of parafermions is challenging, since they are based on the combination of various ingredients, such as crossed Andreev reflection, electron-electron or spin-orbit interaction, and high quality quantum conductors. Thus, the investigation of all these ingredients is essential and timely to achieve further experimental progress.
The main objectives of SuperTop are: a) development of different DNW (double nanowire-based hybrid devices geometries), which consist of two parallel 1D spin-orbit nanowires coupled by a thin superconductor stripe and b) investigation of the emerging exotic bound states at the superconductor/semiconductor interface of the DNW.

TAME-Plasmons. Theoretical chemistry Approach to tiMEresolved molecular Plasmonics. H2020-ERC-CoG-2015; GA 681285. Università di Padova, IT and Cnr Nano Modena (S. Corni). 2016-2021.
www.tame-plasmons.eu

Abstract. Ultrafast spectroscopy is a powerful tool able to disclose the atomistic real-time motion picture of the basic chemical events behind technology and life, such as catalytic reactions or photosynthetic light harvesting. Nowadays, by cleverly harnessing the interaction of the studied molecules with plasmons (collective electron excitations supported, e.g., by metal nanoparticles) it is becoming possible to focus these investigations on specific nanoscopic regions, such as a portion of a catalytic surface or of a photosynthetic membrane. The goal of TAME-Plasmons is to develop a theoretical chemistry approach to directly simulate the real-time evolution of molecules interacting with plasmons and light.

T-CONVERSE (ATTRACT Seed project). Temperature-to-phase conversion THz radiation sensors. H2020-INFRAINNOV-2017-1; GA 777222. INFN, IT (F. Paolucci); Cnr Nano Pisa (F. Giazotto). 2019-2020.
attract-eu.com/selected-projects/temperature-to-phase-conversion-thz-radiation-sensors-t-converse/

Abstract. T-CONVERSE proposes new class cryogenic radiation sensors characterized by operating broadband from 10GHz to 10THz, resolving power larger than 100, and unprecedented noise equivalent power of the order of 10-23W/Hz1/2. These detectors are based on the innovative concept of temperature-to-phase conversion. In a TPC sensor, the latter can be due to the absorption of radiation by antenna coupled to the detection junction. Finally, j across the readout junction is measured by an integrated superconducting quantum interference transistor. Thanks to their unparalleled performances, the TPC detectors could be the cornerstone of novel technologies for THz imaging and spectroscopy. In particular, they could be extensively used for homeland, border and citizen security applications. THz sensors can detect in real-time weapons, illegal goods, drugs or explosives in packs; bringing the sensitivity, the quality and the level of checks beyond any currently existing system devoted to security. Furthermore, the TPC sensors could be employed for food security and citizen health in quality controls of food packaging/adulteration, suspect pharmaceutical freight and fraud inspections.

TeraApps. Doctoral Training Network in Terahertz Technologies for Imaging, Radar and Communication Applications. H2020-MSCA-I-TN-2017; GA 765426. University of Glasgow, UK (E. Wasige); Cnr Nano Pisa (M. S. Vitiello). 2018-2021.
www.gla.ac.uk/research/az/teraapps/

Abstract. This network addresses the future societal need in Teraherz technologies, by addressing the training gap, and crystallizing world leading groups in a concentrated research effort. Emerging research areas in this field link e.g. semiconductor materials synthesis, high-speed electronic device physics and engineering, antenna design, THz optics, and a raft of diverse applications and a new generation of academic and industry leaders in developing these devices and systems in the terahertz spectral band is now required. In particular, the project focuses on tunneling devices that have been shown to be the leading candidate in realizing compact, low cost, high performance THz transmitters and receivers once coupled to suitable antennas. Also, new two-dimensional (2D) materials such as graphene or 1D nanowires are emerging as suitable platforms for realizing highly sensitive detectors of THz radiation.

TERASEC. THz imaging technology for public security. ERC-2019POC; GA 899315. Cnr Nano Pisa (F. Giazotto). 2020-2022.

Abstract. The objectives of TERASEC project entail the activities aimed at pre-commercial validation of the technological performances and market potential of a novel device for the detection of security threats, such as weapons, explosives, drugs, etc. The functionality of TERASEC is enabled through combination of superconducting and ferromagnetic materials that delivers frequency selective THz sensors showing unprecedented sensitivity (single-photon resolution), fast response time, high dynamic range, and low noise-equivalent-power. Specifically, starting from the outstanding outcomes reached so far, the capacity of the TERASEC system to detect the above threats with

given level of accuracy, range and selectivity will be verified in accordance with the requirements of prospect users (to be collected during the project implementation). Moreover, a detailed market, IPR and regulatory compliance study will be carried out, in order to enable smooth implementation of TERASEC in the complicated context of the public security market. To enhance this, an advisory board gathering Key Opinion Leaders of the sector will be secured and involved into project activity throughout all the project duration. In parallel, comprehensive communication strategy addressing all the stakeholders of the relevant value chain will be rolled out, with strong focus on prospect consumers and users, so to ensuring market traction. Overall, the goal of TERASEC is to deliver an unrivalled novel security scanner device leveraging harmless THz waves, that widely overpasses the accuracy performances of all the conventional systems, thus contributing to the safety of European citizens and the security of sensitive infrastructures.

TOPOCIRCUS. Simulations of Topological Phases in Superconducting Circuits. H2020-MSCA-IF-2018; GA 841894. Cnr Nano Pisa (F. Giazotto). 2019-2022.

Abstract. The discovery of topological order characterising novel exotic phases of matter has generated a breakthrough in the comprehension of complex condensed matter phases. Topological invariants entirely determine the behaviour of certain observables and confer to the systems a strong robustness to perturbations. Going beyond condensed matter states, topological order can be engineered in different setups that can benefit form it and represent alternative platform for the simulation of exotic topological phases. Among the most promising candidates for such a plan are the superconducting circuits based on the Josephson effect. This project aims at studying the interconnections between the topological notion and the Josephson effect and to propose superconducting circuits as a platform for the simulation and manipulation of novel topological phases of matter.

xPRINT. 4-Dimensional printing for adaptive optoelectronic components. ERC-2015-COG; GA 682157. Cnr Nano Pisa (A. Camposeo). 2016-2021.
www.xprintlab.eu/

Abstract. Additive manufacturing of three-dimensional objects relies on depositing or curing materials in a layer-by-layer fashion, starting from computer assisted design. These technologies have rapidly evolved from laboratory research to commercially available desktop systems, with costs decreasing continuously. Notwithstanding such astonishing progress, the potentialities of three-dimensional printing are still poorly exploited in terms of both materials and process resolution. This project shed new light on the fundamental aspects of three-dimensional polymerization, thus establishing new process design rules and predictive tools for printing resolution. It also specifically engineered additive manufacturing for printing materials embedding active compounds, thus leading to four-dimensional objects, namely structures that have three-dimensional features and time-changing physical properties at the same time.

National projects

ARTES4.0. Advanced Robotics and enabling digital Technology and Systems. MISE D.D. del 29.01.2018. Cnr Nano Pisa (L. Persano). 2019-2022.

aSTAR. Attosecond transient absorption and reflectivity for the study of exotic materials. MIUR Prin 2017 nr. 2017RKWTMY. Politecnico di Milano (C. Vozzi); Cnr Nano Modena (S. Pittalis). 2019-2022.

Early dysfunctions of intercellular signalling in brain disorders. MIUR Prin 2017 nr. 20175C22WM. Cnr Ibcn (F. Mammano); Cnr Nano Pisa (G. M. Ratto). 2019-2022.

EXC-INS. Excitonic insulator in two-dimensional long-range interacting system. MIUR Prin 2017 nr. 2017BZPKSZ. Università di Modena e Reggio Emilia (E. Molinari); Cnr Nano Modena (M. Rontani). 2019-2022

HARVEST. Learning from natural pigment-protein complexes how to design artificial light-harvesting systems. MIUR Prin2017 nr. 201795SBA3. Politecnico di Milano (G. Cerullo); Cnr Nano Modena (D. Prezzi). 2019-2022.

MONSTRE2D. Monolithic strain engineering platform for two-dimensional materials. MIUR Prin 2017 nr. 2017KFMJ8E. Università di Pisa (A. Tredicucci); Cnr Nano Pisa (V. Tozzini). 2019-2022.

NEMO. Next generation of molecular and supramolecular machines: towards functional nanostructured devices, interfaces, surfaces and materials. MIUR PRIN 2017 nr. 20173L7W8K. Università degli studi di Bologna (A. Credi); Cnr Nano Pisa (L. Persano). 2019-2022.

UTFROM. Understanding and Tuning Friction through nanostructure Manipulation. MIUR Prin 2017 nr. 20178PZCB5. Università di Genova (R. Ferrando); Cnr Nano Modena (G. Paolicelli). 2019-2022.

VIOLoC-Analisi VIno e OLio 4.0: sviluppo di un Laboratorio on-Chip (LoC) a connettività remota (clouding). MIUR FISR 2018-2019. Cnr Nano Pisa (M. Cecchini). 2021-2023.

Cnr projects

Advanced characterization methods for the study of rare-earth single-ion magnets on oxide substrates. Cnr Bilateral project Czech Republic – CAS. Cnr Nano Modena (V. Bellini). 2019-2021.

Regional projects

ADAPTA. Sinonasal cancer: In depth genetic analysis of patients for personalized treatment and disease monitoring. Regione Toscana; Bando Ricerca Salute 2018 -DD15397/2018. Università di Pisa, IT (A. Franchi); Cnr Nano Pisa (L. Persano). 2020-2023. *https://www.unipi.it/index.php/risultati-e-prodotti/item/18731-adapta*

DECODE-EE. Developmental and epileptic encephalopathies: epidemiology, comorbidities, molecular diagnosis, personalized management, and costs analysis. Regione Toscana; Bando Ricerca Salute 2018 -DD15397/2018. Scuola Superiore S. Anna, IT (P. Castoldi); Cnr Nano Pisa (G. M. Ratto). 2020-2023. *https://www.santannapisa.it/en/research/projects/developmental-and-epileptic-encephalopathies-epidemiology-comorbidities-molecular*

DEM-AGING. Neurodegenerative disorders throughout the lifespan. Autophagy-dependent biomarkers for trial readiness from infantile neuronal ceroid-lipofuscinoses to senile dementias. Regione Toscana; Bando Ricerca Salute 2018 -DD15397/2018. IRCCS Stella Maris, IT (F. Santorelli); Cnr Nano Pisa (G. M. Ratto). 2020-2023. *https://www.unipi.it/index.php/risultati-e-prodotti/item/18615-dem-aging?tmpl=component&print=1*

Materiali Innovativi per celle a Combustione (Rif PA 2019-11475/RER). POR-FESR EMILIA ROMAGNA 2014.2020 OBIETTIVO TEMATICO 10. Cnr Nano Modena (P. Luches). 2019-2020.

RIMMEL - RIvestimenti Multi-funzionali e multi-scala, per componenti MEccanici in acciaio e Leghe di alluminio fabbricati con additive manufacturing. Regione Emilia-Ro-

magna POR FESR 2014-2021 - Azione 1.2.2. Cnr Nano Modena (S. Valeri). 2019-2022. *https://rimmel.nano.cnr.it/*

SENSOR. Nuovi Sensori Real Time per la Determinazione di Contaminazioni Chimiche e Microbiologiche in Matrici Ambientali e Biomedicali. Regione Toscana POR CREO FESR Toscana 2014-2020. Laboratori ARCHA S.R.L., Pisa; Cnr Nano Pisa (M. Cecchini). 2018-2020.

SUPER Supercomputing Unified Platform. Regione Emilia-Romagna POR-FESR 2014-2020, Asse 1 - Ricerca e Innovazione, Azione 1.5.1. Cineca, IT (S. Bassini); Cnr Nano Modena (E. Molinari). 2019-2020.

TOSCANO. The Omics SCiences AgaiNst Osteosarcoma. Regione Toscana - Bando Ricerca Salute 2018 -DD15397/2018. Cnr Nano Pisa (M. Cecchini). 2020-2023.

Other funding agencies

ANCIENT_ROME. Study of many body excitations in defective titanium dioxide materials by ab-initio Methods. PRACE Project Access (Call 19). 30M core hours. CNR Nano Modena (C. Cardoso). 2019-2020.

Balzan Research Project. Fondazione Internazionale Premio Balzan. Cnr Nano Pisa (M. S. Vitiello). 2017-2022.

EXTEND. Excitonic instability in two-dimensional tungsten Ditelluride. PRACE Project Access (Call 19). 45M core hours. CNR Nano Modena (D. Varsano). 2019-2020.

Intracellular chloride dynamics in autistic brain: a better understanding is needed for tailored cures. Telethon 2018. Cnr Nano Pisa (G. M. Ratto). 2019-2022.

Molecular Spins for Quantum Technologies. AOARD 2017-2020. Osaka City University, JP; Cnr Nano Modena (M. Affronte). 2017-2020.

Nanotecnologie per la determinazione di marker molecolari tumorali e per la diagnostica precoce. Fondazione Pisa Bando 2016. Cnr Nano Pisa (G. M. Ratto). 2017-2020.

SAWINE – Laboratorio on-chip basato su onde acustiche di superficie. Bando CARI-LUCCA 2019 – 2021 "Ricerca". Cnr Nano Pisa (M. Cecchini). 2020-2022

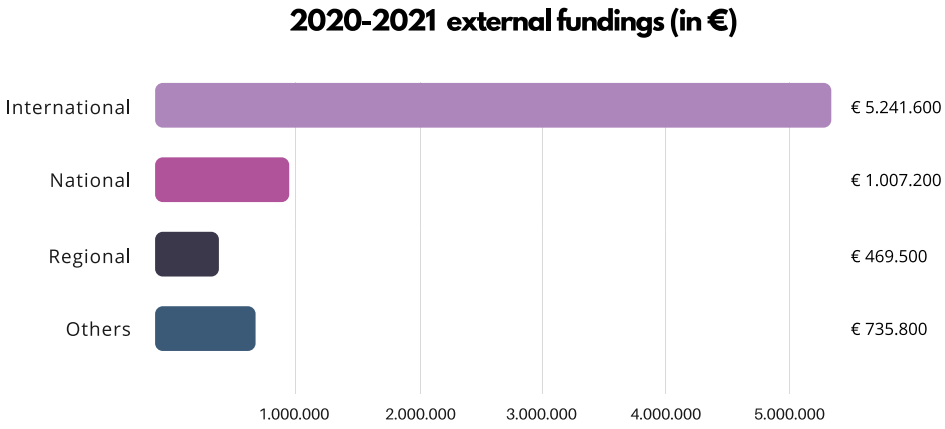

Publications

A list of publications from journals with IF ≥ 9.185 (i.e., Physical Review Letter's IF in 2021) ordered by their JCR 2021 IF is given. A full and updated list of publications is available on the Institute website at the page "Publications" (http://www.nano.cnr.it/publications). Publications marked with © earned a cover in the corresponding journal. Covers are displayed at the end of this section.

2021

Intermolecular conical intersections in molecular aggregates.
A. De Sio, E. Sommer, X.T. Nguyen, L. Gross, D. Popovic, B.T. Nebgen, S. Fernandez-Alberti, S. Pittalis, C.A. Rozzi, E. Molinari, E. Mena-Osteritz, P. Bäuerle, T. Frauenheim, S. Tretiak, and C. Lienau. Nat Nanotechnol 16, 63-68 (2021).

Anyons in quantum Hall interferometry.
M. Carrega, L. Chirolli, S. Heun, and L. Sorba. Nat Rev Phys 3, 698-711 (2021).

On the evaluation of output voltages for quantifying the performance of pyroelectric energy harvesters.
Q. Li, S. Li, D. Pisignano, L. Persano, Y. Yang, and Y. Su. Nano Energy 86, 106045 (2021).

Toward Mechanochromic Soft Material-Based Visual Feedback for Electronics-Free Surgical Effectors.
G. Giordano, M. Gagliardi, Y. Huan, M. Carlotti, A. Mariani, A. Menciassi, E. Sinibaldi, and B. Mazzolai. Advanced Science 8, 2100418 (2021).

Chip-Scalable, Room-Temperature, Zero-Bias, Graphene-Based Terahertz Detectors with Nanosecond Response Time.
M. Asgari, E. Riccardi, O. Balci, D. De Fazio, S.M. Shinde, J. Zhang, S. Mignuzzi, F.H.L. Koppens, A.C. Ferrari, L. Viti, and M.S. Vitiello. ACS Nano 15, 17966-17976 (2021).

Circularly Polarized Laser with Chiral Nematic Cellulose Nanocrystal Cavity.
D. Qu, M. Archimi, A. Camposeo, D. Pisignano, and E. Zussman. ACS Nano 15, 8753-8760 (2021).

Dielectric Engineering Boosts the Efficiency of Carbon Nanotube Photodiodes.
M.J. Senger, A. Kefayati, A. Bertoni, V. Perebeinos, and E.D. Minot. ACS Nano 15, 10472-10479 (2021).

Hot-Carrier Cooling in High-Quality Graphene Is Intrinsically Limited by Optical Phonons.
E.A.A. Pogna, X. Jia, A. Principi, A. Block, L. Banszerus, J. Zhang, X. Liu, T. Sohier, S. Forti, K. Soundarapandian, B. Terres, J.D. Mehew, C. Trovatello, C. Coletti, F.H.L. Koppens, M. Bonn, H.I. Wang, N. Van Hulst, M.J. Verstraete, H. Peng, Z. Liu, C. Stampfer, G. Cerullo, and K.-J. Tielrooij. ACS Nano 15, 11285-11295 (2021).

Ultrafast, All Optically Reconfigurable, Nonlinear Nanoantenna.
E.A.A. Pogna, M. Celebrano, A. Mazzanti, L. Ghirardini, L. Carletti, G. Marino, A. Schirato, D. Viola, P. Laporta, C. De Angelis, G. Leo, G. Cerullo, M. Finazzi, and G. Della Valle. ACS Nano 15, 11150-11157 (2021).

Wafer-scale integration of graphene-based photonic devices.
M.A. Giambra, V. Miseikis, S. Pezzini, S. Marconi, A. Montanaro, F. Fabbri, V. Sorianello, A.C. Ferrari, C. Coletti, and M. Romagnoli. ACS Nano 15, 3171-3187 (2021).

Magnetization dependent tunneling conductance of ferromagnetic barriers
Z. Wang, I. Gutierrez-Lezama, D. Dumcenco, N. Ubrig, T. Taniguchi, K. Watanabe, E. Giannini, M. Gibertini, and A.F. Morpurgo. Nat Commun 12, 6659 (2021).

Mapping propagation of collective modes in Bi2Se3 and Bi2Te2.2Se0.8 topological insulators by near-field terahertz nanoscopy.
E.A.A. Pogna, L. Viti, A. Politano, M. Brambilla, G. Scamarcio, and M.S. Vitiello. Nat Commun 12, 6672 (2021).

Publisher Correction: Mapping propagation of collective modes in Bi2Se3 and Bi2Te2.2Se0.8 topological insulators by nearfield terahertz nanoscopy (Nature Communications, (2021), 12, 1, (6672), 10.1038/s41467-021-26831-6).
E.A.A. Pogna, L. Viti, A. Politano, M. Brambilla, G. Scamarcio, and M.S. Vitiello. Nat Commun (12), 7339 (2021).

Millimeter wave photonics with terahertz semiconductor lasers.
V. Pistore, H. Nong, P.-B. Vigneron, K. Garrasi, S. Houver, L. Li, A. Giles Davies, E.H. Linfield, J. Tignon, J. Mangeney, R. Colombelli, M.S. Vitiello, and S.S. Dhillon. Nat Commun 12, 1427 (2021).

Preliminary demonstration of a persistent Josephson phase-slip memory cell with topological protection.
N. Ligato, E. Strambini, F. Paolucci, and F. Giazotto. Nat Commun 12, 5200 (2021).

Graphene Confers Ultralow Friction on Nanogear Cogs.
A. Mescola, G. Paolicelli, S.P. Ogilvie, R. Guarino, J.G. McHugh, A. Rota, E. Iacob, E. Gnecco, S. Valeri, N.M. Pugno, V. Gadhamshetty, M.M. Rahman, P. Ajayan, A.B. Dalton, and M. Tripathi. Small 17, 2104487 (2021).

Quantitative Ultrafast Electron-Temperature Dynamics in Photo-Excited Au Nanoparticles.
M. Sygletou, S. Benedetti, M. Ferrera, G.M. Pierantozzi, R. Cucini, G. Della Valle, P. Carrara, A. De Vita, A. di Bona, P. Torelli, D. Catone, G. Panaccione, M. Canepa, and F. Bisio. Small 17, 2100050 (2021).

Chip-Scale Terahertz Frequency Combs through Integrated Intersubband Polariton Bleaching.
F.P. Mezzapesa, L. Viti, L. Li, V. Pistore, S. Dhillon, A. Giles Davies, E.H. Linfield, and M.S. Vitiello. Laser & Photonics Rev 15, 2000575 (2021).

Two-Photon Laser Writing of Soft Responsive Polymers via Temperature-Controlled Polymerization.
I. De Bellis, S. Nocentini, M.G. Delli Santi, D. Martella, C. Parmeggiani, S. Zanotto, and D.S. Wiersma. Laser & Photonics Rev 15, 2100090 (2021).

Effect of pressure on the properties of a NASICON Li1.3Al0.3Ti1.7(PO4)3 nanofiber solid electrolyte.
A. La Monaca, G. Girard, S. Savoie, H. Demers, G. Bertoni, S. Krachkovskiy, S. Marras, E. Mugnaioli, M. Gemmi, D. Benetti, A. Vijh, F. Rosei, and A. Paolella. J Mater Chem A 9, 13688-13696 (2021).

Altered Cl- homeostasis hinders forebrain GABAergic interneuron migration in a mouse model of intellectual disability.
A. Maset, L. Galla, S. Francia, O. Cozzolino, P. Capasso, R.C. Goisis, G. Losi, A. Lombardo, G.M. Ratto, and C. Lodovichi. PNAS 118, e2016034118 (2021).

Evidence of ideal excitonic insulator in bulk MoS2 under pressure.
S.S. Ataei, D. Varsano, E. Molinari, and M. Rontani. PNAS 118, e2010110118 (2021).

Electrostatic Field-Driven Supercurrent Suppression in Ionic-Gated Metallic Superconducting Nanotransistors.
F. Paolucci, F. Crisà, G. De Simoni, L. Bours, C. Puglia, E. Strambini, S. Roddaro, and F. Giazotto. Nano Lett 21, 10309-10314 (2021).

Large Enhancement of Critical Current in Superconducting Devices by Gate Voltage.
M. Rocci, D. Suri, A. Kamra, G. Vilela, Y. Takamura, N.M. Nemes, J.L. Martinez, M.G. Hernandez, and J.S. Moodera. Nano Lett 21, 216-221 (2021).

Quantum-Dot Single-Electron Transistors as Thermoelectric Quantum Detectors at Terahertz Frequencies.
M. Asgari, D. Coquillat, G. Menichetti, V. Zannier, N. Diakonova, W. Knap, L. Sorba, L. Viti, and M.S. Vitiello. Nano Lett 21, 8587-8594 (2021).

Strong Coupling between Localized Surface Plasmons and Molecules by Coupled Cluster Theory.
J. Fregoni, T.S. Haugland, S. Pipolo, T Giovannini, H. Koch, and S. Corni. Nano Lett 21, 6664-6670 (2021).

Ultrafast dynamics of plasmon-mediated charge transfer in Ag@CeO2 studied by free electron laser time-resolved x-ray absorption spectroscopy.
J.S. Pelli Cresi, E. Principi, E. Spurio, D. Catone, P. O'Keeffe, S. Turchini, S. Benedetti, A. Vikatakavi, S. D'Addato, R. Mincigrucci, L. Foglia, G. Kurdi, I.P. Nikolov, G. De Ninno, C. Masciovecchio, S. Nannarone, J.K. Kesavan, F. Boscherini, and P. Luches. Nano Lett 21, 1729-1734 (2021).

Glial-fibrillary-acidic-protein (GFAP) biomarker detection in serum-matrix: Functionalization strategies and detection by an ultra-high-frequency surface-acoustic-wave (UHF-SAW) lab-on-chip.
M. Agostini, F. Amato, M.L. Vieri, G. Greco, I. Tonazzini, L. Baroncelli, M. Caleo, E. Vannini, M. Santi, G. Signore, and M. Cecchini. Biosens Bioelectron 172, 112774 (2021).

©Hyperbolic Metamaterials with Extreme Mechanical Hardness.
A. Calzolari, A. Catellani, M. Buongiorno Nardelli, and M. Fornari. Adv Opt Mat 9, 2001904 (2021).

Unusual Red Light Emission from Nonmetallic Cu2Te Microdisk for Laser and SERS Applications.
Q. Li, H. Rao, X. Ma, H. Mei, Z. Zhao, W. Gong, A. Camposeo, D. Pisignano, and X. Yang. Adv Opt Mat 10, 2101976 (2021).

Inhibitor binding influences the protonation states of histidines in SARS-CoV-2 main protease.
A. Pavlova, D.L. Lynch, I. Daidone, L. Zanetti-Polzi, M.D. Smith, C. Chipot, D.W. Kneller, A. Kovalevsky, L. Coates, A.A. Golosov, C.J. Dickson, C. Velez-Vega, J.S. Duca, J.V. Vermaas, Y.T. Pang, A. Acharya, J.M. Parks, J.C. Smith, and J.C. Gumbart. Chem Sci 12, 1513-1527 (2021).

Challenges in Controlled Thermal Deposition of Organic Diradicals.
T. Junghoefer, N.M. Gallagher, K. Kolanji, E. Giangrisostomi, R. Ovsyannikov, T. Chassé, M. Baumgarten, A. Rajca, A. Calzolari, and M.B. Casu. Chem Mater 33, 2019-2028 (2021).

In situ decoration of laser-scribed graphene with TiO2 nanoparticles for scalable high-performance micro-supercapacitors.
L. Fornasini, S. Scaravonati, G. Magnani, A. Morenghi, M. Sidoli, D. Bersani, G. Bertoni, L. Aversa, R. Verucchi, M. Riccò, P. P. Lottici, and D. Pontiroli. Carbon 176, 296-306 (2021).

Synthesis of large-area rhombohedral few-layer graphene by chemical vapor deposition on copper.
C. Bouhafs, S. Pezzini, F.R. Geisenhof, N. Mishra, V. Mišeikis, Y. Niu, C. Struzzi, R.T. Weitz, A.A. Zakharov, S. Forti, and C. Coletti. Carbon 177, 282-290 (2021).

Enhanced Coherence in Superconducting Circuits via Band Engineering.
L. Chirolli and J.E. Moore. Phys Rev Lett 126, 187701 (2021).

Ensemble Reduced Density Matrix Functional Theory for Excited States and Hierarchical Generalization of Pauli's Exclusion Principle.
C. Schilling and S. Pittalis. Phys Rev Lett 127, 023001 (2021).

Estimating Quantum and Private Capacities of Gaussian Channels via Degradable Extensions.
M. Fanizza, F. Kianvash, and V. Giovannetti. Phys Rev Lett 127, 210501 (2021).

Experimental Demonstration of an Electrostatic Orbital Angular Momentum Sorter for Electron Beams.
A.H. Tavabi, P. Rosi, E. Rotunno, A. Roncaglia, L. Belsito, S. Frabboni, G. Pozzi, G.C. Gazzadi, P.-H. Lu, R. Nijland, M. Ghosh, P. Tiemeijer, E. Karimi, R.E. Dunin-Borkowski, and V. Grillo. Phys Rev Lett 126, 094802 (2021).

Microscopic Understanding of Ultrafast Charge Transfer in van der Waals Heterostructures.
R. Krause, S. Aeschlimann, M. Chávez-Cervantes, R. Perea-Causin, S. Brem, E. Malic, S. Forti, F. Fabbri, C. Coletti, and I. Gierz. Phys Rev Lett 127, 276401 (2021).

Quantum Energy Lines and the Optimal Output Ergotropy Problem.
S. Tirone, R. Salvia, and V. Giovannetti. Phys Rev Lett 127, 210601 (2021).

Reinforcement Learning Approach to Nonequilibrium Quantum Thermodynamics.
P. Sgroi, G.M. Palma, and M. Paternostro. Phys Rev Lett 126, 020601 (2021).

Sauter-Schwinger Effect in a Bardeen-Cooper-Schrieffer Superconductor.
P. Solinas, A. Amoretti, and F. Giazotto. Phys Rev Lett 126, 117001 (2021).

Vacancy-like Dressed States in Topological Waveguide QED.
L. Leonforte, A. Carollo, and F. Ciccarello. Phys Rev Lett 126, 063601 (2021).

Models of polymer solutions in electrified jets and solution blowing.
M. Lauricella, S. Succi, E. Zussman, D. Pisignano, and A.L. Yarin. Rev Mod Phys 92, 35004 (2020).

A Josephson phase battery.
E. Strambini, A. Iorio, O. Durante, R. Citro, C. Sanz-Fernández, C. Guarcello, I.V. Tokatly, A. Braggio, M. Rocci, N. Ligato, V. Zannier, L. Sorba, F.S. Bergeret, and F. Giazotto. Nat Nanotechnol 15, 656-660 (2020).

A monolayer transition-metal dichalcogenide as a topological excitonic insulator.
D. Varsano, M. Palummo, E. Molinari, and M. Rontani. Nat Nanotechnol 15, 367-372 (2020).

Ultrafast terahertz saturable absorbers using tailored intersubband polaritons.
J. Raab, F.P. Mezzapesa, L. Viti, N. Dessmann, L.K. Diebel, L. Li, A. Giles Davies, E.H. Linfield, C. Lange, R. Huber, and M.S. Vitiello. Nat Commun 11, 4290 (2020).

Optical Properties of Lead-Free Double Perovskites by Ab Initio Excited-State Methods.
M. Palummo, E. Berrios, D. Varsano, and G. Giorgi. ACS Energy Lett 5, 457-463 (2020).

Allosteric Control of Naphthalene Diimide Encapsulation and Electron Transfer in Porphyrin Containers: Photophysical Studies and Molecular Dynamics Simulation.
L. Zanetti-Polzi, R. Djemili, S. Durot, V. Heitz, I. Daidone, and B. Ventura. Chem 26, 17514-17524 (2020).

Strong Coupling with Light Enhances the Photoisomerization Quantum Yield of Azobenzene.
J. Fregoni, G. Granucci, M. Persico, and S. Corni. Chem 6, 250-265 (2020).

Electrically controlled white laser emission through liquid crystal/polymer multiphases.
A. Adamow, A. Szukalski, L. Sznitko, L. Persano, D. Pisignano, A. Camposeo, and J. Mysliwiec. Light Sci Appl 9, 19 (2020).

Highly efficient surface-emitting semiconductor lasers exploiting quasi-crystalline distributed feedback photonic patterns.
S. Biasco, A. Ciavatti, L. Li, A. Giles Davies, E.H. Linfield, H. Beere, D. Ritchie, and M.S. Vitiello. Light Sci Appl 9, 54 (2020).

Unveiling the detection dynamics of semiconductor nanowire photodetectors by terahertz near-field nanoscopy.
E.A.A. Pogna, M. Asgari, V. Zannier, L. Sorba, L. Viti, and M.S. Vitiello. Light Sci Appl 9, 189

(2020).

Maneuvering the Migration and Differentiation of Stem Cells with Electrospun Nanofibers.
J. Xue, D. Pisignano, and Y. Xia. Advanced Science 7, 2000735 (2020).

Naturally Degradable Photonic Devices with Transient Function by Heterostructured Waxy-Sublimating and Water-Soluble Materials.
A. Camposeo, F. D'Elia, A. Portone, F. Matino, M. Archimi, S. Conti, G. Fiori, D. Pisignano, and L. Persano. Advanced Science 7, 2001594 (2020).

Conformable Nanowire-in-Nanofiber Hybrids for Low-Threshold Optical Gain in the Ultraviolet.
A. Portone, R. Borrego-Varillas, L. Ganzer, R. Di Corato, A. Qualtieri, L. Persano, A. Camposeo, G. Cerullo, and D. Pisignano. ACS Nano 14, 8093-8102 (2020).

Gate-controlled suspended titanium nanobridge supercurrent transistor.
M. Rocci, G. De Simoni, F. Giazotto, C. Puglia, D. Degli Esposti, E. Strambini, V. Zannier, L. Sorba, and F. Giazotto. ACS Nano 14, 12621-12628 (2020).

Intelligent non-colorimetric indicators for the perishable supply chain by non-wovens with photo-programmed thermal response.
L. Romano, A. Portone, M.-B. Coltelli, F. Patti, R. Saija, M.A. Iatì, G. Gallone, A. Lazzeri, S. Danti, O.M. Maragò, A. Camposeo, D. Pisignano, and L. Persano. Nat Commun 11, 5991 (2020).

Low-voltage 2D materials-based printed field-effect transistors for integrated digital and analog electronics on paper.
S. Conti, L. Pimpolari, G. Calabrese, R. Worsley, S. Majee, D.K. Polyushkin, M. Paur, S. Pace, D.H. Keum, F. Fabbri, G. Iannaccone, M. Macucci, C. Coletti, T. Mueller, C. Casiraghi, and G. Fiori. Nat Commun 11, 3566 (2020).

Modelling genetic mosaicism of neurodevelopmental disorders in vivo by a Cre-amplifying fluorescent reporter.
F. Trovato, R. Parra, E. Pracucci, S. Landi, O. Cozzolino, G. Nardi, F. Cruciani, V. Pillai, L. Mosti, A.W. Cwetsch, L. Cancedda, L. Gritti, C. Sala, C. Verpelli, A. Maset, C. Lodovichi, and G.M. Ratto. Nat Commun 11, 6194 (2020).

Direct evidence for efficient ultrafast charge separation in epitaxial WS2/graphene heterostructures.
S. Aeschlimann, A. Rossi, M. Chávez-Cervantes, R. Krause, B. Arnoldi, B. Stadtmüller, M. Aeschlimann, S. Forti, F. Fabbri, C. Coletti, and I. Gierz. Sci Adv 6, eaay0761 (2020).

When nanocellulose meets diffraction grating: Freestanding photonic paper with programmable optical coupling.
G. Chu, D. Qu, A. Camposeo, D. Pisignano, and E. Zussman. Mater Horiz 7, 511-519 (2020).

30°-twisted bilayer graphene quasicrystals from chemical vapor deposition.
S. Pezzini, V. Mišeikis, G. Piccinini, S. Forti, S. Pace, R. Engelke, F. Rossella, K. Watanabe, T. Taniguchi, P. Kim, and C. Coletti. Nano Lett 20, 3313-3319 (2020).

Extremely Efficient Photocurrent Generation in Carbon Nanotube Photodiodes Enabled by a Strong Axial Electric Field.
D.R. McCulley, M.J. Senger, A. Bertoni, V. Perebeinos, and E.D. Minot. Nano Lett 20, 433-440 (2020).

Graphene promotes axon elongation through local stall of nerve growth factor signaling endosomes.
D. Convertino, F. Fabbri, N. Mishra, M. Mainardi, V. Cappello, G. Testa, S. Capsoni, L. Albertazzi, S. Luin, L. Marchetti, and C. Coletti. Nano Lett 20, 3633-3641 (2020).

HBN-Encapsulated, Graphene-based, Room-temperature Terahertz Receivers, with High Speed and Low Noise.
L. Viti, D.G. Purdie, A. Lombardo, A.C. Ferrari, and M.S. Vitiello. Nano Lett 20, 3169-3177 (2020).

Orbital Tuning of Tunnel Coupling in InAs/InP Nanowire Quantum Dots.
Z. Sadre Momtaz, S. Servino, V. Demontis, V. Zannier, D. Ercolani, F. Rossi, F. Rossella, L. Sorba, F. Beltram, and S. Roddaro. Nano Lett 20, 1693-1699 (2020).

Quantitative Nanoscale Absorption Mapping: A Novel Technique to Probe Optical Absorption of Two-Dimensional Materials.
M. Negri, L. Francaviglia, D. Dumcenco, M. Bosi, D. Kaplan, V. Swaminathan, G. Salviati, A. Kis, F. Fabbri, A. Fontcuberta i Morral. Nano Lett 20, 567-576 (2020).

Bandgap determination from individual orthorhombic thin cesium lead bromide nanosheets by electron energy-loss spectroscopy.
R. Brescia, S. Toso, Q. Ramasse, L. Manna, J. Shamsi, C. Downing, A. Calzolari, and G. Bertoni. Nanoscale Horiz 5, 1610-1617 (2020).

Transforming colloidal Cs4PbBr6 nanocrystals with poly(maleic anhydride-alt-1-octadecene) into stable CsPbBr3 perovskite emitters through intermediate heterostructures.
D. Baranov, G. Caputo, L. Goldoni, Z. Dang, R. Scarfiello, L. De Trizio, A. Portone, F. Fabbri, A. Camposeo, D. Pisignano, and L. Manna. Chem Sci 11, 3986-3995 (2020).

Erratum: Transforming colloidal Cs4PbBr6nanocrystals with poly(maleic anhydride-: Alt -1-octadecene) into stable CsPbBr3perovskite emitters through intermediate heterostructures (Chemical Science (2020) (11) (3986-3995) DOI: 10.1039/D0SC00738B)
Baranov D., Caputo G., Goldoni L., Dang Z., Scarfiello R., De Trizio L., Portone A., Fabbri F., Camposeo A., Pisignano D., Manna L. Chem Sci (11), 6923-6924 (2020)

Dye Stabilization and Wavelength Tunability in Lasing Fibers Based on DNA.
L. Persano, A. Szukalski, M. Gaio, M. Moffa, G. Salvadori, L. Sznitko, A. Camposeo, J. Mysliwiec, R. Sapienza, B. Mennucci, and D. Pisignano. Adv Opt Mat 8, 2001039 (2020).

Monitoring water and oxygen splitting at graphene edges and folds: Insights into the lubricity of graphitic materials.
P. Restuccia, M. Ferrario, and M.C. Righi. Carbon 156, 93-103 (2020).

Enhanced Electrospinning of Active Organic Fibers by Plasma Treatment on Conjugated Polymer Solutions.
V. Fasano, R. Laurita, M. Moffa, C. Gualandi, V. Colombo, M. Gherardi, E. Zussman, G. Vasilyev, L. Persano, A. Camposeo, M.L. Focarete, and D. Pisignano. ACS Appl Mater Inter 12, 26320-26329 (2020).

Enhanced Piezoelectricity of Electrospun Polyvinylidene Fluoride Fibers for Energy Harvesting.
P.K. Szewczyk, A. Gradys, S.K. Kim, L. Persano, M. Marzec, A. Kryshtal, T. Busolo, A. Toncelli, D. Pisignano, A. Bernasik, S. Kar-Narayan, P. Sajkiewicz, and U. Stachewicz. ACS Appl Mater Inter 12, 13575-13583 (2020).

Novel Ultrathin Films Based on a Blend of PEG- b-PCL and PLLA and Doped with ZnO Nanoparticles.
L. Vannozzi, P. Gouveia, P. Pingue, C. Canale, and L. Ricotti. ACS Appl Mater Inter 12, 21398-21410 (2020).

Surface Reactivity of Ag-Modified Ceria to Hydrogen: A Combined Experimental and Theoretical Investigation.
S. Benedetti, G. Righi, P. Luches, S. D'Addato, R. Magri, and A. Selloni. ACS Appl Mater Inter 12, 27682-27690 (2020).

Beyond the Swap Test: Optimal Estimation of Quantum State Overlap.
M. Fanizza, M. Rosati, M. Skotiniotis, J. Calsamiglia, and V. Giovannetti. Phys Rev Lett 124, 60503 (2020).

Bosonic Quantum Communication across Arbitrarily High Loss Channels.
L. Lami, M.B. Plenio, V. Giovannetti, and A.S. Holevo. Phys Rev Lett 125, 110504 (2020).

Ensemble Density Functional Theory: Insight from the Fluctuation-Dissipation Theorem.
T. Gould, G. Stefanucci, and S. Pittalis. Phys Rev Lett 125, 233001 (2020).

Ferromagnetic Resonance Assisted Optomechanical Magnetometer.
M.F. Colombano, G. Arregui, F. Bonell, N.E. Capuj, E. Chavez-Angel, A. Pitanti, S.O. Valenzuela, C.M. Sotomayor-Torres, D. Navarro-Urrios, and M.V. Costache. Phys Rev Lett 125, 147201 (2020).

Geometric Phase through Spatial Potential Engineering.
S. Cusumano, A. De Pasquale, and V. Giovannetti. Phys Rev Lett 124, 190401 (2020).

Inverse Currents in Hamiltonian Coupled Transport.
J. Wang, G. Casati, and G. Benenti. Phys Rev Lett 124, 110607 (2020).

Magnetic-Field-Dependent Equilibration of Fractional Quantum Hall Edge Modes.
T. Maiti, P. Agarwal,S. Purkait, G.J. Sreejith, S. Das, G. Biasiol, L. Sorba, and B. Karmakar. Phys Rev Lett 125, 076802 (2020).

Nonlinear Thermoelectricity with Electron-Hole Symmetric Systems.
G. Marchegiani, A. Braggio, and F. Giazotto. Phys Rev Lett 124, 106801 (2020).

Nonlocal Thermoelectricity in a Superconductor-Topological-Insulator-Superconductor Junction in Contact with a Normal-Metal Probe: Evidence for Helical Edge States.
G. Blasi, F. Taddei, L. Arrachea, M. Carrega, and A. Braggio. Phys Rev Lett 124, 227701 (2020).

Quantum Advantage in the Charging Process of Sachdev-Ye-Kitaev Batteries.
D. Rossini, G.M. Andolina, D. Rosa, M. Carrega, and M. Polini. Phys Rev Lett 125, 236402 (2020).

Quantum Flags and New Bounds on the Quantum Capacity of the Depolarizing Channel.
M. Fanizza, F. Kianvash, and V. Giovannetti. Phys Rev Lett 125, 020503 (2020).

G. Bertoni et al.
Surface Science 691, 2020.

F. Fabbri, L. Persano, A. Camposeo, D. Pisignano, et al. Applied Nano Materials 3 (10), 2020.

D. Pisignano, A. Camposeo, et al. The Journal of Physical Chemistry C 124 (46), 2020.

A. Calzolari et al.
Chemistry of Materials 33 (6), 2021.

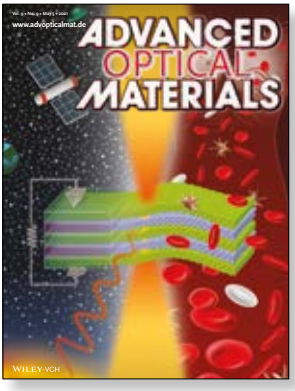

A. Calzolari, A. Catellani, et al. Advanced Optical Materials 9 (9), 2021.

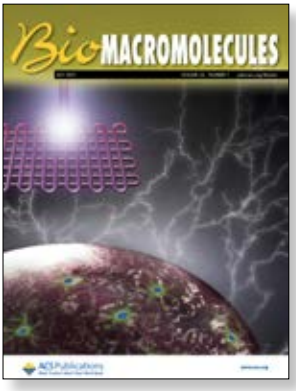

A. Camposeo, D. Pisignano, et al. Biomacromolecules 22 (7), 2021.

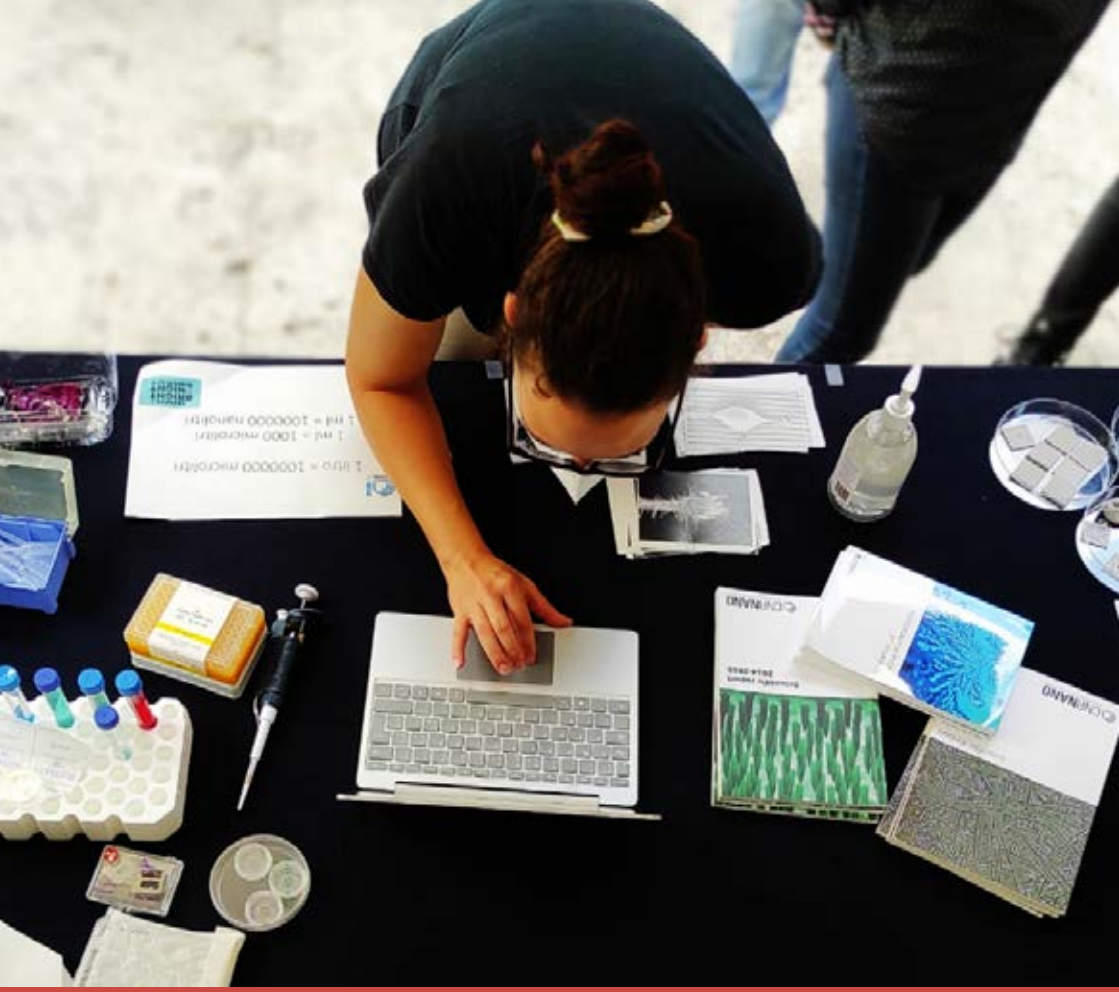

Cnr Nano Life

Cnr Nano events in 2020

JANUARY
The science to come

"La scienza che verrà" (The science to come) was the new year's opening episode of the radio program Aula 40 by the Cnr Pisa Area (broadcasted on January 16). Francesca Telesio was among the researchers invited to summarize the future opportunities in different science areas: she illustrated the exciting possibilities opened up by the research on graphene and 2D materials to the listeners and the high-school students attending the live broadcast.

JANUARY
A deep dive into Yambo

On January 27 the Computational School on Electronic Excitations in Novel Materials Using the Yambo Code, organized by Cnr Nano within the MaX Centre of Excellence, kicked off at ICTP (Trieste). 50 students from 23 countries attended a week of lively theoretical and technical lectures to learn how to fully master the Yambo code to simulate fundamental properties of materials.

FEBRUARY
New Institute board

On February 19, the Cnr Nano Institute board was renewed by the election of new members. The new board elected with a large participation of the voters is made up of 9 members, for the 60% women and for the 60% new; M. Grazia Angelini, Stefania Benedetti, Giorgia Brancolini, Marco Cecchini, Stefan Heun, Elisa Molinari, Valentina Tozzini, Alessandro Tredicucci, Filippo Troiani, will remain in office for the next four years, supporting the Director in planning the scientific activity of the institute.

FEBRUARY

Cnr Nano paper in PSS in Showcase 2020

The article by Cnr Nano researchers Stefano Guiducci, Matteo Carrega, Lucia Sorba, and Stefan Heun "Towards Quantum Hall Effect in a Josephson Junction", was chosen for the Physica Status Solidi Showcase 2020, a selection of the most interesting contents published in the Wiley's Physica Status Solidi journal.

MARCH

Equipment donation to support the COVID19 emergency

About a month after the outbreak of the COVID-19 pandemic in Italy, Cnr Nano and NEST Laboratory of Scuola Normale Superiore offered their personal protective equipment available to local hospitals. Masks, gloves, overshoes, and disposable coveralls used by researchers in their clean rooms were donated to support the dramatic shortage of protective equipment that health workers faced in the early stages of the pandemic.

APRIL

"25 Encores" for G.M. Ratto's lessons

More than 1300 high-school students from all over Italy had the chance to follow Gian Michele Ratto's free video lessons on brain functioning and on the advanced techniques to study it. Lessons were given within the Scuola Normale Superiore's initiative to support high schools and educational institutions in distance learning during the lockdown. Due to the high number of applications, Ratto's lessons were broadcasted more than 25 times from April 28 to June 5.

MAY

Activity Report 2020 is out!

The fifth edition of our biennial report spotted the main scientific highlights of the Institute, along with glimpses from its outreach activity, and many other important topics such as publications and funded projects of the years 2018-2019. It is a must-read to have an overview of what is done and who is who there, downloadable from the Institute's website.

MAY

An Innovation award

Cnr Nano researcher Giovanni Bertoni was among the winners of the Canada-Italy Award for Innovation 2020, a prize dedicated to strengthen the ties between the countries in the fields of science, technology, and innovation. Giovanni Bertoni was awarded for his project with Hydro-Québec, a Center of Excellence in Electric Transportation and Storage of Energy, focussing on Li ion batteries materials.

MAY

#TuttiInMusica with Carlo Andrea Rozzi

On May 19, researcher and expert violinist Carlo Andrea Rozzi took part in the live broadcast #TuttiInMusica - produced by the CNR Communication Office - to talk about the art of decomposing the sound: he discussed how to study the sound, how to dismantle, recombine, and reassemble it, and how these actions can have consequences beyond the purely scientific and technological scope.

JUNE

The Quantum Phase Battery is real

A research published in Nature Nanotechnology by Francesco Giazotto's group reporting the first fabrication of a quantum phase battery, hit the media with a featured article in the major Italian newspaper La Repubblica. The quantum device provides a persistent phase bias to the wave function of a quantum circuit and is a key element for quantum technologies based on phase coherence.

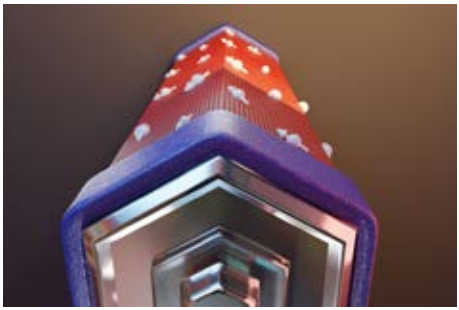

JUNE

Mind the mind traps!

Another live broadcast of #TuttiInMusica entitled 'Mind traps - Game, music and science to go further', hosted our researcher Carlo Andrea Rozzi to talk about acoustic illusions that can deceive our senses. Rozzi contributed to an illuminating discussion on how game, science, and music can be good allies to understand, face, and overcome the traps of the mind.

AUGUST

An iontronic community

On August 31 and September 1, Francesco Rossella chaired the mini-colloquium "Nanodevice iontronics" hosted at CMD2020GEFES, the international conference on all aspects of condensed matter physics. At the colloquium, held online, invited and regular speakers presented the most recent results achieved within the interdisciplinary community working on nanoscale electric double layer transistors.

SEPTEMBER

Extreme computing talking

Among the many top-quality events going on at the EuroScience Open Forum 2020, Cnr Nano participated in a hot-topic one, dedicated to the frontiers of High-Perfomance Computing. The meeting "Super-computing and the science & technology of the future", held on September 5, saw a top-quality scientific discussion among Elisa Molinari (UniMore & Cnr Nano) Roberto Cingolani (Leonardo SpA), Erik Lindahl (BioExcel CoE), and was moderated by Carlo Cavazzoni (Leonardo SpA).

OCTOBER

A winning business idea

Digital Superconducting Quantum Machines, an innovative business idea conceived by Cnr Nano and NEST Laboratory researchers, was awarded at the business competition StartCup Toscana 2020. The project aims at developing ultra-fast and low-energy devices towards the 6G revolution. DSQM also participated to the National Innovation Award as one of the shortlisted finalist projects (November 2020).

Cnr Nano events in 2021

FEBRUARY

Smart materials on TV

On February 16, Luana Persano's laboratories hosted a TV crew from Rai, the main national television network, that filmed a report on future light-based innovations. In a long interview she illustrated her recent development on smart materials published in Nature Communications: new nanomaterials with thermal properties that can be programmed using light and used to design smart labels for temperature monitoring.

APRIL

Molecular diagnostics to the market

INTA Systems, the first spin-off of Cnr Nano institute, closed its first seed investment with 350.000 € from the venture companies Eureka! and A11. INTA, founded by Matteo Agostini from Scuola Normale Superiore, Marco Cecchini from Cnr Nano, and Marco Calderisi, aims at bringing to the market a novel lab-on-a-chip called BRAIKER, capable of detecting biomarkers of traumatic brain injuries with rapid blood analysis.

APRIL

Lucia Sorba honored by the EPS

The Director of Istituto Nanoscienze was nominated a 2021 EPS Fellow by the European Physical Society in recognition of her scientific contributions "to the conception and engineering of reliable semiconducting nanostructures". The EPS president Petra Rudolf congratulated Lucia Sorba and expressed “appreciation for Lucia Sorba’s work not only personally, but also on behalf of the 130.000 physicists of the EPS”.

APRIL

A sound interview

The perception of sound is a complex issue, for example in many situations it is not easy to distinguish a sound from a noise. In the Cnr webzine ‘Almanacco della Scienza’, researcher Carlo Andrea Rozzi discussed a smartphone-based citizen science experiment he coordinated, aimed to evaluate the impact of environmental noise in residential areas.

JUNE

Innovating electron microscopy

On June 8, Cnr Nano Modena unit hosted the kick-off meeting of the MINEON FET project, a follow-up of another successful FET project, Q-SORT. Thanks to MINEON, leading experts in the field of electron microscopy and quantum light optics, coordinated by Vincenzo Grillo from Cnr Nano, will finalize a miniaturized electron-optical component to improve the electron-microscope imaging of a vast class of systems, e.g., biological samples for medical imaging.

JUNE

A week as a scientist

"Una settimana da scienziato" is a week-long event aimed at introducing and engaging high-school students in STEM disciplines, organized by the FIM Department of the University of Modena and Reggio Emilia on June 14-18. Cnr Nano researchers contributed to the Physics section of this summer school with talks about computing materials (Claudia Cardoso), quantum computers (Filippo Troiani), and international networks and large scale facilities (Paola Luches). The session was attended by more than 60 students.

JUNE

Optogenetic challenges

In three busy days full of presentations (June 14-16), more than 80 leading scientists from the fields of excited state properties of biological matter and charge transfer processes in proteins, shared and discussed their theoretical and experimental approaches, thanks to the virtual Psi-k workshop CT4OPTO, organised by Cnr Nano (Rosa Di Felice and Laura Zanetti Polzi) with the University of L'Aquila and the University of Southern California.

JULY

RAITH Micrograph Award 2021

Congratulations to Sedighe Salimian, young researcher at Cnr Nano and the NEST Lab, for her honorable mentions at the RAITH Micrograph Award 2021 – Special Edition, one of the most important awards in the world on e-beam lithography. She was awarded for her image 'Charge carrier separation in InAs/InP/GaAsSb core-dualshell based multifunctional device'.

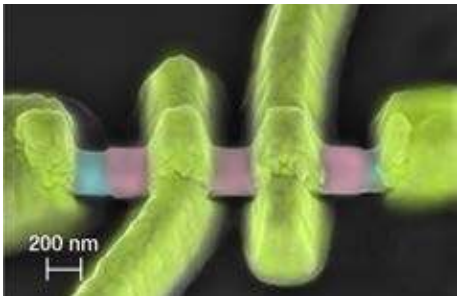

AUGUST

Talking of ourselves

A long-standing tradition in the Institute, the series of Nano Colloquia spotted again several Nano scientists from Modena and Pisa, who presented their work to colleagues. It is a good chance of sharing knowledge and finding new collaborations, as well as the first stage for many early stage researchers. All talks are given virtually and presentations can be downloaded from our website.

AUGUST

A toast to nanotechnologies

An unusual project for Cnr Nano was launched: the VIOLoC project aims to start a technological revolution in the world of wine and oil analytics by exploiting micro and nano-technologies and artificial intelligence. Its technological core is a micron-sized lab-on-a-chip with remote connectivity based on microfluidics that will be designed by the Marco Cecchini's group at Cnr Nano.

AUGUST

A special URSI GASS edition

The 2021 edition of the General Assembly and Scientific Symposium of the International Union of Radio Science (URSI GASS 2021, August 28-September 4) was a special one: it celebrated the URSI 100th anniversary! It hosted, among many others, a session on "Metasurfaces-enabled polarisation control" organized and chaired by Cnr Nano (Simone Zanotto) featuring an invited talk by Prof. Federico Capasso.

SEPTEMBER

At the forefront of electron microscopy

Cross-fertilisation and stimulating new ideas was the aim at the core of the "Science and Applications of coherent electron beam manipulation" conference, jointly organised by Vincenzo Grillo and four projects (Q-SORT, 3D MAGiC, SMART-electron, and MINEON), held online on September 1-3, focussed on exploring concepts at the forefront of electron microscopy research, such as electron coherence, electron phase control & holography, and many others.

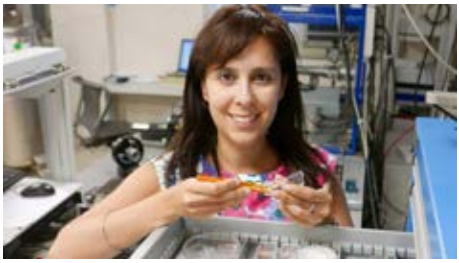

SEPTEMBER

Miriam Serena Vitiello awarded with the Friedel-Volterra Prize

Cnr Nano researcher Miriam Serena Vitiello was awarded the Friedel-Volterra Prize by the Italian and the French Physics Societies. She received the prize, awarded annually to a physicist active in the Italian-French collaboration, for her important experimental research in the field of light-matter interaction phenomena, in particular for the development of innovative devices in the terahertz frequency range.

SEPTEMBER

The Researcher's night is back!

On September 24, Cnr Nano joined the EU event where scientists meet citizens to talk science. In the city centre of Modena, a number of Cnr Nano researchers engaged in nanoscience outreach and played with pencils, diodes, and sheets of paper to present 2D materials. In Pisa, they showed new 3D printed materials and lab-on-a-chip to be used as innovative tools for medicine and health.

SEPTEMBER

Jacopo Fregoni awarded with the Premio Primo Levi

Young post-doc Jacopo Fregoni was awarded the "Premio Primo Levi 2020" by the Italian Chemical Society, devoted to an under-35 scientist active in the field of chemical sciences. Fregoni received the prize for his contribution "Strong coupling with light enhances the photoisomerization quantum yield of azobenzene", published in the journal Chem, realized during his PhD at the University of Modena and Reggio Emilia and Cnr Nano.

OCTOBER
Scienza quo vadis?

Take a seat, make yourself comfortable, and listen to science stories. Cnr Nano contributed to the Science cafè series, organized by Unimore, with a talk by Stefano Ossicini titled "Science quo vadis? Pinocchi in science, stories of scams and misconduct in modern scientific research", on October 26.

NOVEMBER
Intersect workshop

The outstanding building Casa Convalecència in Barcelona hosted for 3 days an audience of experimental and theoretical experts in electrical engineering, physics, chemistry, and materials science gathered in person and online to discuss the main open problems and solutions for the development of volatile and non-volatile memories and memristors. The International Workshop on Advanced Materials-to-Device Solutions for Synaptic Electronics (November 10-12) was organized within the H2020 project INTERSECT, led by Arrigo Calzolari, by ICN2 and Cnr Nano and attended by more than 80 people.

DECEMBER
Super-slippery graphene

After being published in the journal Small, Guido Paolicelli's group study on the frictional properties of graphene, hit the media. In two long interviews broadcasted on Radio24, a major Italian all-news radio station, Andrea Mescola and Guido Paolicelli explained how they could control and regulate friction of deposited graphene with a textured substrate, with the goal to reduce friction in the design of nano gears.


Fabio Taddei
Lucia Sorba
Paola Corezzola
Maria Spies
Valentina Tozzini
Luca Belluci
Massimo Rontani
Stefan Heun
Daniele Varsano
Antonella Battisti
Tavani Francesco
Paola Luches
Isha
Maddalena
Melissa Santi
Sara
Enzo Rotunno
Riccardo Nilosi
Vacondio
vincenzo Grillo
Claudio Bonizzoni
PATRIZIA PUCCI
Ale Pitanti
Deborah Prezzi
Claudia Cardoso
Stefania Benedetti
Francesco Giacotto
Alessandro di Bona
Luisa Neri
Andrea Mescola
Ivan Villani
Nicola Spallanzani
Barbara
MARIA BARTOLACELLI
Davide Calanca
FRANCESCO BAESSO
Paolo Rosi
Miki Bonacci
Giancarlo Gazzadi
Giorgio De Simoni
Antonella Sparbossa
Alessandro Braggio
Federica Bianco
Sergio Pezzini
Pino D'Amico
VZ
Valentina Zannier

People

The list below includes all researchers and staff active at Cnr Nano in 2020-2021. A total of 261 people have been working in our institute (32,1% female, 67,9% male), coming from 21 different countries besides Italy (Brazil, China, Colombia, Cuba, Germany, Greece, India, Iran, Malaysia, Morocco, Nepal, The Netherlands, Nigeria, Pakistan, Portugal, Romania, Russia, Spain, UK, Ukraine, and US).

Cnr Nano researchers

Antonella Battisti
Valerio Bellini
Luca Bellucci
Stefania Benedetti
Andrea Bertoni
Giovanni Bertoni
Federica Bianco
Alessandro Braggio
Giorgia Brancolini
Arrigo Calzolari
Michele Campisi
Andrea Camposeo
Matteo Carrega
Alessandra Catellani
Marco Cecchini
Valdis Corradini
Alessandro Crippa
Pino D'Amico
Giorgio De Simoni
Alessandro di Bona
Rosa Di Felice
Alessandra Di Gaspare
Filippo Fabbri
Riccardo Farchioni
Andrea Ferretti
Gian Carlo Gazzadi
Francesco Ghetti
Alberto Ghirri
Francesco Giazotto
Vincenzo Grillo
Stefan Heun
Nadia Ligato
Paola Luches
Francesca Matino
Francesco Mezzapesa
Riccardo Nifosì
Guido Paolicelli
Federico Paolucci
Claudia Maria Pereira Cardoso
Luana Persano
Sergio Pezzini
Valentino Pistore
Alessandro Pitanti
Stefano Pittalis
Eva Arianna Aurelia Pogna
Deborah Prezzi
Gian Michele Ratto
Elisa Riccardi
Massimo Rontani
Francesco Rossella
Enzo Rotunno
Carlo Andrea Rozzi
Melissa Santi
Andrea Secchi
Antonella Sgarbossa
Lucia Sorba
Nicola Spallanzani
Barbara Storti
Elia Strambini
Fabio Taddei
Francesco Tavanti
Ilaria Tonazzini
Valentina Tozzini
Filippo Troiani
Daniele Varsano
Stefano Veronesi
Leonardo Viti
Miriam Vitiello
Laura Zanetti Polzi
Valentina Zannier
Simone Zanotto

Cnr Nano Post Docs

Lyudmyla Adamska
Bamidele Ibrahim Adetunji
Matteo Archimi
Omer Arif
Mahdi Asgari
Seyedehsamaneh Ataei
Laura Bellentani

Claudio Bonizzoni
Luca Bursi
Sara Carpi
Davide Casotti
Luca Chirolli
Rajiv Kumar Chouhan
Lucian Aurel Constantin
Federica Cruciani
Eugenio Damiano
Jose Gustavo De La Ossa Guerra
Miriam De Sarlo
Ambra Del Grosso
Francesco Delfino
Andrea Di Ciolo
Behnood Dianat
Dayong Fan
Zacharias Fthenakis
Mariacristina Gagliardi
Sujoy Kumar Ghosh
Peter Nicholas Oliver Gillespie
Simone Giubbolini
Alberto Guandalini
Leonardo Lamanna
Savio Laricchia
Dario Alejandro Leon Valido
Chiara Liberatore
Francesco Lunardelli
Giampiero Marchegiani
Daniel Margineda De Godos
Maria Celeste Maschio
Andrea Mescola
Alessio Massimiliano Miranda
Fulvio Paleari
Gabriele Parlanti
Riccardo Parra
Vinoshene Pillai Rajan
Alessandro Porcelli
Alberto Portone
Claudio Puglia
Mirko Rocci
Luigi Romano
Paolo Rosi
Pavel Rukin
Luca Salemi
Elisabetta Salerno
Sedighe Salimian
Amine Slassi
Maria Spies
Francesca Telesio
Francesco Trovato
Leonardo Vicarelli
Avinash Vikatakavi
Francesco Vischi

Affiliated researchers

Marco Affronte
Andrea Alessandrini
Maria Allegrini
Fabio Beltram
Giuliano Benenti
Roberto Biagi
Pietro Bonfà
Paolo Bordone
Marilia Junqueira Caldas
Francesco Cardarelli
Franco Carillo
Giovanni Carlotti
Ciro Cecconi
Francesco Ciccarello
Stefano Corni
Sergio D'Addato
Valentina De Renzi
Elena Degoli
Angelo Di Bernardo
Alberto Di Lieto
Sebastiano Di Pietro
Daniele Ercolani
Rosario Fazio
Stefano Frabboni
Simone Gasparinetti
Marco Gibertini
Vittorio Giovannetti

Guido Goldoni
Alessandro Lascialfari
Stefano Luin
Rita Magri
Franca Manghi
Fabio Mencarelli
Claudia Menozzi
Elisa Molinari
Stefano Ossicini
Gioacchino Massimo Palma
Pasqualantonio Pingue
Dario Pisignano
Maria Clelia Righi
Stefano Roddaro
Alberto Rota
Alice Ruini
Alessandra Toncelli
Mauro Tonelli
Alessandro Tredicucci
Sergio Valeri
Giovanni Maria Vanacore
Giampaolo Zuccheri

Affiliated Post Docs

Matteo Agostini
Vittorio Buccheri
Dhawal Choudhary
Sutapa Dutta
Andrea Ottomaniello
Enrico Pracucci
Teresa Tommasini

Affiliated PhD students

Annachiara Albanese
Luca Basta
Bibek Bhandari
Gianmichele Blasi
Miki Bonacci
Lennart Bours
Giada Bucci
Dario Cilluffo
Gloria Conte
Samuele Cornia
Naeimeh Eghbali Fam
Paolo Andrea Erdman
Jacopo Fregoni
Gaia Germanese
Davide Giambastiani
Sara Khorshidian
Didi Lamers
Lorenzo Lavista
Riccardo Magrin Maffei
Nicola Melchioni
Roberta Mezzena
Daniele Montepietra
Gabriele Nardi
Samuele Pelatti
Francesco Pisani
Domenic Prete
Frank Ernesto Quintela Rodriguez
Gregorio Ragazzini
Cinzia Scorzoni
Giacomo Sesti
Eleonora Spurio
Simone Vacondio
Isha Verma
Andrea Vezzosi
Matteo Zanfrognini

Administrative staff

Maria Grazia Angelini
Francesco Baesso
Michela Balderi
Elisa Bolognesi
Michele Corradi
Giovanna Diprima
Sandro Guerrazzi
Patrizia Pucci
Federica Sighinolfi
Anna Grazia Stefani

Technical staff

Maria Bartolacelli
Davide Calanca
Daniele Desiati
Mara Di Berardo
Luisa Neri
Riccardo Pallini
Maria Jesus Rodriguez Douton
Maddalena Scandola

Support Staff in Genova

Alberto Arnone
Matilde Bolla
Barbara Cagnana
Enrico Camauli
Marco Campani
Paolo Ciocia
Paola Corezzola
Monica Dalla Libera
Roberta De Donatis
Piero Di Lello
Fabio Distefano
Francesca Fortunati
Maria Carla Garbarino
Giuseppe Genovese
Danilo Imperatore Antonucci
José Carlos Manganaro
Diletta Miceli
Elisabetta Narducci
Marco Punginelli
Liliana Sciaccaluga
Simone Spinozzi

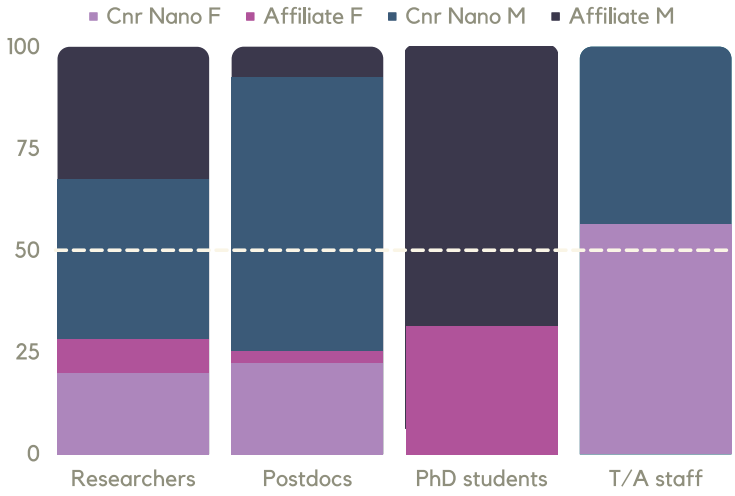

All categories have been normalized to 100 to show the gender distribution within the Institute.

Image credits

Cover image
Close up of a plasmonic metasurface realized by FIB milling used for optical beam shaping.
Courtesy of Paolo Rosi, Giancarlo Gazzadi (Cnr Nano Modena)

pag. 5
False-color scanning electron microscopy image of Helicobacter pylori ATCC43504 fixation residues on a silicon wafer.
Courtesy of Antonella Battisti, Antonella Sgarbossa (Cnr Nano Pisa)

pag. 23
Photoswitch of interface polaritons in black phosphorus heterostructures.
Courtesy of Miriam Serena Vitiello, Leonardo Viti (Cnr Nano Pisa)

pag. 43
Coil of nanowires: semiconductor nanowires grown on a patterned substrate defining a spiral with curved rays.
Courtesy of Valentina Zannier, Lucia Sorba (Cnr Nano Pisa)

pag. 67
An electrostatic MEMS device to produce a near exact tunable electron vortex beam. The device includes innovative boundary condition controls.
Courtesy of Paolo Rosi (Cnr Nano Modena), Alberto Roncaglia (Cnr Imm Bologna)

pag. 85
Hydrogen adsorption within nanoporous graphene scaffolds. Hydrogen is represented in orange as is iso-density surface. The nanoporous graphene structure is in black.
Courtesy of Luca Bellucci, Francesco Delfino, Valentina Tozzini (Cnr Nano Pisa)

—

Finito di stampare nel mese di luglio 2022.
Progetto editoriale: Luisa Neri, Cnr Nano.
Progetto grafico: mediamo.net, Modena.

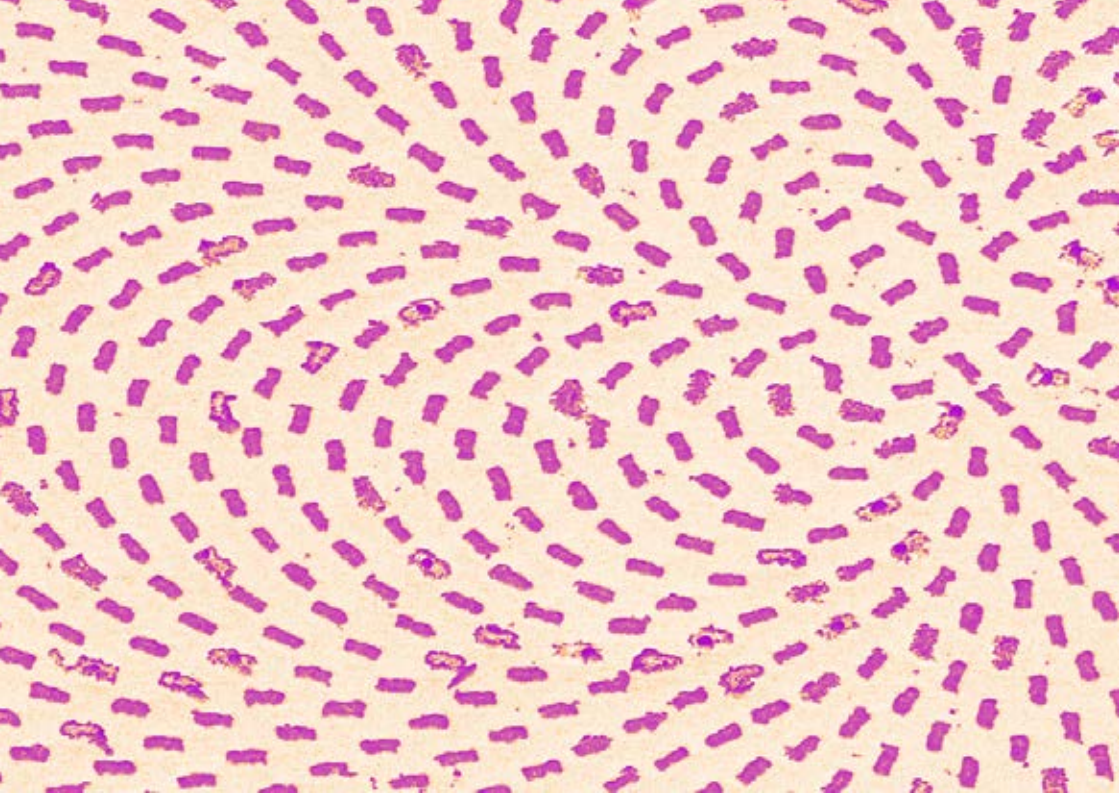

CNRNANO

ISTITUTO NANOSCIENZE CONSIGLIO NAZIONALE DELLE RICERCHE